Modelling bushfire changes for South Australian regions

Final Report – January 2015

Jacqueline Balston & Associates

Department of Environment, Water and Natural Resources
South Australian Prospering in a Changing Climate Program

Contact for enquiries: Dr. Jacqueline Balston, Jacqueline Balston & Associates, P.O. Box 315, Bridgewater, South Australia 5155.

Title: Modelling bushfire changes for South Australian regions.

This report should be cited as:
Balston, J.M. and Williams, A. (2014), Modelling bushfire changes for South Australian regions, Department of Environment, Water and Natural Resources South Australia, Adelaide, South Australia. pp.88.

Contributors:
Dr. Balston, J.M. – Jacqueline Balston & Associates.
Dr. Williams, A.J. – Tjuringa Products and Services.

A copy of this report and further information on climate change in South Australia is available at the South Australian Government Environment website: (http://www.environment.sa.gov.au/firemanagement/Fire_and_the_Environment/Fire_research)

Acknowledgements:
Thanks to: the project collaborators for their support and guidance (Lauren Burton and Mike Wouters, Department of Environment, Water and Natural Resources; Liz Connell, SAFECOM; Leigh Miller, CFS; Adam Gray, LGASA; Natasha Hall, Central Region LGA; Jarrod White Northern and Yorke NRM; Darren Ray, Bureau of Meteorology SA; Jacqueline Frizenschaf, SA Water).This project was funded by the South Australian Department of Environment, Water and Natural Resources, Northern and Yorke NRM and SA Water.

TABLE OF CONTENTS

LIST OF FIGURES

LIST OF TABLES

EXECUTIVE SUMMARY

Bushfire is a regular feature of the natural environment in South Australia (SA). Even prior to the arrival of humans, the region was subject to regular and extensive bushfires. However, over the past thirty years, the climate of SA has changed as greenhouse gas emissions in the atmosphere have increased and the resultant global warming. Observations show: increased mean, maximum and minimum temperatures; an increase in the intensity and frequency of heatwave events; changes to rainfall patterns; an increase in evaporation; and a corresponding increase in the Forest Fire Danger Index. As greenhouse gas emissions continue to rise, fire weather in SA is expected to become more severe.

Prior to this study, fire weather data (temperature, rainfall, evaporation, wind) and fire danger data (Forest Fire Danger Index (FFDI) and Grass Fire Danger Index (GFDI)) were available in a number of formats and spatial and temporal resolutions. However, projections of changes to fire danger as a result of climate change had only been done for four locations in SA – Adelaide, Ceduna, Mt. Gambier and Woomera. As a result, the capacity to plan for, and adapt to, future bushfire threats in regional areas of SA was limited.

This project undertook to review existing bushfire studies and examine current data sets of fire weather to determine if they were fit for use in assessing the likely impacts of climate change on fire behaviour for other areas of SA. Once rigorous data was identified, a methodology was developed to calculate the likely changes to future bushfire weather for regions across the State. The methodology was tested for two pilot areas: one within the Central LGA Region (Spring Gully Conservation Park – SGCP); and the other in the Mt. Bold Reserve (MBR) in the Adelaide Hills. No assessment of climate change on fire danger had previously been undertaken in these areas.

The methodology developed asks the researcher two questions: Is the location to be analysed close to an historical weather observing station that collects all the necessary variables required to calculate the FFDI / GFDI? If so, does the observing station have a time series long enough to calculate a baseline FFDI / GFDI? If each of these criteria is met then observed data can be used for the historical baseline analysis. If observed data is not available then patched observed data or a range of synthetic gridded data can be used instead. For climate change analyses a range of methods that capture the projected change in future climate can be applied to the historical data set or Global Climate Model (GCM) data can be used. Each of these options was assessed and the best selected for use in the two pilot areas.

The SILO Patched Point data set contains Bureau of Meteorology (BOM) observed historic data with gaps filled for temperature, rainfall and evaporation. This data set in conjunction with the closest observed wind data sets were used for each of the pilot sites to calculate the baseline FFDI. A high emissions scenario (A1FI) climate for the year 2050 as modelled by three GCMs was then created using the Change Factor technique utilized by CSIRO in the OZCLIM data sets. Historical and future fuel load and curing data were not available for SGCP and MBR and so GFDI could not be calculated at this stage. Analysis of the changes in the FFDI between the 1990 baseline climate indicate that at both locations, the cumulative monthly and annual FFDI is most likely to increase by 2050. The fire danger season is also likely to increase in both length and intensity. The number of days when the FFDI>25 (very high fire danger days) are projected to increase from 16 to 25 at SGCP and from 17 to 20 at MBR. These results support those from previous studies in South Australia.

These results can be included in the Integrated Climate Change Vulnerability Assessments (IVA) for each study area as well as the strategic plans of relevant government agencies, project partners and the State Emergency Risk Management Planning processes. In addition, there is the opportunity in the future to expand the analysis to other areas either at point locations or, using gridded data sets, the whole State. Future analysis could also use the outputs from the CMIP5 suite of GCM scenario runs or include analysis of the GFDI using modelled fuel data.

1 BACKGROUND TO THE PROJECT

1.1 PROJECT CONTEXT

Warming of the climate as a result of human activities that release greenhouse gasses into the atmosphere is now considered by the global scientific community to be “unequivocal” (IPCC 2013). South Australia has already experienced a number of climate changes as a result of global warming that has affected fire weather including increased mean, maximum and minimum temperatures, an increase in heatwave events, changes to rainfall patterns, an increase in evaporation and an increase in the Forest Fire Danger Index. Despite current greenhouse gas mitigation strategies, levels in the atmosphere will continue to rise over the coming decades and so the climatic changes expected to enhance bushfire weather in South Australia (SA) are expected to continue.

Prior to this study fire weather data (including temperature, rainfall, soil moisture, wind) and fire danger index data (Forest Fire Danger Index (FFDI) and Grass Fire Danger Index (GFDI) was available in a number of formats and spatial and temporal resolutions for Australia. However, projections of changes to fire danger as a result of climate change had only been done for four point locations in SA: Adelaide, Ceduna, Mt. Gambier and Woomera (Lucas, Hennessy et al. 2007).

Information on the likely impacts of climate change to bushfire weather in other regions of SA including the Central Region and Adelaide Hills did not exist and so the capacity to plan for, and adapt to future bushfire risks in these areas by way of regional integrated climate change vulnerability assessments (IVAs) and other processes was limited.

1.2 PROJECT AIM AND OUTPUTS

The aim of this project was to determine if it is possible to calculate the likely impacts of climate change on future bushfire danger for regional areas of SA.

Outputs from the project include: a final report (this document); a literature review of previous studies that have assessed the likely impacts of climate change on bushfire weather in SA including methodology and data sets analysed (Appendix 1); detailed development of a methodology and analysis of data sets (Appendix 2); and the analysis and results for each of the two pilot study sites (Appendix 3). An additional two page communication factsheet was also developed to meet the requirements of project partners. This report is available on the web at: (http://www.environment.sa.gov.au/firemanagement/Fire_and_the_Environment/Fire_research)

1.3 PROJECT METHODOLOGY

The project comprised six key tasks:

- Undertake a literature review of current studies to assess fire behaviour in Australia and SA;
- Assess existing fire weather and danger index data for appropriateness in SA;
- Develop a fire and climate change model / methodology to determine likely impacts of climate change on fire behaviour in SA;
- If the data supported it, analyse historical fire weather and compare it to future climate change fire weather for two pilot areas in SA;
- Develop project outputs and deliverables.

2 CLIMATE CHANGE AND BUSHFIRE – A REVIEW OF THE LITERATURE OF RELEVANCE TO SOUTH AUSTRALIA

A detailed literature review (Appendix 1 of this report) examined the context of fire in the SA landscape, current approaches to forecasting fire weather, observed and future changes to the climate for SA and previous studies of climate change and bushfire that have been undertaken. This chapter provides a brief overview of the review.

2.1 BUSHFIRE IN THE SOUTH AUSTRALIAN LANDSCAPE

Bushfire is a natural part of the Australian environment that has shaped the biota of the continent over many millennia. Australia today is considered to be the most bushfire prone of all continents (Bradstock 2010). However, even prior to the arrival of humans, Australia was subject to regular and extensive bushfires as is evident in the diverse range of floral and faunal responses to fire that have evolved since the Eocene. The native vegetation of Australia is well adapted to fire and many species are able to regrow either vegetatively after a fire from protected buds (above or below ground), or from seeds stored in protective woody fruits in the canopy seed bank (serotiny). Other species exhibit fire stimulated flowering, and / or heat and smoke stimulated germination of soil-stored seeds (Williams, Bradstock et al. 2009).

The relationship between climate, vegetation and fire varies across the continent. For example, in southern, forested regions the rainfall is higher and drought is associated with the major fires. In arid, central Australia, it is above average rainfall that leads to burning of very large areas. This variation is because fire in arid woodland communities is limited by biomass (fuel) growth, whereas in wet areas where forests dominate, fires are driven by fuel moisture (availability to burn) and fire weather (Bradstock 2010).

2.2 CURRENT BUSHFIRE FORECASTING IN AUSTRALIA

Bushfire is controlled by four switches: biomass (fuel) production; the dryness of the fuel; occurrence of suitable fire weather; and a source of ignition. Each of these switches must be “on” for a bushfire to occur (Bradstock 2010). Weather parameters that intensify potential bushfires are high maximum temperatures, strong winds and low relative humidity.

Fire danger indices are used in many parts of the world as a measure of the suppression difficulty of a bushfire. In Australia the McArthur Forest Fire Danger Index (FFDI) (McArthur 1967) is widely used to forecast the influence of weather on fire behaviour. The Australian Bureau of Meteorology routinely issues forecasts of the FFDI and the Grassland Fire Danger Index (GFDI) for use by fire authorities.

The fire danger rating scale was introduced by Lucas et al (2007). The original scale had five levels: low, moderate, high, very high and severe. However, after the February 2009 Black Saturday fires in Victoria, and the extreme fire danger weather recorded during the event, the fire danger rating scale was changed in October 2010 to include two additional levels: extreme and catastrophic (Bureau of Meteorology 2014a).

2.3 GLOBAL GREENHOUSE GAS EMISSIONS

Between 1750 and 2011 human activity released 375 billion tonnes of carbon dioxide into the atmosphere as a result of fossil fuel burning (coal, oil, gas) and cement production. Another 180 billion tonnes were released as a result of land clearing (IPCC 2013). This carbon dioxide is a unique isotope that can only be attributed to the burning of carbonate fuels and so is not from other sources such as volcanoes. Other greenhouse gases including methane and nitrous oxide have also been released as part of industrial processes.

2.4 OBSERVED CHANGES IN THE SOUTH AUSTRALIAN CLIMATE

An increase in greenhouse gas concentrations warms the earth as the atmosphere has an enhanced capacity to prevent heat from escaping back into space. In response to the increase in greenhouse gas concentrations, the mean temperature across South Australia has increased by 0.8^{o}C to 1.2^{o}C between 1970 and 2011.The number of very hot days (days above 40^{o}C) has also increased by 4.5 to 9.0 days since 1970. In addition, the number of heatwave events or 'warm spell durations' (defined by the Bureau of Meteorology as an annual count of days with at least four consecutive days when daily maximum temperature greater than the 90th percentile) has also increased. Annual rainfall since 1970 has decreased by 10 to 40 mm/decade – most dramatically across the north-east of the state. Changes in evaporation have varied across the state from +5 mm to -5 mm per year (Bureau of Meteorology 2014b). Across Australia between 1975 and 2006 there has been a recorded widespread stilling in daily wind run of 0.009 m/s per year (McVicar, Van Niel et al. 2008).

2.5 FUTURE EXPECTED CHANGES IN THE SOUTH AUSTRALIAN CLIMATE

Future greenhouse gas emission levels are unknown and so a range of different possible emissions scenarios and resultant climates are calculated using Global Climate Models (GCMs). Projections of future warming for South Australia have been undertaken by the CSIRO and Bureau of Meteorology. As a whole, the average annual temperature is expected to further increase by between 0.6^{o}C and 2.0^{o}C by 2030 and 1.0^{o}C and 5^{o}C by 2070 compared to average temperature from 1980 to 1999 – a period known as the 1990 baseline. This warming is expected be greater inland and less along the coast.

Projected changes in annual rainfall for South Australia are more difficult to model than changes in temperature. By 2030, annual average rainfall is expected to change from -20% to +10% and by 2070 from–60% to +20% compared to 1990 levels (CSIRO and BoM 2007).

Projections for future wind are calculated for 10 m above the ground and have only been undertaken at the continent scale (CSIRO BOM 2007). Average wind speed in South Australia is expected to increase in coastal regions by 2% to 10% by 2030 in summer and increase or decrease by 2% in winter. By 2050, the magnitude of the change increases depending on the emissions scenario used.

Eyre Peninsula 2005. (Sourced: melbourneblogger.blogspot.com 10 Jan 2013).

2.6 GLOBAL BUSHFIRE STUDIES

As a result of climate change and in some cases changes to forest management, the has been a decrease in fire frequency over some regions of the globe, including the USA and Europe, and an increase in others, including Amazonia, Southeast Asia, and Canada (IPCC 2007). An IPCC assessment of future fire risk to the year 2100 indicates for Australia that the FFDI is expected to increase by 12% in coastal area and by up to 50% inland (Caesar and Golding 2011).

2.7 AUSTRALIAN BUSHFIRE STUDIES

As identified earlier, bushfire intensity is a function of biomass production, availability of fuel to burn, fire weather and ignition. As the climate of SA warms and potentially dries it is expected that an increase in dryness in arid woodland communities will decrease potential fire frequency as fuel loads diminish, but increase in wetter temperate forests where fire is driven by fuel moisture and fire weather (Bradstock 2010).

Because the monitoring of fuel loads for each of the fire danger indices is a complex process that may need to take into account a range of fuel types and characteristic, most previous studies that considered changes in past and future bushfire intensity and frequency assessed the changes in bushfire weather alone (Bradstock 2010).

Between 2001 and 2007 fire danger weather has increased in many areas by 10% to 40% compared to the 1980 – 2000 period (Steffen 2009). Four of the five fire seasons (2003 to 2007) were among the longest on record since 1942, a trend that has increased since the early 1990s (Lucas, Hennessy et al. 2007).

A number of studies have considered the impact of future climate change on the Forest Fire Danger Index (FFDI). Results show that the expected increase in CO_2 in the atmosphere, and resultant increased temperature, reduced humidity and increased frequency of cold front events (that bring dangerous wind shifts and increase fire exposure) significantly increase the fire weather risk across south-eastern Australia to an extent dependant on location and future scenario (Williams, Karoly et al. 2001; Hennessy, Lucas et al. 2005; Pitman, Narisma et al. 2007; Hasson, Mills et al. 2009). In one study the mean and extreme FFDI were projected to decrease or remain close to 20th century levels in the summer rainfall-dominated tropical north-east of Australia. However, in the uniform and winter rainfall regions that occupy south-east continental Australia the FFDI was projected to increase strongly by 2100 (Clarke, Smith et al. 2011). The role of lightning in future fire frequency is at this stage unknown.

Changes in wind speed were shown to contribute very little to the projected changes although only daily average wind speed was available for the study (Clarke, Lucas et al. 2012). Currently about 30% of fires are started by lightning. In a warmer future climate we may have less thunderstorms overall but those that do occur may be more intense (Price 2009).

Only one study considered the effect of a changing climate *and* atmospheric CO_2 on grass curing, fuel load, and the GFDI. The study showed that changes in temperature and moisture determined curing, while atmospheric CO_2 concentration had no significant effect. Results indicated that the monthly 95th percentile GFDI was generally predicted to increase as climates became warmer and drier compared with the historical climate, particularly in the warmer months (November to March). However, the combined effects of generally higher GFDI and generally lower fuel loads modelled for future climate and atmospheric CO_2 combinations resulted in relatively small changes in modelled future potential fire-line intensity for the majority of grassland types, months and study locations (King, Cary et al. 2012). The authors also noted that "for the exotic annual grasslands at all locations and the exotic perennial grasslands in Canberra and Melbourne, the mean fuel load between October and April, when the majority of fire activity occurs, was a good approximation for the assumed mean fuel load of 4.5 t/ha used in earlier studies".

2.8 SOUTH AUSTRALIAN BUSHFIRE STUDIES

An analysis of climate change impacts on bushfire by Lucas, Hennessy et al. (2007) included 28 stations across southern Australia including Adelaide, Ceduna, Woomera and Mt. Gambier in SA. Historical data were analysed to determine trends and the current number of days when the fire danger rating exceeded high, very high, severe, extreme and catastrophic. Data for Adelaide showed that the average number of days each year when the FFDI score went above 25 (very high) was 17.3 and the average number of days each year when the FFDI score went above 50 (severe) was 10.9. To 2007 when the study was undertaken there had been no days when the FFDI exceeded 75 (extreme) or 100 (catastrophic) in Adelaide. An assessment of future climate changes showed that a mean temperature increase of up to 1.0^{o}C would lead to a 10% to 30% increase in the average number of very high fire days across southern Australia, and the average number of extreme fire days would rise by 15% to 65% depending on location. In addition, it is expected that fire seasons will start earlier, end later and be "generally more intense throughout their length. For Adelaide, a high greenhouse gas emissions scenario would result in an estimated increase of four days each year when the FFDI was above 25 by 2020 and an additional twelve days by 2050. In addition, the annual cumulative FFDI was likely to increase by between 5% and 8% and 16% to 25% for high emission scenarios for the years 2020 and 2050 respectively.

A follow up study by Clarke, Lucas et al (2012) examined changes in Australian fire weather as measured by the FFDI between 1973 and 2010 and included four South Australian locations. Annual cumulative FFDI increased significantly at 16 of the 38 stations tested, mostly those in the interior south-east of the continent and less along the coast. None of the stations showed a negative trend. The largest increases were shown to have happened in spring and autumn. The multi-station mean showed that on average across Australia, there had been an increase in annual cumulative FFDI since 1973 of 212 points per decade. Locations in the study in SA were Adelaide, Ceduna, Mt. Gambier and Woomera. For SA, there were significant increases in both the annual FFDI and seasonal values – particularly in the spring and autumn.

2.9 LITERATURE REVIEW SUMMARY

Bushfire weather in South Australia (SA) has been observed to have changed over the past 100 years: annual total rainfall has decreased although summer rainfall has increased in some areas; maximum temperatures have increased State wide; relative humidity has increased in some parts of the State and decreased in others; and wind speeds display mixed trends, increasing in some locations, decreasing in others. When included in the calculation of the historical FFDI for SA, there have been significant increases in both the annual FFDI and seasonal values – particularly in the spring and autumn. Trends were higher at the upper end of the distributions, an indication that the shape of the distribution is changing and not just the mean. In addition, at the locations considered across southern Australia, the length of the bushfire season has extended by 2.4 days per decade (Clarke, Lucas et al. 2012).

The one study that considered the impacts of climate change on SA bushfire weather included Adelaide, Ceduna, Mt. Gambier and Woomera. For Adelaide, a high greenhouse gas emissions scenario would result in an estimated increase of four days each year when the FFDI was above 25 by 2020 and an additional twelve days each year by 2050 (Lucas, Hennessy et al. 2007). In addition, the annual cumulative FFDI was likely to increase by between 5% and 8% and 16% to 25% for high emission scenarios for the years 2020 and 2050 respectively (Lucas, Hennessy et al. 2007).

3 FIRE AND CLIMATE CHANGE ANALYSIS METHODOLOGY AND DATA

Each of the publications reviewed in Appendix 1 were further examined to identify the methodology and data sets used in each study (Appendix 2). A methodology for future studies was then developed. As would be expected a range of different approaches and data sets were used. Studies were an assessment of either historical or future FFDI or GFDI and used either the historic observed or gridded data for analysis of past fire weather and global climate model outputs or modified historic data sets for future assessments.

Past analyses also considered a range of spatial scales from individual points, to larger regions based on an average for the region from a number of points or a spatially gridded surface. Temporal scales also varied from the daily scale up to monthly, seasonal and even annual. A summary of the methodology and data sets used in previous studies is provided in the tables on the following pages (Table 1 and Table 2).

Each of these approaches and the data sets used were considered in the development of a methodology or future climate change and bushfire studies Figure 1. The methodology developed is presented as a flow chart and asks the researcher: Is the location to be analysed close to an historical weather observing station that collects all the necessary variables required to calculate the FFDI / GFDI? If so, does the observing station have the necessary time series to calculate a baseline FFDI / GFDI that takes into account climate variability? If each of these criteria are met then observed data can be used for the historical analysis.

If observed data is not available then patched observed data or a range of synthetic gridded data can be used instead. Patched Point data sets include that developed by the Queensland Government as part of the SILO project. Patched Point data is only available for point locations that correspond with actual observed historical data collected by the Bureau of Meteorology (BOM) observing network but fills any gaps in the observed data using a range of methods.

Synthetic data sets use observed data to generate a value for each climate variable for a grid that spans across the landscape. In addition to the observed data, the synthetic data set may take into account topography, distance from the coast and other variables. The grids range in scale from 5 km up to 25 km. Synthetic data sets of relevance for this study include the BOM high quality gridded data set (AWAP), the Mc Vicar wind gridded data set, the Finkele drought Index data set and the Aussie Grass gridded data set. Synthetic gridded data sets do not usually replicate the actual observed values at a single point as the Patched Point data sets do. The further one moves away from the observed recorded data the more errors are likely in the values at a particular location.

For climate change analyses a range of methods that capture the projected change in future climate can be applied to the historical data set or Global Climate Model (GCM) output data set. The analysis of historic and future changes in the FFDI / GFDI can then be calculated.

Based on methodology developed and data available we undertook the following calculations so as to allow for comparison between this and the original study by Lucas et al (2007). The approach is highlighted as a red pathway on the methodological flowchart provided in Figure 1.

- Change in the annual cumulative FFDI (∑FFDI, as per Beer and Williams 1995). This value is the sum of the daily FFDI for each year;
- The monthly ∑FFDI was also examined – the sum of the daily FFDI for each month;
- Changes in the number of days the FFDI exceeds a particular threshold;
- Changes in the frequency of certain threshold events. Lucas et. al. used the number of ‘very high’ and ‘extreme’ days - the number of days where the FFDI >25. We also examined the number of days of the FFDI > 40 (as per Blanchi, Lucas et al. 2010), and FFDI > 50 (as per Bradstock and Gill 2001).

Table 1: Review of bushfire and climate studies in Australia and South Australia including methodology and data sets used.

Author/s	Date	Study locations	Historical	Future	Methodology	Data sets used	FFDI/GFDI	Outputs	Notes / Limitations
Williams, A.J. Karoly, D.J. Tapper, N.	2001	Eight GCM grids across northern and southern Australia.	√	√	Calculated changes in daily and seasonal fire weather and the McArthur FFDI using the CSIRO9 GCM to simulate current and double CO_2 climate. GCM outputs were validated using historical data at a number of point locations to compare GCM and observed daily FFDI distributions. Historical analysis used observed station data 1960-1992.	CSIRO-9 GCM forced for double CO_2	FFDI	Frequency distributions of daily fire weather and FFDI. Historical daily and seasonal fire danger and fire weather 1960-1992.	GCM outputs may underestimate extreme events in future climate. Temporal and spatial limitations of grid resolution for future climate projections. No sites in SA.
Hennessy, K.J. Lucas, C. Nicholls, N. Bathols, J. Suppiah, R. Ricketts, J.	2005	17 sites in NSW, ACT, VIC and TAS.	√	√	Fire danger indices were calculated for "present conditions" using historical weather records from 1974-2003. Two CSIRO global climate models (Mark 2 and Mark 3 downscalled to 50 km grids using the CCAM Mark 2 model) were then used to generate pojected changes in daily temperature, humidity, wind and rainfall for the years 2020 and 2050, relative to 1990. Changes were then applied to the historical data sets.	CSIRO Mark 2 GCM and CSIRO Mark 3 GCM.	FFDI	FFDI and GFDI for 2020 and 2050.	Temporal and spatial limitations of grid resolution for future climate projections. Use of historical data adjusted by GCM outputs retains observed distributions and so captures full variabiity but does not allow for shift in distribution shape. No sites in SA.
Pitman, A.J. Narisma, G.T. Mc Aneney, J.	2009	Across all Australia at a resolution of 56 km grids.		√	Assessed the impact of climate change on the risk FFDI and GFDI in Australia for January using a high resolution regional climate model (RAMS) driven at the boundaries by data from a transitory coupled climate model. Two future emission scenarios (relatively high and relatively low) were used for 2050 and 2100 and four realisations for each scenario were run.	AUSLIG data set to identify vegetation cover. CSIRO Mark 2 to force the boundaries of RAMS.	FFDI & GFDI	Probability density function for the fire risk for a single point in New South Wales for January 2050 and 2100. Mapped change in FFDI and GFDI for all Australia for January 2050 and 2100.	Analysis for January only. GCM outputs may underestimate extreme events in future climate. Change in probability distribution undertaken for one location only.
Hasson, A.E.A. Mills, G.A. Timbal, B. Walsh, K.	2009	850 hPa temperature gradient as indicator of cold front activity.		√	Analysed the 850 hPa temperature gradient from ten GCMs from the Coupled Model Intercomparison Project to estimate the frequency of cold front events at the middle and end of the 21st Century for low and high greenhouse gas emissions scenarios.	Ten GCMs from the Coupled Model Intercomparison Project.	Neither	The change in the frequency of cold fronts responsible for extreme fire weather across southern Australia.	Analysis of only one weather parameter.
Lucas, C.	2010	77 locations across southern Australia. In SA: Adelaide, Ceduna, Port Lincoln, Mt Gambier, Renmark, Snowtown, Woomera.	√		Development of a national historic fire weather data set. Calculated the FFDI for each location.	Bureau of Meteorology observing station data.	FFDI	Fire weather data set.	Development of data set only. Analysis of inhomogeneities in the data sets for temperature, rainfall, wind and humidity and impact of those on the FFDI. No analysis of the FFDI undertaken.
Douglas, G.	2011	30 locations in 21 fire regions in NSW.	√		Historical analysis of FFDI and GFDI for 16 stations across New South Wales using BOM data.	BOM station data.	FFDI & GFDI	Historical change in FFDI and GFDI.	Preliminary results only - find follow up report. No sites in SA.
Clarke, H.G. Smith, P.L. Pitman, A.J.	2011	Four 600,000 km^2 regions in eastern Aust: Central QLD; southern QLD /northern NSW; southern NSW; VIC.		√	World Climate Research Program's (WCRP) Coupled Model Intercomparison Project phase 3 (CMIP3) multimodel dataset used to calculate daily FFDI for current climate (1961 to 2000), 2050 climate (2046 to 2065) and 2100 climate (2081 to 2100). Model runs used the A2 SRES future. Models selected had the highest skill score over Australia (Perkins et al. 2007). MRI ranked fifth but was included because daily data for all variables were not available for MIROC-m, which would otherwise have been used.	CMIP3 multi-model daily archive. CSIRO, ECHO-G, IPSL and MRI.	FFDI	FFDI distributions for current, 2050 and 2100 for each study region.	East coast regions only. The CMIP3 archive includes simulations of past, present and future climate so the same data set can be used for all analysis. However, no validation was made with observed FFDI. GCM outputs can underestimate future extreme events. No sites in SA.
King, K.J. Cary, G.J. Gill, A.M. Moore, A.D.	2012	Three sites in south eastern Australia near Canberra, Sydney and Melbourne.	√	√	Assessed effect of both a changing climate and atmospheric CO_2 combinations on grass curing, fuel load, and thus GFDI and potential fire-line intensity for an A1B emissions scenario for 2030, B1 for 2070 and A1FI for 2070. Patched point historical, daily weather datasets (Jeffrey et al. 2001) were used as input for GRAZPLAN modelling. Daily weather was derived for alternative future climates by applying the 50th percentile (median) projected seasonal changes in temperature, rainfall, wind speed, relative humidity and solar radiation to each historical daily weather value (1 January 1965 to 30 April 2011) for each location. Future climate scenarios were 2030 under the A1B SRES emissions scenario with 450 ppm CO_2; 2070 under the B1 emission scenario with 518 ppm CO_2 and 2070 under the A1FI emission scenario with 707 ppm CO_2.	GRAZPLAN model to calculate grass growth and curing rates. Suite of GCM output mean changes applied to historic weather data. Projected atmospheric CO_2 concentrations from the Bern Carbon Cycle model.	GFDI	Change in grass growth rates, curing and GFDI for each location for each future climate year.	Good assessment of GFDI. FFDI not included. Future climate a current climate mean shifted by GCM output average changes for each parameter - not a single model output and so might have issues about loss of model output integrity. No sites in SA.
Lucas, C. Hennessy, K. Mills, G. Bathols, J.	2007	28 stations across south east Australia. In SA: Adelaide, Ceduna, Woomera, Mt. Gambier.	√	√	Historical data were analysed to determine trends and the current number of days when the fire danger rating exceeded high, very high, severe, extreme and catastrophic. Future climate changes used two CSIRO global climate models to calculate daily values for temperature, humidity, wind and rainfall for the years 2020 and 2050, relative to 1990. The modelled changes from the various scenarios were then projected onto the observed daily time series of temperature, rainfall, wind and relative humidity from 1973 to early 2007.	Observed historic data set from BOM stations. CSIRO CCAM Mark 2 and Mark 3 for future simulations as per Hennessy et al. 2005.	FFDI	Change in the the annual cumulative FFDI and the number of high, very high, severe, and catastrophic fire days at each location.	Point locations only. Only four sites in SA. Change factor methodology.
Clarke, H. Lucas, C. Smith, P.	2012	38 stations across Australia, most in the south east. SA stations as above.	√		Examined changes in Australian fire weather as measured by the FFDI between 1973 and 2010. No future climate change considered.	Observed historic data set described in Lucas et al 2007.	FFDI	Observed change in FFDI for each location.	Historical study only. Point locations only. Only four sites in SA.

Table 2: Review of data sets used in previous studies of bushfire in Australia and South Australia.

	Data set	Source	Spatial scale	Temporal scale	Temp	Precip.	Humidity	Wind (10 m)	VP	Strengths	Weaknesses	Notes
Climate change data	CSIRO Mark 3	CSIRO, Australia	200kms	1 hourly. Depends on storage space, download time, analysis requirements.	√	√	√	√	√	A 'hot dry' model: allows us to assess a worst case scenario.	There are GCMs in terms of ability to simulate ENSO and other key features of Australia's climate.	
	CCAM (McGregor and Dix 2008)	BOM, Australia	60kms (0.5deg).	As above	√	√	√	√	√	Good spatial resolution.	Not freely available.	Bertrand Timbal did model runs for SA.
	SILO Consistent Climate Change Scenarios. CMIP 3 Multi-model	Queensland Government	Station locations	Daily	√	√	x	x	√	Easy access to climate change scenarios that are all in a consistent form.	Change factor methodology.	ALL SRES scenarios for 2030. Patched point data locations as per SILO.
Synthetic and observed historical data	**Point datasets**											
	BoM station data	BOM, Australia	Point	n/a	√	√	√	√	√	This is observed data.	Data quality may be poor.	Check: The use of 3 pm values (cf daily mins or maxs, eg as in Hennessy et al 2005) decreases extreme FFDI by approx 20%.
	Gridded data sets											
	AWAP (Jones et al. 2009)	BOM, Australia	Gridded	Daily	√	√	x	x	√	Gridded dataset allow for greater spatial consistency. Gridded datasets aim to produce a representation of the area-average rainfall, not rainfall at individual points.	(1) The differences in the rainfall amount between the value representing a grid cell and a point location can be large, such as in complex terrain or in convective small-scale rain events. Extreme rainfall events are not well captured. Gridded datasets tend to underestimate wet events and overestimate dry events. (2) The difference in maximum temperature between grid value and point value is generally rather smaller due to the greater spatial homogeneity (and perhaps also to the less-dense observation network) of the maximum temperature observations.	Observed data is decomposed into averages and anomalies (anomalies are weakly related to topography). The averages are interpolated using 3-dimensional smoothing splines, and the anomalies are interpolated using the Barnes successive correction technique. Similar to SILO, but different algorithms.
	SILO (Jefferies et al 2001)	QCCCE	Gridded 0.01 deg.	Daily	√	√	x	x	√	As above	As above	Observed data is interpolated using kriging. The process is designed to accurately reproduce the observed data.
	Daily near-surface wind speed. (McVicar et al. 2008)	CSIRO DOI:10.4225/08/510B50F8DBB30	Gridded (from BoM point data) 0.01 deg.	Daily 1975-2012	x	x	x	√	x	Good spatial resolution of wind speed.	This is daily mean WS that will underestimate FFDI. We need daily max WS or 3 pm WS. Use Guo 2013 to convert. Or ECMWF to compare, or nearby point stations.	
	Drought Factor (Finkele et al. 2006)	BOM, Australia	Gridded 0.01 deg and 0.25 deg.	Daily (1965-2005)	x	x	x	x	x	Fine spatial resolution.	Derived from BOM NCC gridded Tmax and P (Weymouth et al 1999, Jones 1999). These are different datasets to SILO and AWAP.	
	Modelled data											
	BoM MESOLAPS forecast data (Puri et al. 1998)	BOM, Australia	0.125 deg lat/long	2000 til present. 3 hrly	0600UTC unless 0300 is greater	KBDI	√	√		Fine spatial and temporal resolution.	Only available since 2006. (2) Forecast data: less reliable than reanalysis.(3) An FFDI derived from gridded forecast field will differ to single station analysis.	BoM MESOLAPS (as per Dowdy et al 2010).Used for daily FFDI forecasts since 2006.
	ECMWF (as per Kepert et al. 2012)	United Kingdom Met. Office	Gridded 75 km.	3 hourly	√	x Keppert uses Finkele SMD/KBDI (BoM)	√	√	√	(1) Data is available every 3 hours.(2) Data is available every 75kms (3) There are many more variables available cf BoM observing stations, such as measures of atmospheric instability that have been shown to relate to fire danger.	(1) Rainfall is hard to estimate in reanalysis, therefore use other source such as BoM. (2) 75 km is relatively coarse resolution.	
	Datasets that could be used for validating other datasets											
	FFDI (derived by Lucas et al. 2010)	BOM, Australia	Point (77 BoM stations)	Daily FFDI	Daily Tmax	KBDI	3:00 PM	10 min average	x	The input data have been highly scrutinised.	There are only a few locations in SA. Despite the data being of the highest quality (relative to other data), in general the data is still not homogeneous due to the introduction of AWS in 1990s.	

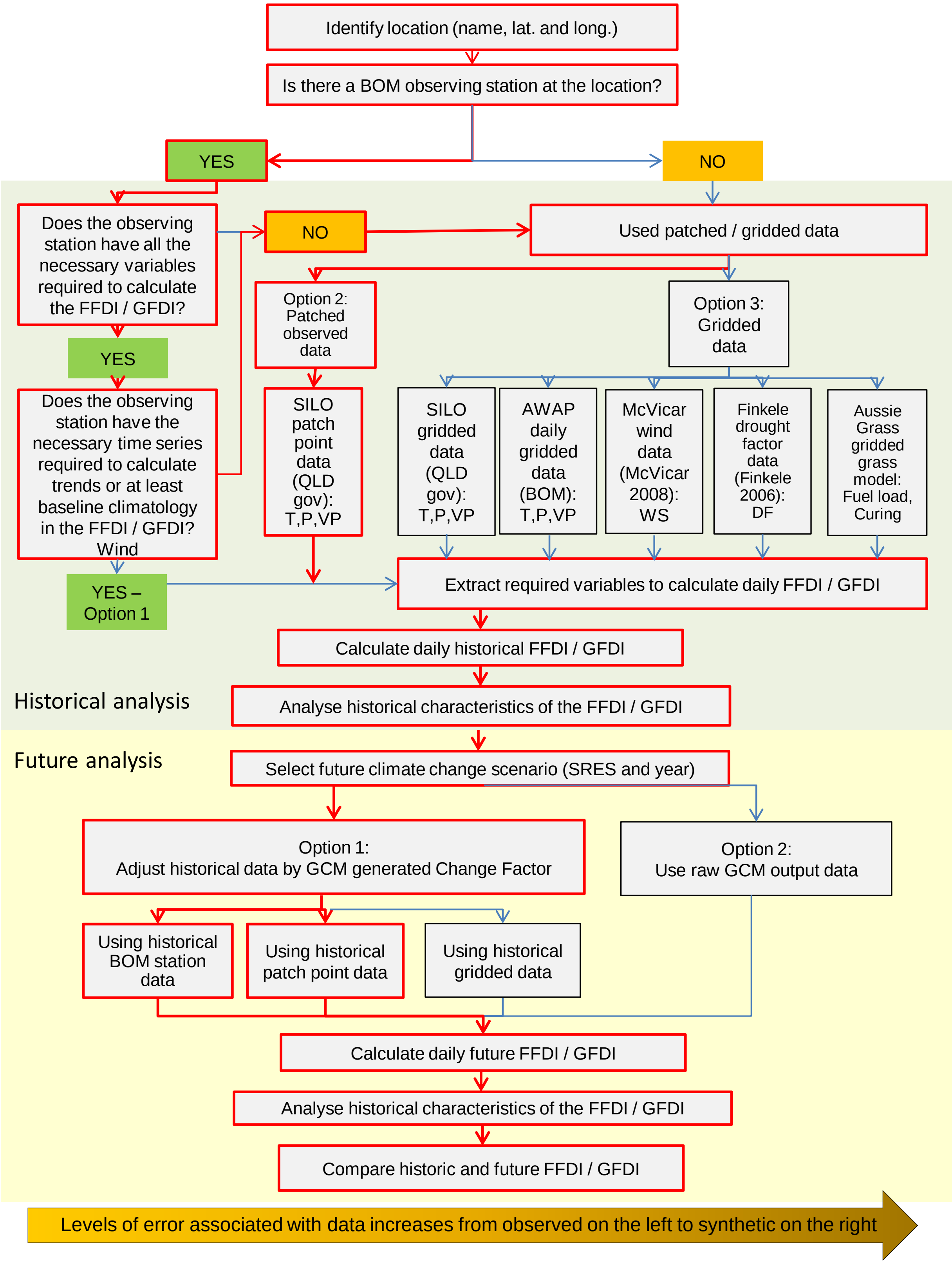

Figure 1: Flow chart of data and methodological approaches to the analysis of historical and future changes in the Forest Fire Danger Index (FFDI) and Grassland Fire Danger Index (GFDI). The pathway highlighted in red is the one taken in this study for the analysis of historic and future changes to bushfire weather at each of the pilot study areas. SRES refers to the range of greenhouse gas emissions scenarios and GCM is for global climate model (also known as General Circulation Model).

4 PILOT STUDY AREAS IN SOUTH AUSTRALIA

Input from project partners identified two study areas in which to use the methodology developed. The study areas were to be: different from those that had already been assessed and identified in the literature; provide a range of both urban and rural landscapes; and represent areas that had a high intrinsic bushfire hazard and impacts risk. The two areas selected were: Spring Gully Conservation Park in the Clare Valley; and the Mt. Bold Reservoir Reserve in the Adelaide Hills.

4.1 STUDY AREA 1 – SPRING GULLY CONSERVATION PARK IN THE CLARE VALLEY

The first of the two study areas selected for this project was the Spring Gully Conservation Park in the Clare Valley. The park is located 8 km south of Clare in the mid-north region of South Australia and extends over 400 hectares. It includes the two springs that give the park its name (Figure 2). The park conserves important habitat for wildlife and vegetation within the largely cleared and settled Clare district. It includes some of the most picturesque native landscapes in the region including, rocky sandstone outcrops, natural springs and steep sided valleys. Species of interest in the park include the red stringybark (*Eucalyptus macrorhyncha*) an abundance of native orchids, kangaroos, euros, echidnas and up to 50 species of birds.

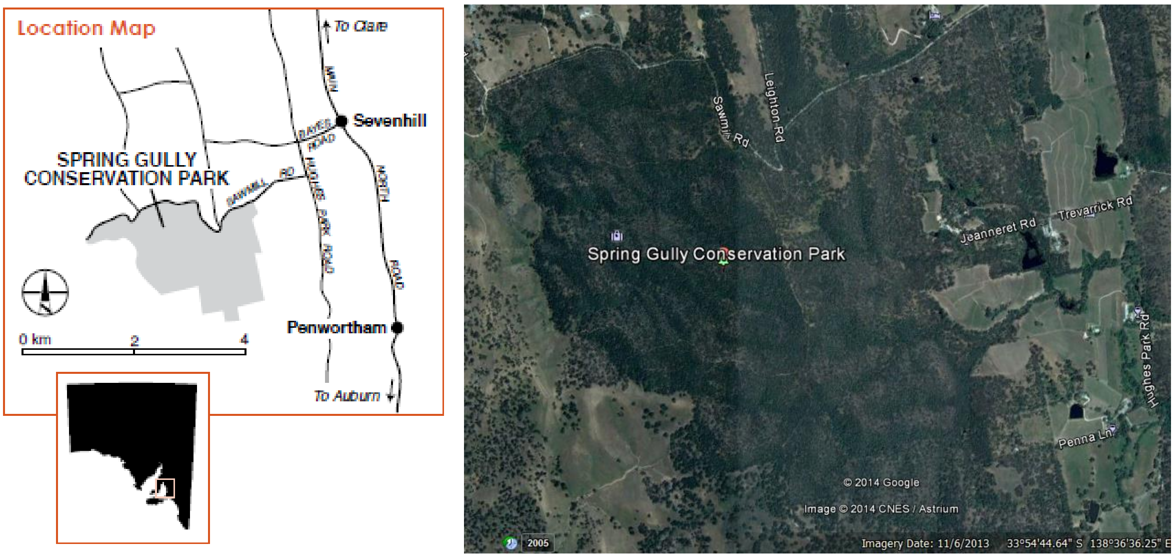

Figure 2: (left) A map showing the location of the Spring Gully Conservation Park in the Mid-North region of South Australia (Department of Environment and Natural Resources 2010); and (right) an aerial image of the region (Google Maps 2014).

4.2 STUDY AREA 2 – MT. BOLD RESERVOIR IN THE ADELAIDE HILLS

The second of the two study areas was the Mt. Bold Reservoir Reserve in the Adelaide Hills (Figure 3). The reserve is 23 km south-south-east of Adelaide Central Business District and contains the Mt. Bold Reservoir. The reservoir is the largest in South Australia and contains over 46 thousand megalitres of water supplied for agricultural and domestic uses.

The reserve is also an important conservation area for a diverse range of native fauna and flora. The dominant species is Messmate Stringbark (*Eucalyptus oblique)* with some Cup Gum (*Eucalyptus cosmophylla*) present. A vulnerable ecosystem of Pink Gum (*Eucalyptus fasciculosa*) remains in the park and there are also areas of the rare and endangered Candlebark Gum (Eucapyptus dalrympleana spp.) and Bracken Fern / Silky Tea-tree closed shrubland. In total seven rare and 27 uncommon floral species are to be found in the reserve. Fauna in the reserve includes the endangered Southern Brown Bandicoot, the Bush Rat, Yellow Footed Antichinus and Water-rat.

On 10 January 2007 a bushfire burned through the Mount Bold Valley area, and affected properties between Kangarilla and Echunga. The fire destroyed two houses, gutted over ten sheds and killed livestock and horses. Two people were injured and fencing was damaged (The Advertiser 2007). Fire also threatens water quality and so an understanding of the fire hazard for the region is important on many levels.

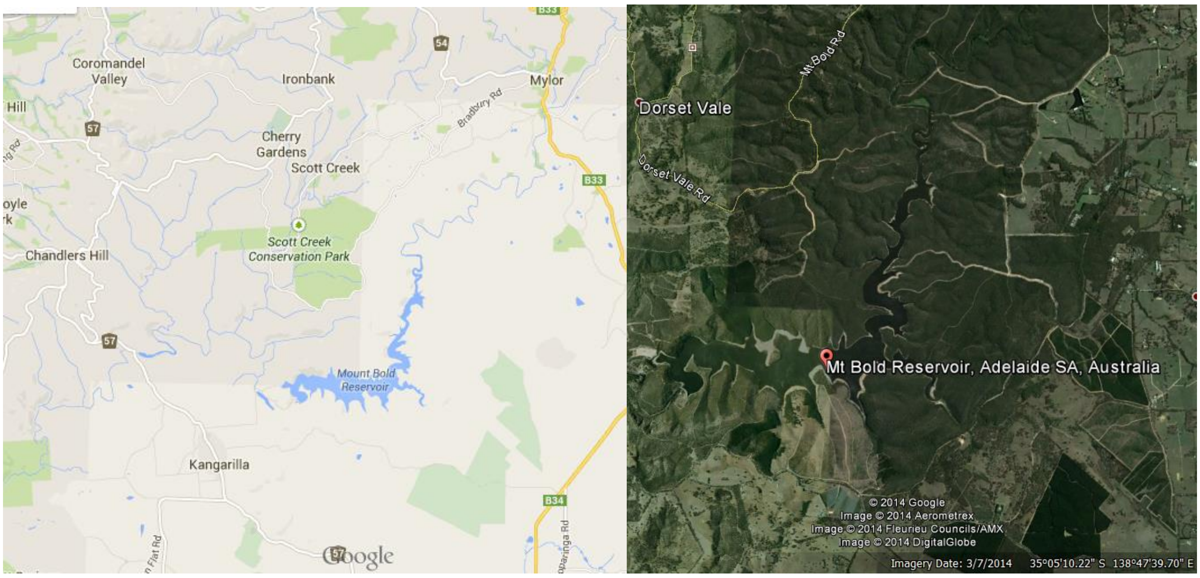

Figure 3: (left) A map showing the location of the Mt. Bold Reserve in the Adelaide Hills region of South Australia (Google Maps 2014); and (right) an aerial image of the region (Google Maps 2014).

CFS crew fight a fire at Mount Bold, January 2007 (Sourced: http://mvcfs.asn.au/latest-archive.htm)

5 ANALYSIS AND RESULTS FOR PILOT STUDY AREAS

On the basis of the methodology developed and the data sets available for the two study sites identified, an assessment of historical and future bushfire hazard was undertaken. Future bushfire risk will be dependent on changes in a range of factors including climate, land use, population, and vegetation. This study has focussed solely on a range of projected changes of fire weather variables by 2050 that were then used to assess changes in fire danger as described by the FFDI.

For the two study areas, Spring Gully Conservation Park (SGCP) and Mt Bold Reservoir (MBR) a range of metrics were used to assess the possible change to fire danger climatology that may occur with global climate change. Historical fire danger was assessed using the FFDI model with daily historical observed data. The FFDI was then calculated using daily data modified by a climate change scenarios to integrate projected changes into precipitation, temperature, relative humidity, and wind speed. The observed historical fire danger was then compared with that of the period 2046 to 2065 ("2050").

HISTORICAL ANALYSIS

On the basis of the detailed assessment of data for the historical analysis and flow chart methodology developed, we used a slightly different approach for SGCP than for MBR, described as follows. Neither of the two study areas, SGCP or MBR are in the BoM observing network and so are not in the SILO Patch Point database either. As use of observed data is preferable to gridded data where it is available we selected the nearest stations with **all** of the required data as proxy locations for SGCP and MBR. The observing stations closest to SGCP and MBR are the Clare Post Office and Kuitpo (Bureau of Meteorology site numbers: 021014 and 023887 respectively). The benefits of using the observed data from the SILO Patch Point data base have been explained (in summary in Section 3 and in detail in Appendix 2) and so we examined data availability for the Clare Post Office and Kuitpo. Clare Post Office is in the SILO Patch Point Database, however, Kuitpo is not. Therefore, for Clare Post Office we obtained historical daily maximum temperature, rainfall data and vapour pressure data from 1960 to 2010 from SILO, and for Kuitpo we obtained the data from BOM historical records from 1998-2014.

As discussed in Appendix 2, wind speed data is not available in the SILO database. As Lucas et al. 2007 identified, the poor quality of wind data in the observing station network is the primary reason why long term studies of FFDI have only been done for a very limited number of locations. Examining the BOM observing station network, the closest stations to SGCP and MBR that recorded daily wind speed (at 3pm and 10 meters height) were Clare Post Office (site number 021014) and Kuitpo (site number 023887). Years of availability (between 1960 and 2010) are 1960 to 1994 for Clare PO, and 1998 to 2010 for Kuitpo. There were some missing data and these have been in-filled using the long term median value. An analysis of the differences in wind speeds in the study area was undertaken and results provided in Appendix 3 (Figure A3.1).

FUTURE ANALYSIS

For the climate change analysis, future climate scenarios for the 30 year period 2050 were obtained from the SILO Consistent Climate Change Scenarios (CCCS) database. As per the historical data, the key variables required for the fire danger model are future projections of maximum temperature, relative humidity, rainfall, and wind speed data. Given the current trajectory of emissions we have used the A1FI scenario as the most likely, albeit worst-case, scenario.

The future climate data used in this study was obtained from the CCCS using the Change Factor methodology developed by the CSIRO (Whetton et al. 2001). The Change Factor technique changes the climatological mean of a specific climate variable from its historical value to a future value. The resolution of the final climate change scenario data is the same as the historical data set. The CCCS has utilised the OZCLIM methodology (Page and Jones 2001) to transform the 1975 to 2004 baseline climatology SILO historical daily climate data into monthly climate scenarios for the year 2050.

Three Global Climate Models (GCMs) were selected from the CMIP3 collection of climate models: MIROC-H; HADGEM1; and GFDL-21 to generate the changes to fire weather projected to occur by 2050.

RESULTS

Temperature and relative humidity were the only variables for which all three GCMs projected changes in the same direction across all months compared to the historic data. That is, an increase in temperature and a decrease in relative humidity (except for the MIROC-H projection of changes in July). The projections of monthly rainfall were also mostly consistent and showed a strong decrease in winter and spring compared to history. There was more variation between models in summer. The projections of wind speed, however, varied greatly between the GCMs, except for a consistent decrease in May wind speed. Greatest change to wind was in the winter months.

Therefore, with the exception of the uncertainty in the wind speed projections, the changes in fire weather conditions as a result of rainfall, temperature and evaporation by 2050 would suggest an increase in fire danger. This change is verified by the calculated changes in the mean annual cumulative FFDI (Figure 4), and also the change in interannual variability of annual ΣFFDI (Figure 5). As can be seen from the graphs, the fire seasons are likely to increase (as measured by higher cumulative annual and monthly FFDI) and also last longer and start earlier in the year (as measured by an increase in the higher monthly values for the FFDI in Spring and Autumn compared to the baseline climate). Note there are slight differences between the two regions.

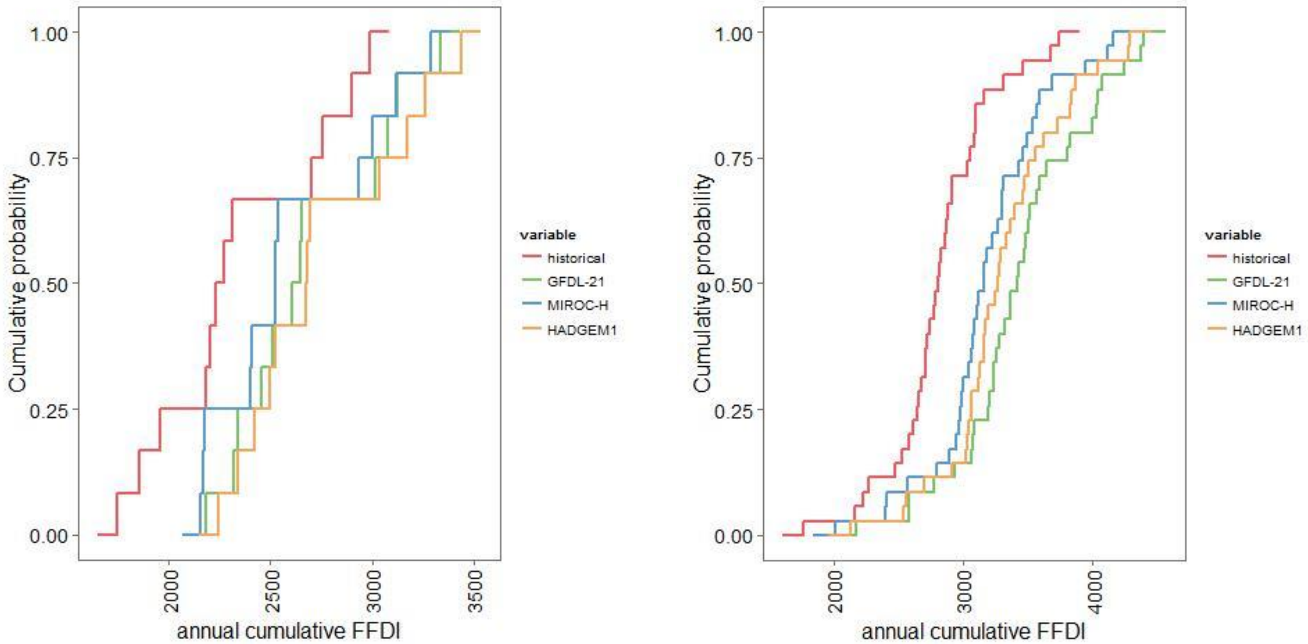

Figure 4: The cumulative probability of annual ∑FFDI for MBR (left) and SGCP (right) for the historical climate (red) and three possible future climates in 2050 as modelled by GFDL -21(green), MIROC-H (blue), and HADGEM1 (orange) using the A1FI high emissions SRES scenario.

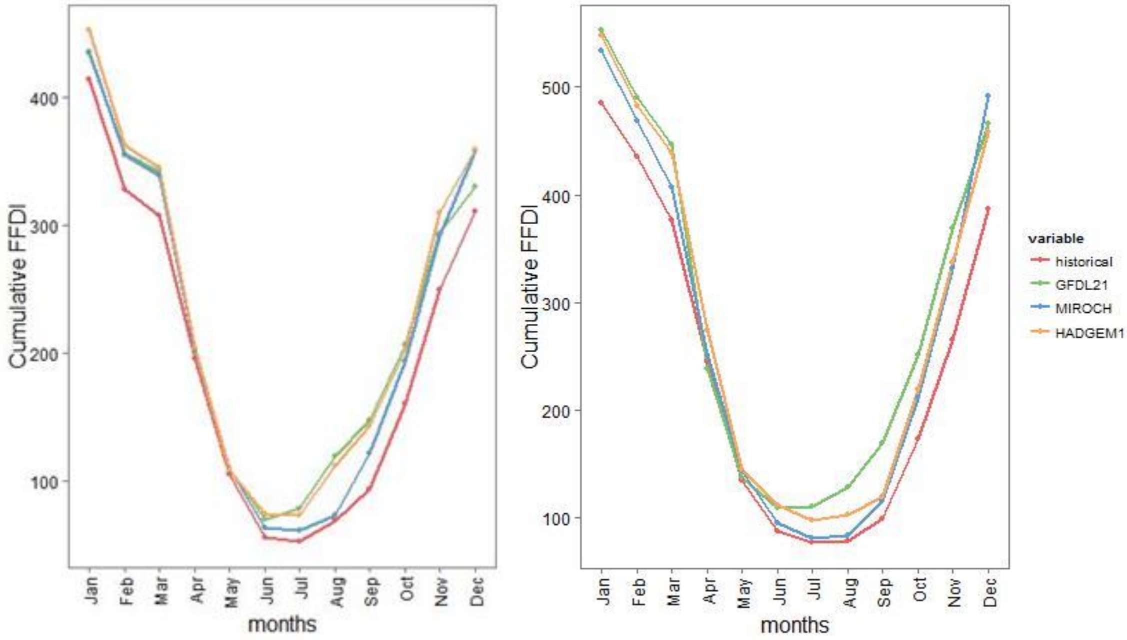

Figure 5: The cycle of mean monthly ∑FFDI for MBR (left) and SGCP (right) for the historical climate (red) and three possible future climates in 2050 as modelled by GFDL -21(green), MIROC-H (blue), and HADGEM1 (orange) using the A1FI high emissions SRES scenario. A high ∑FFDI indicates greater fire danger.

With this increase in cumulative monthly and annual FFDI, a higher number of days with a FFDI of 'very high' or 'extreme' are also expected. The number of high fire danger days and above generally increases by 50-60% (Table 3 and Table 4).

Table 3. The mean number of days where the FFDI is above a certain threshold at SGCP for the historical dataset and the three GCMS using the A1FI high emissions SRES scenario for the year 2050.

	FFDI>25	FFDI>40	FFDI>50
Historical	15.97	0.77	0.03
GFDL-21	25.34	2.26	0.09
MIROC-H	23.37	1.77	0.06
HADGEM1	24.46	2.11	0.06

Table 4. The mean number of days where the FFDI is above a certain threshold at MBR for the historical dataset and the three GCMS using the A1FI high emissions SRES scenario for the year 2050.

	FFDI>25	FFDI>40	FFDI>50
Historical	16.77	3.38	0.62
GFDL-21	19.15	4.69	1.08
MIROC-H	19.92	4.92	1.15
HADGEM1	21	5.62	1.77

These results should be placed in the context of the current climate and its tendencies.

The previous study on bushfire weather in SA by Lucas et. al. (2007) used all of the locations in the State that had long historical time series (especially for wind) and consequently was able to put future changes in an historical perspective. He concluded that during the last several years in southeast Australia, including the 2006-07 season, particularly severe fire weather conditions have been observed. In many cases, the conditions far exceed the projections in the high scenarios of 2050. Unfortunately there are not any other locations in addition to those studied by

Lucas et al (2007) that are suitable for creating a long-term historic FFDI timeseries based on observed data. This limitation is mostly because of the lack of lengthy wind speed records.

However, an alternative methodology that would provide relatively long term data would be to use the SILO gridded dataset for temperature, rainfall, and vapour pressure, and a separate gridded wind speed dataset developed by CSIRO (McVicar et. al.). This wind speed dataset was designed specifically to be integrated with SILO. Assessment of this option as part of this study indicates that the approach is possible and would be rigorous, however, there is a cost to source the data sets. In addition, the McVicar wind data set requires GIS software to extract it. However, it must be remembered that a long dataset is only required if a historical analysis to be done. It is not required for a climate change analysis.

Finally, the size and complexity of the analysis and data sets and the number of steps involved to fill gaps and prepare data sets prior to analysis did not allow us to develop a simple Excel spreadsheet tool that could be used. Instead the analysis were undertaken in a software package called “R” that is freely available on the web for those with the technical expertise to replicate the analysis. The programming code that was developed to do the FFDI computations have been provided as an output of this study.

Finally, it is important to note the following caveats with respect to these analyses:

1. We have used proxies to represent the study areas of interest. We have used Clare as a proxy for SGCP and Kuitpo for MBR which we believe are relatively robust. However, local knowledge may need to be used to further interpret these results in terms of SGCP and MBR.

2. All climate change impact modelling studies have inherent uncertainties based on the future likely emissions, how the climate responds to those emissions and the accuracies of the GCMs to model the climate. This study has utilised the SRES A1FI emissions scenario, but has not addressed uncertainty that may arise from other scenarios or uncertainties.

3. We have aimed to capture a measure of the uncertainty resulting from the use of different GCMs by undertaking the analysis for three models. However, there may be GCMs that simulate other climate projections that may increase the range of risk from future climate change than that used in this analysis.

4. The primary assumption in the CCCS and Ozclim approach is that the spatial and temporal climate variability observed over the past 30 years will be maintained. With climate change, there may be changes in the frequency of certain types of events, for example the number of days of zero rainfall.

Port Lincoln, Eyre Peninsula November 2012 (Sourced: sbs.com.au 10 Jan 2013).

6 RECOMMENDATIONS AND CONCLUSIONS

6.1 RECOMMENDATIONS

There appears to be three main avenues of work possible for future fire assessment of bushfire behaviour in South Australia:

1. Assess the impact of climate change on fire danger in other areas of the State.

   This project has developed a rigorous methodology and identified the data sets required to duplicate this analysis of bushfire risk for other regions in the State. Options for future expansion of the analysis would be to select further point locations of interest for Integrated Climate Change Vulnerability Assessments, water management or other climate change research currently underway in SA. Alternatively, the analysis could be expanded to use the gridded data sets identified to create a GIS surface of historical and or future bushfire danger across the entire State.

2. Use updated climate change assessments from the CMIP5 suite of models.

   Although the future CMIP5 climate scenarios are not significantly different to the CMIP3 scenarios in many regions, it is important to update them to enable continuity with climate change impact assessments in other sectors or areas of adaptation. This analysis could be replicated for other areas using the CSIRO Climate Futures Tool to assess a full range of possible futures with the most recent CMIP5 GCM output. The CSIRO NRMAdapt project (website) has utilised the GCMs in the CMIP5 scenarios. One of the outputs of this project is the Climate Change in Australia webpage (not yet released), and the Climate Future Tool (not yet released). The Climate Futures Tool is essentially an archive of climate data from 42 CMIP5 GCMs for four emissions scenarios at a range of spatial and temporal scales across Australia. The Climate Futures Tool provides users with a methodology to select the most appropriate GCM to represent a range of possible climate futures for their region of interest. At the time of writing this report, these results were not available. However, CSIRO expect them to be available early 2015. In any future analysis, we suggest this new data be used in the same way that we have done in this project. That is:
   a. Use the flowchart methodology developed to select relevant data;
   b. For the future scenario use change factors for each variable, perturb the historical data to create future climate dataset.
   c. Use more than one GCM and thereby capture the range of possible scenarios.

3. Include the assessment of GFDI.
   To undertake computations of the GFDI will require overcoming the limited availability of historical assessments of fuel loads and curing, and also the need to compute future fuel loads and curing. As described in this report each of these requirements can be achieved using historical data perturbed by change factors derived from CMIP3 GCMs. This information is conveniently contained in the SILO database. To undertake such a study for SA would involve validating the Aussie Grass model parameters for the State (this has been done for some locations) and then running the model using historic data to create a baseline fuel load and curing data set and then using the perturbed future climate data set for a future scenario and run the Aussie Grass model again. Staff at SARDI would be able to undertake these computations if requested. Finally, the GFDI would be calculated using the baseline historical and the future climate, fuel load and curing data and results compared.

6.2 CONCLUSIONS

Prior to this study, fire weather data including temperature, rainfall, evaporation, wind and fire danger data (FFDI and GFDI) were available in a number of formats and spatial and temporal resolutions for a range of areas across Australia. However, projections of changes to fire danger as a result of climate change had only been undertaken for four locations in SA – Adelaide, Ceduna, Mt. Gambier and Woomera. As a result, the capacity to plan for, and adapt to, future bushfire threats in regional areas of SA was limited.

The key aims of this project were to:

- Undertake a literature review of current studies to assess fire behaviour in Australia and SA;
- Assess existing fire weather and danger index data for appropriateness in SA;
- Develop a fire and climate change model / methodology to determine likely impacts of climate change on fire behaviour in SA;
- If the data supported it, analyse historical fire weather and compare it to future climate change fire weather for two pilot areas in SA;
- Develop project outputs and deliverables.

A detailed literature review of the studies that had assessed fire behaviour of relevance to SA was undertaken and is provided in Appendix 1. Key findings from the review were that bushfire weather in SA has been observed to have changed over the past 100 years: annual total rainfall has decreased although summer rainfall has increased in some areas; maximum temperatures have increased State wide; relative humidity has increased in some parts of the State and decreased in others; and wind speeds display mixed trends, increasing in some locations, decreasing in others. When included in the calculation of the historical FFDI for SA, there have been significant increases in both the annual FFDI and seasonal values – particularly in the spring and autumn. Trends were higher at the upper end of the distributions, an indication that the shape of the distribution is changing and not just the mean. In addition, at the locations across southern Australia considered, the length of the bushfire season has extended by 2.4 days per decade (Clarke, Lucas et al. 2012).

The data and methodology used in these studies was then reviewed in further detail (Appendix 2) and assessed for relevance and possible use in future SA studies. Findings from the review were collated into two summary tables (Table 1 and 2) and a simple to use methodology flow chart that supports future researchers determine the best approach when assessing historical and future bushfire danger by identifying the key methods and data sets available (Figure 2.4). A range of calculations were then developed that can be applied to the selected data so as to ensure that future studies are rigorous and comparable with those done previously.

The methodology flowchart developed was then applied to two pilot study areas: Spring Gully Conservation Park (SGCP) in the Clare region; and the Mount Bold Reserve (MBR) in the Adelaide Hills. Metrics were then calculated and plotted (Appendix 3). A lack of historical and projected grass fuel load and curing data prevented an analysis of the GFDI and so all analysis for this study focussed on the FFDI. Due to a lack of long-term historic data at each of the two locations historical trend analysis of the FFDI was not possible. However, a range of other metrics were assessed including projected changes in each of the climate parameters relevant to bushfire weather, the cumulative annual and monthly changes to the FFDI, and the number of days when the FFDI exceeded certain critical thresholds. These analyses enabled an assessment of different components of the fire danger at an annual or seasonal scale both in history and for a future projection. Importantly projected change between the observed historical data and projected future climate in both mean and interannual variability were examined. The use of more than one GCM enabled an assessment of the certainty of the results.

Results from the analysis of data indicate that for a high-emissions (A1FI) mid-century climate (2050) fire danger weather is projected to increase at each of the two pilot study areas when compared to present day values. In addition, the fire season is projected to become longer because of an earlier start and there will be more days when the FFDI is greater than 25, 40 and 50. These results concur with others from previous studies both in SA and other areas of southern Australia. It is important to note that these results may not apply across all of SA as although most regions are projected to warm in the future, projected increases in precipitation and/or relative humidity in some areas may well increase uncertainty in future fire danger projections.

GLOSSARY

ADAPTATION
Adaptations are actions taken to help communities and ecosystems moderate, cope with, or take advantage of actual or expected changes in climate conditions.

ADAPTIVE CAPACITY
Adaptive capacity is the ability of a system to adjust to climate change (including climate variability and extremes) to moderate potential damages, to take advantage of opportunities, or to cope with the consequences. The adaptive capacity of a system or society describes its ability to modify its characteristics or behaviour so as to cope better with changes in external conditions. The more adaptive a system the less vulnerable it is. Adaptive capacity is also defined as the property of a system to adjust its characteristics or behaviour to expand its coping range under existing climate variability or future climate conditions.

AR4
The IPCC Fourth Assessment Report.

BOM
Bureau of Meteorology.

CLIMATE
Climate summarises the average, range and variability of weather elements, e.g. precipitation, wind speed, air temperature, humidity, and sunshine hours (solar radiation), observed over many years (typically > 30 years) at a location or across an area (Bureau of Meteorology 2009).

CLIMATE VARIABILITY
Climate variability refers to variations in the mean state of climate on all temporal and spatial scales beyond that of individual weather events. Examples of climate variability include extended droughts, floods, and conditions that result from periodic El Niño and La Niña events.

CLIMATE CHANGE (global warming)
Climate change refers to shifts in the mean state of the climate or in its variability, persisting for an extended period (decades or longer). Contemporary climate change refers to anthropogenically driven changes in the climate as a result of changes to the composition of the atmosphere via the addition of greenhouse gases.

CRITICAL INFRASTRUCTURE
Infrastructure which, if destroyed, degraded or rendered unavailable for an extended period, will impact on social or economic well-being or affect national security or defence.

CSIRO
Commonwealth Scientific and Industrial Research Organisation.

EMERGENCY MANAGEMENT
A range of measures to manage risks to communities and the environment. It involves the development and maintenance of arrangements to prevent or mitigate, prepare for, respond to, and recover from emergencies and disasters in both peace and war.

EMERGENCY RISK MANAGEMENT
A systematic process that produces a range of measures that contribute to the well-being of communities and the environment. The process considers the likely impacts of hazardous events and the treatment measures by which they can be reduced.

FFDI
Forest Fire Danger Index.

GCM
Global Climate model.

GIS
Global Information Systems.

HAZARD
A potential or existing condition that may cause harm to people or damage to property or the environment.

IPCC
Intergovernmental Panel on Climate Change

ISO
International Standards Organisation

IVA
Integrated climate change vulnerability assessment

LGAs
Local Government Areas.

LGASAs
Local Government Association of South Australia.

NRM
Natural Resource Management

OZCLIM
A climate change scenario generator developed by CSIRO.

PREPAREDNESS
Action designed to minimise loss of life and damage, and to organise and facilitate timely and effective response and recovery actions. Preparedness is concerned with understanding the threat; forecasting and warning; educating and training officials and the public; and establishing organisations for the management of disaster situations including preparation of operational plans, training relief groups, stockpiling supplies, and earmarking necessary funds.

PREVENTION
In relation to an emergency includes the identification of hazards, the assessment of threats to life and property, and the taking of measures to reduce or eliminate potential loss to life or property and protect economic development. Measures taken to eliminate or reduce the incidence or severity of emergencies

RISK
Risk is the product of consequences and likelihood - what can happen, and what are the odds of it happening. Both of these factors are important in determining whether and how we address specific risks.

RISK ANALYSIS
A systematic use of available information to determine how often specified events may occur and the magnitude of their likely consequences on a community. In emergency risk management, risk analysis is the systematic use of available information to study risk.

RISK ASSESSMENT
The process used to determine risk management priorities by evaluating and comparing the level of risk against predetermined standards, target risk levels or other criteria.

RISK EVALUATION
The process in which judgments are made on the tolerability of the risk on the basis of risk analysis and taking into account factors such as socioeconomic and environmental aspects.

RISK MANAGEMENT
The systematic application of management policies, procedures and practices to the task of identifying, analysing, evaluating, treating and monitoring risk.

SA
South Australia.

SAFECOM
South Australia Fire and Emergency Services Commission

SEMC
State Emergency Management Committee

SRES
Special Report on Emissions Scenarios.

UNCERTAINTY
Uncertainties can be classified in several different ways according to their origin. Two primary types are 'value uncertainties' and 'structural uncertainties'. Value uncertainties arise from the incomplete determination of particular values or results, for example, when data are inaccurate or not fully representative of the phenomenon of interest. Structural uncertainties arise from an incomplete understanding of the processes that control particular values or results, for example, when the conceptual framework or model used for analysis does not include all the relevant processes or relationships. Value uncertainties are generally estimated using statistical techniques and expressed probabilistically. Structural uncertainties are generally described by giving the authors' collective judgment of their confidence in the correctness of a result. In both cases, estimating uncertainties is intrinsically about describing the limits to knowledge and for this reason involves expert judgment about the state of that knowledge (IPCC 2007).

WEATHER
Weather describes atmospheric conditions at a particular place in terms of air temperature, precipitation, wind speed, pressure, and humidity.

APPENDIX 1: CLIMATE CHANGE AND BUSHFIRE – A REVIEW OF THE LITERATURE OF RELEVANCE TO SOUTH AUSTRALIA

A1.1 BUSHFIRE IN THE AUSTRALIAN LANDSCAPE

Bushfire is a natural part of the Australian environment that has shaped the biota of the continent over many millennia. Australia today is considered to be the most bushfire prone of all continents (Bradstock 2010). However, even prior to the arrival of humans, Australia was subject to regular and extensive bushfires as is evident in the diverse range of floral and faunal responses to fire that have evolved since the Eocene. Cooler and drier conditions 40-25 million years before present caused a shift to fire prone biomes and sclerophylls (eucalyptus). Then a probable intensification of the El Nino Southern Oscillation 130,000 years ago intensified the trend to even more frequent fires (Williams, Bradstock et al. 2009).

Fire stick farming by the Aboriginal peoples on their arrival to the continent 50,000 to 46,000 years before present, and possible changes to the monsoon, again increased the proportion of fire adapted vegetation in the landscape and altered the fauna (Williams, Bradstock et al. 2009). As a result of this environment the native vegetation of Australia is well adapted to fire and many species are able to regrow either vegetatively after a fire from protected buds (above or below ground), or from seeds stored in protective woody fruits in the canopy seed bank (serotiny), or exhibit fire stimulated flowering, and heat and smoke stimulated germination of soil-stored seeds (Williams, Bradstock et al. 2009).

The relationship between climate, vegetation and fire vary across the continent. For example, in southern, forested regions the rainfall is higher and drought is associated with the major fires. In arid, central Australia, it is above average rainfall that leads to burning of very large areas. This variation is because fire in arid climate woodland communities is limited by biomass (fuel) growth, whereas in wet climates where forests dominate, fires are driven by fuel moisture (availability to burn) and fire weather (Bradstock 2010).

Currently, around 5% of the Australian land surface burns annually, a process that consumes approximately 10% of the net primary productivity of the continent (Pittock 2003).

A1.2 CURRENT BUSHFIRE FORECASTING IN AUSTRALIA

To understand the drivers of bushfire and recent changes that have been obvserved in fire frequency and behaviour, there has been a large investment in bushfire research since the turn of the century. Some studies have examined the many drivers of bushfire events and others have focussed on the weather and climate conditions within which bushfires are most damaging.

In 2010, Bradstock developed a framework within which bushfire in the Australian landscape can be considered. The author identified that the incidence of bushfire is controlled by four switches: biomass (fuel) production; the dryness of the fuel; occurrence of suitable fire weather; and a source of ignition. Each of these switches must be “on” for a bushfire to occur (Bradstock 2010). Weather parameters that intensify potential bushfires are high maximum temperatures, strong winds and low relative humidity.

“Fire danger indices are used in many parts of the world to integrate meteorological and fuel information into a single or small number of measures. These measures can then be applied to regions for the issuing of warnings, or more locally to estimate the suppression difficulty of a single fire or fire complex. In Australia the McArthur Forest Fire Danger Index (FFDI) (McArthur 1967) is widely used to forecast the influence of weather on fire behaviour, and the Australian Bureau of Meteorology routinely issues forecasts of Grassland and Forest Fire Danger Index (GFDI and FFDI) for use by fire authorities” (Dowdy, Mills et al. 2009).

THE FOREST FIRE DANGER INDEX (FFDI)

The McArthur Forest Fire Danger Index Mark 5 (FFDI) was developed by McArthur in 1967 and was derived from approximately 400 experimental forest fires in south-eastern Australia, and conducted in a variety of fuels in low to medium quality dry sclerophyll forests with a fuel loading of 12 t/ha,. Fire danger is indicative of the chances of a fire starting, its rate of spread, intensity and difficulty of suppression.

The index is calculated from daily maximum temperature, daily minimum relative humidity, daily mean wind speed, and a drought factor that is based upon daily precipitation (McArthur 1967). The model was converted to algorithms by Noble in 1980 to allow for computer calculation of the index (Noble, Barry et al. 1980).

$$\text{FFDI} = 1.275D^{0.987} \times [\exp(0.0338T - 0.0345H)] \times \exp[0.0234V]$$

Where: T = maximum daily air temperature ^{o}C;
V = daily mean wind speed km/hr in the open at 10 m height;
H = daily minimum relative humidity %, and D is a drought factor.

$$\text{D} = [0.191(I + 104)(N + 1)^{1.5}] / [3.52(N + 1)^{1.5} + R - 1)]$$

where I = Keetch Byram Drought Index, a number between 0 and 10 (Keetch and Byram 1968), R = precipitation, N = days since rain.

Griffiths (1999) modified the original Drought Factor described above so it would better capture recent daily rainfall. As with the previous drought factor it is dimensionless, and ranges between 0 and 10 and was calculated using the Keetch–Byram Drought Index (KBDI; Keetch and Byram 1968), following (Griffiths 1999), as:

$$DF = 10.5 \times (1\text{- } \exp(-(\text{KBDI}/30)/40)) \;\; \times (41\text{X}^2 + \text{X})/40\text{X}^2 + \text{X} + 1)$$

Where: X expresses the influence on the drought factor of past rainfall. X is defined as:

$$X = \text{N}^{1.3} / \text{N}^{1.3} + \text{p} - 2\text{) for } N \geq 1 \text{ and } p > 2$$
$$X = 0.8^{1.3} / 0.8^{1.3}\text{)p} - 2\text{) for } N = 0 \text{ and } p > 2$$
$$X = 1 \text{ for } p \leq 2$$

Where: p is the sum of rainfall within the last rain event; and
N is the number of days since the day with the largest daily rainfall amount within the rain event. A rainfall event is defined as a set of consecutive days, each with rainfall above 2 mm, within the last 20 days.

Note that although the Griffiths DF is used operationally by most fire authorities, it is not always used in climatological studies, especially climate change studies. This is due to the lack of daily resolution in climate change studies that use a change factor methodology that does not change the frequency of dry days.

The Mount Soil Dryness Index (Mount 1972) is a possible alternative to KBDI. While it is used operationally in South Australia, it is not commonly used for climatological studies. Instead, the soil moisture deficit index (i.e. the KBDI) is used across a range of climate regions to enable comparison of FFDI values.

For operational fire management and response fuel loads are monitored by authorities and involve a complex process that may take into account: a range of fuel types including size, quantity, and arrangement; and ideally the topographic aspect and slope of the landscape.

Overall fuel hazard is calculated as the sum of bark hazard, elevated fuel hazard and surface fine fuel hazard. Elevated fuels include those up to 2 m, near surface fuels include suspended litter and low shrubs, and surface fuels include leaves, bark, twigs and grassy fuels at the surface (Department of Environment and Natural Resources 2012).

THE GRASSFIRE FIRE DANGER INDEX (GFDI)

The Grassland Fire Danger Index (FFDI) was also developed by McArthur (1973), and is usually used as described by the Australian Bureau of Meteorology for operational purposes (Noble, Barry et al. 1980):

$$\mathrm{GFDI} = 2.0 \times \exp(-23.6 + 5.0 \times \ln(curing) + 0.0281 \times T - 0.226 \times \sqrt{RH} + 0.663 \times \sqrt{u})$$

Where: *curing* is the proportion of dead aboveground grass material (%);
T is the temperature at 1500 hours (8C);
RH is relative humidity at 1500 hours (%); and
u is wind speed at 1500 hours (km/h).

Daily potential fire-line intensity (kW/m) was calculated according to Byram (1959):

$$\mathrm{Intensity} = H \times w \times r$$

Where: *H* is the heat yield and often included at a value of 16150 kJ /kg, representing the average of values for a range of grassland types (Cheney and Sullivan 1997);
w is the fuel load (kg/m^2) (total aboveground herbage mass); and
r is the forward rate of spread in undisturbed grasslands (m/s), that is calculated from curing, wind speed and dead fuel moisture content using the equations of Cheney, Gould et al. (1998) for undisturbed pastures (King, Cary et al. 2012).

The monitoring of curing rates for the GFDI is undertaken at the local level by fire authorities in each state.

OTHER FIRE DANGER INDICES

Use of the Canadian Forest Fire Weather Index (FWI) in Australia was assessed by Dowdey, Mills et al. (2009). The study investigated the spatial and temporal differences between the FWI and the FFDI for Australian conditions using eight years of gridded data across the continent. The authors found that “the indices are found to be similar to each other on a broad scale in that they are both most sensitive to wind speed, then secondly to relative humidity and thirdly to temperature. On a finer scale, derivatives of the indices show that the McArthur Forest Fire Danger Index is relatively more sensitive to temperature and relative humidity, and less sensitive to wind speed and rainfall, than the Canadian Fire Weather Index”. The FWI is not typically used in Australia and so is not included in this study.

FIRE DANGER RATING SCALE

The fire danger rating scale was introduced by Lucas et al (2007). The original scale have five levels: low, moderate, high, very high and severe, However, in the wake of the February 2009 Black Saturday fires in Victoria, and the extreme fire danger weather recorded during the event, the fire danger rating scale was changed in October 2010 to include two additional levels: extreme and catastrophic (Bureau of Meteorology 2014a).

In Australia, fire agencies are responsible for calculating the fire danger ratings based on the FFDI and the GFDI. Because of local differences, there are some variations in the cut off levels of each index for each fire danger rating level. The Bureau of Meteorology issues fire weather warnings when weather conditions are conducive to the spread of dangerous bushfires. Warnings are generally issued within 24 hours of the potential onset of hazardous conditions and are broadcast on radio and television. In most States and Territories it is the fire agencies that declare fire bans. However, in South Australia, Northern Territory, Victoria, New South Wales and Tasmania, the Bureau does issue Total Fire Ban Advices to assist publicising and distributing the message (Bureau of Meteorology 2014a). The fire danger ratings, scales and advice for South Australia are shown in Table A1.1.

Table A1.1: Categories and advice for the South Australian Fire Danger Ratings (CFS 2014; CFS 2014). Fire intensity and maximum flame height were provided by Mike Wouters, Fire Ecologist, South Australian Department of Environment, Water and Natural Resources.

Fire Danger Rating	FFDI / GFDI Range	Fire Intensity (kW/m)	Maximum Flame Height (m)	Advice
Low - Moderate	0-11 / 0-11	0-3000	6.0	If a fire starts, it is likely to be controlled in these conditions and homes can provide safety. Be aware of how fires can start and reduce the risk.
High	12-24 / 12-24	3000-7000	15.0	As above.
Very High	25-49 / 25-49	>7000	>15	As above.
Severe	50-74 / 50-99			These are hot, dry and possibly windy conditions for a bush or grass fire. If a fire starts and takes hold, it will be hard for fire fighters to bring under control. Well prepared homes that are actively defended can provide safety.
Extreme	75-99 / 100-149			These are very hot, dry and windy conditions for a bush or grass fire. If a fire starts and takes hold, it will be unpredictable, move very fast and very difficult for fire fighters to bring under control. Spot fires will start and move quickly. Embers may come from many directions. Homes that are prepared to the highest level, have been constructed to bushfire protection levels and are actively defended **may** provide safety. The safest place to be is away from bushfire prone areas.
Catastrophic (Code Red)	>100 / >150			These are the worst conditions for a bush or grass fire. If a fire starts and takes hold, it will be extremely difficult to control and will take significant fire fighting resources and cooler conditions to bring it under control. Spot fires will start well ahead of the main fire and cause rapid spread of the fire. Embers will come from many directions. Homes are not designed or constructed to withstand fires in these conditions. The safest place to be is away from bushfire prone areas.

A1.3 GLOBAL WARMING IMPACTS ON SA CLIMATE

Each of the climate variables that influences fire behaviour has been, and will continue to be, affected by global warming. Between 1750 and 2011 human activity released 375 billion tonnes of carbon dioxide into the atmosphere as a result of fossil fuel burning (coal, oil, gas) and cement production and another 180 billion tonnes as a result of land clearing (IPCC 2013).

The future impact of continued increases in greenhouse gasses on the climate is calculated using Global Climate Models (GCMs). GCMs take into account changes in solar radiation from the sun, volcanic eruptions and the presence of other particulates in the atmosphere as well as changes in greenhouse gases and aerosols. Model outputs have been tested for accuracy against historical data, and calculations of future climates take into account what the future emissions of greenhouse gases will be, how much aerosols and clouds will influence future temperatures (Sherwood 2011), and how sensitive the climate is to the extra warming.

This carbon dioxide is of a unique isotope that can only be attributed to the burning of carbonate fuels and so is not from other sources such as volcanoes. Over the same period the levels of oxygen in the atmosphere have declined as would be expected when carbon burns to form carbon dioxide (CO_2). The concentration of CO_2 in the atmosphere at the end of August 2014 was 397 ppm (CO_2 Now.org 2014). Other greenhouse gases including methane and nitrous oxide have also been released as part of industrial processes (Figure A1.1).

An increase in greenhouse gas concentrations warms the earth as the atmosphere has an enhanced capacity to prevent heat from escaping back into space. As a result of these emissions, the extent of ice, acidity of the oceans, and climate systems on Earth have changed over the past century. This phenomenon has been measured and continues to be monitored at a global scale using a range of instruments and proxies.

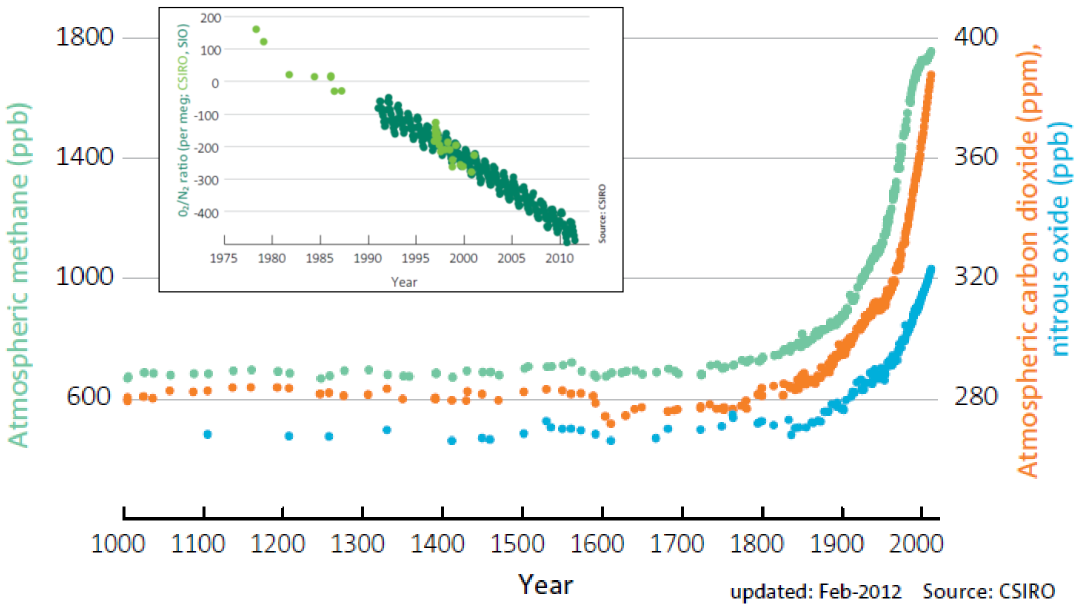

Figure A1.1: Change in the concentration of greenhouse gasses in the atmosphere including carbon dioxide (CO_2 - red), nitrous oxide (NO_2 - blue), and methane (CH_4 – green), between the years 1000 and 2012 (CSIRO and BoM 2012). The smaller inset graph shows the corresponding decline in atmospheric oxygen levels (1975 – 2010).

A1.4 FUTURE GREENHOUSE GAS EMISSION SCENARIOS

To determine what the likely changes to future bushfire danger will be we need to know how the climate is likely to change into the future. However, because we don't know how many tonnes of greenhouse gases are yet to be emitted by human activities, the future climate is unknown and so a range of different possible emissions scenarios and climates are calculated. In the IPCC Fourth Assessment Report (AR4) in 2007, climate projections made by global climate models were based on future emissions scenarios in the Special Report on Emissions Scenarios (SRES) used in previous assessments (Figure A1.2). In the IPCC Fifth Assessment Report (AR5), new emissions scenarios known as “Representative Concentration Pathways” (Figure A1.2 bottom) used instead (Moss, Edmonds et al. 2010).

The four concentration pathways represent the full range of greenhouse gas emission concentrations that may occur in the atmosphere by the year 2100 and range from 450 ppm up to 1300 ppm CO_2 equivalents (CO_2e). A CO_2e is a measure of the warming capacity of all of the greenhouse gas emissions including carbon dioxide, methane, nitrous oxide and others. The scenarios are named according to the level of radiative forcing in W/m^2 by the year 2100. For example, RCP 8.5 represents the emissions pathway that will result in 8.5 W/m^2 by the year 2100. Figure A1.2 compares the two scenarios out to the year 2100.

The two sets of future climate scenarios align somewhat. The highest RCP 8.5 (1465 ppm CO_2e by 2100) in the new set of scenarios corresponds closely to the SRES A1FI emissions scenario (1360 ppm by 2100). This scenario sees greenhouse gas emissions continue to rise beyond the end of the century. The mid-low RCP 4.5 (600 ppm by 2100) corresponds most closely to SRES B1 (640 ppm by 2100). As is the case with the RCP 6.0, these two mid-range scenarios describe a stabilisation of greenhouse gas emissions not long after 2100. The lowest RCP 2.6 projects a future where emissions are significantly lower than even the lowest SRES scenario, as although CO_2e concentrations in the atmosphere rise to nearly 500 ppm, they then fall to 450 ppm by the end of the century.

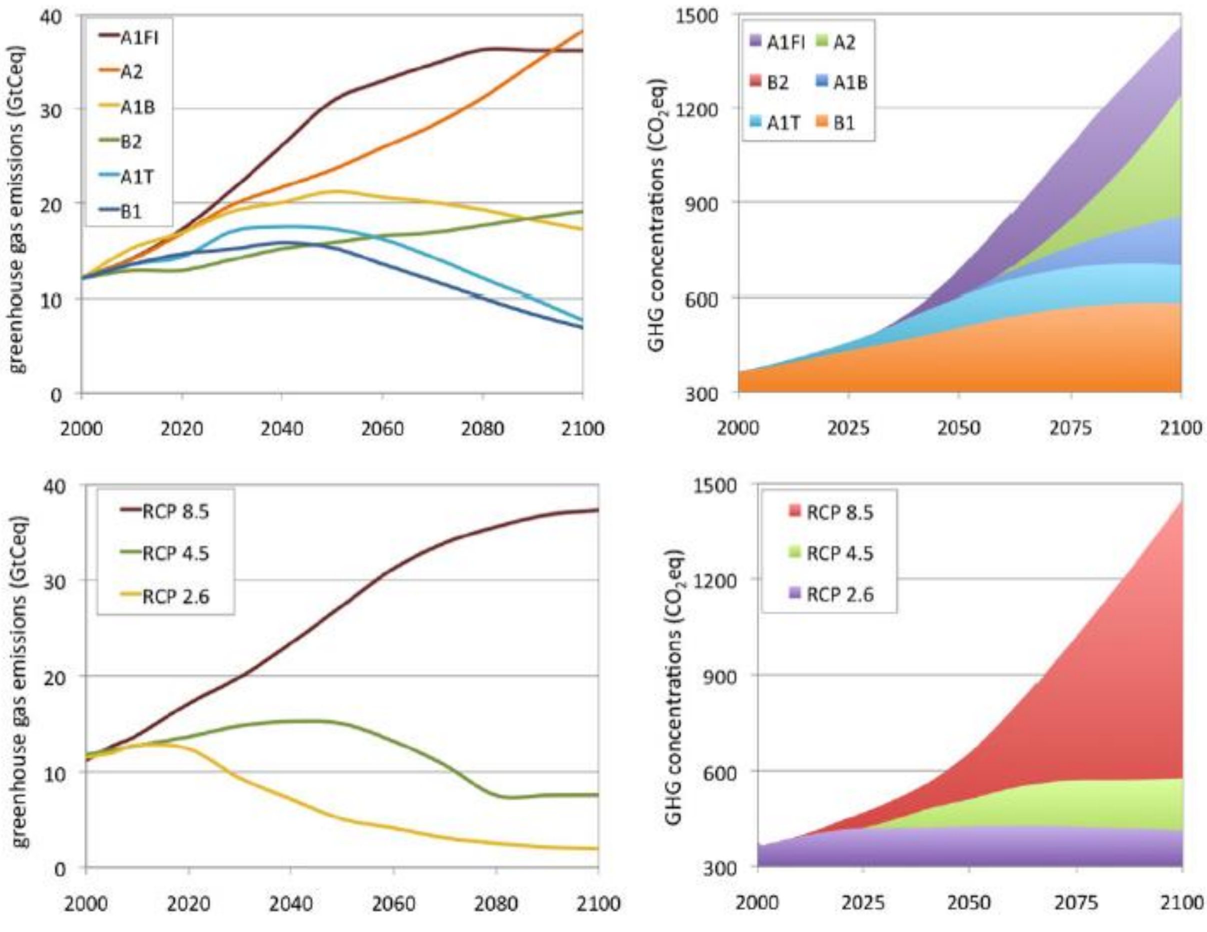

Figure A1.2: (Top) IPCC AR4 future climate scenarios expressed as greenhouse gas emissions in gigatonnes of CO_2 equivalents (left) and total greenhouse gas concentrations in the atmosphere in parts per million out to 2100 (right). The two plots at the bottom of the figure show the AR5 representative concentration pathways (Source: Moss, Edmonds et al. 2010).

A1.5 OBSERVED AND EXPECTED FUTURE CHANGES TO BUSHFIRE WEATHER IN SA

As is the case in Australia, all of the climate and weather systems that affect South Australia are driven by differences in temperature at the surface of the earth and higher altitudes and so have been, and will continue to be, affected by global warming.

TEMPERATURE

South Australia has what is described as a Mediterranean climate with hot, dry summers and cool, wet winters. In the north of the State the climate is hotter and dryer whilst in the south it tends to be cooler and wetter. Mean annual temperature ranges from 18 ^{o}C to 6^{o}C (Figure A1.3).

In response to the increase in greenhouse gas concentrations, the mean temperature across South Australia has increased by 0.8^{o}C to 1.2^{o}C between 1970 and 2011(Bureau of Meteorology 2014b) (Figure A1.4).

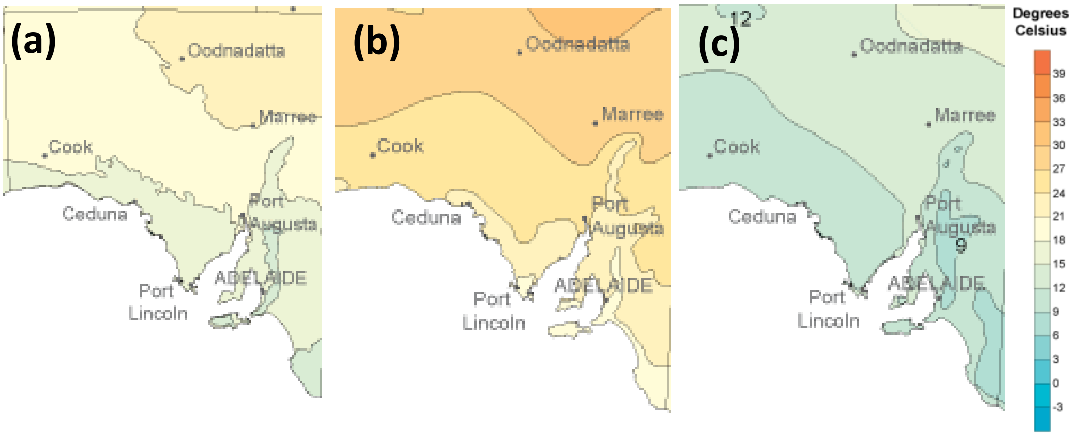

Figure A1.3: Mean temperature for South Australia: (a) Annual mean; (b) Annual maximum; and (c) Annual minimum. Values are based on the standard 30 year period from 1961-1990 (Source: Bureau of Meteorology 2013).

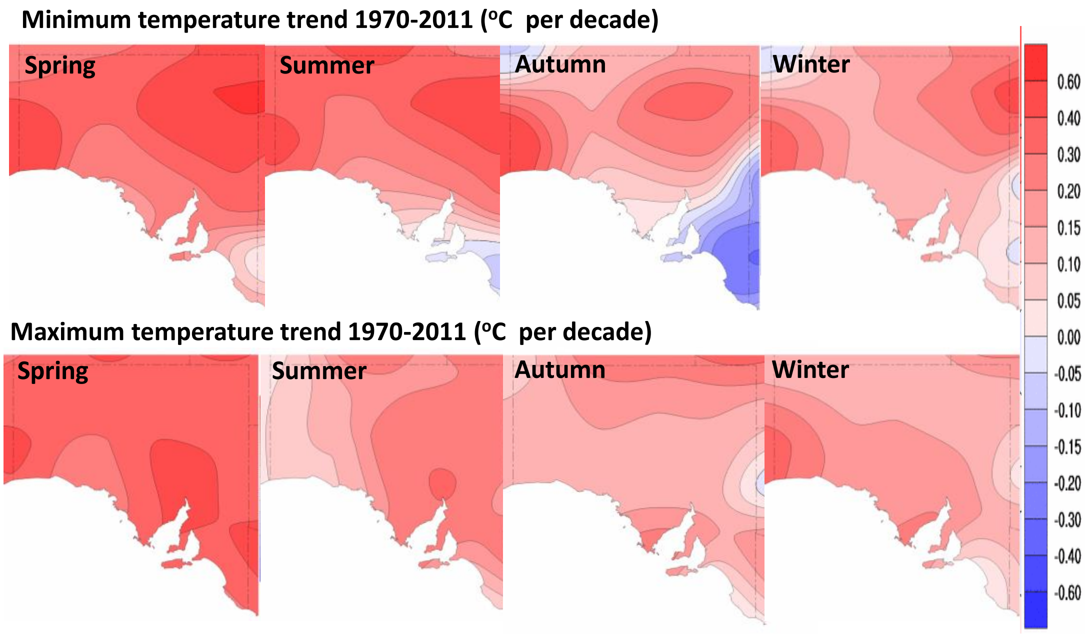

Figure A1.4: Observed change in seasonal minimum (top) and maximum (bottom) temperatures across South Australia between 1970 and 2011 in ^{o}C per decade (Source: Bureau of Meteorology 2013).

Projections of future warming for South Australia have been undertaken by the CSIRO and Bureau of Meteorology (2007). As a whole, the average annual temperature is expected to further increase by between 0.6°C and 2.0°C by 2030 and 1.0°C and 5°C by 2070 compared to average temperature from 1980 to 1999 – a period known as the 1990 baseline (Figure A1.5). This warming is expected be greater inland and less along the coast.

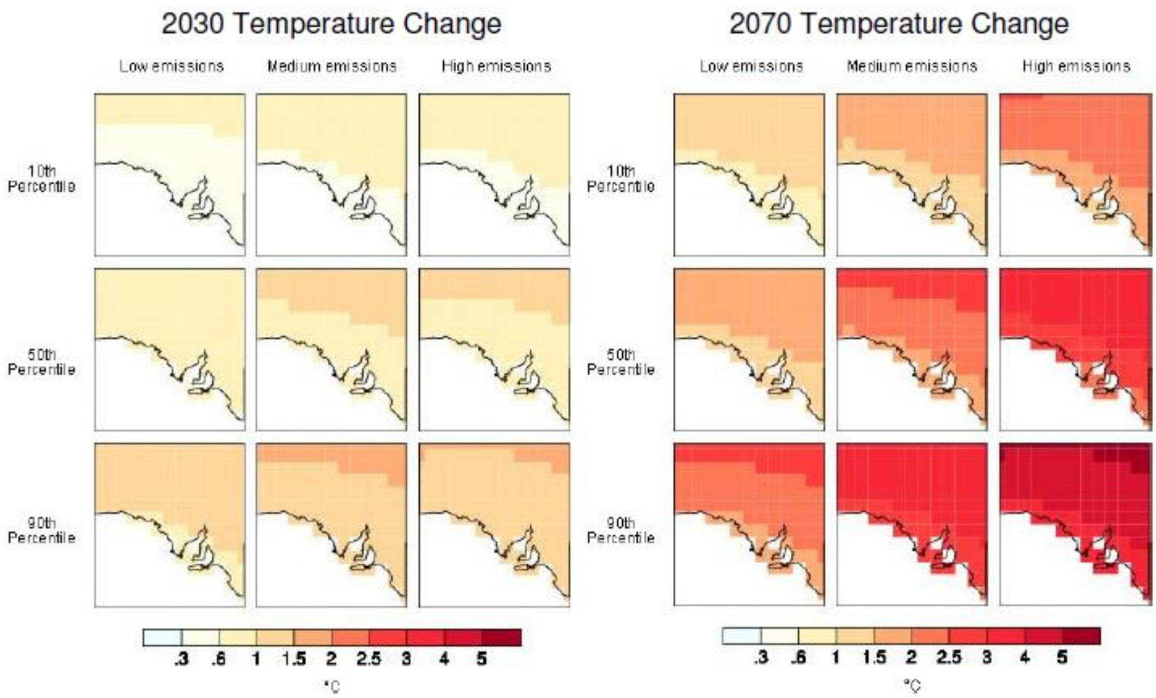

Figure A1.5: Expected range of changes to annual temperature (°C) for South Australia as predicted by a suite of Global Climate Models under low medium and high greenhouse gas emissions scenarios for the year 2030 (left) and 2070 (right) compared to the 1990 baseline (1980-1999 average) (Source: CSIRO and BoM 2007). The median expected change across all models is shown in the 50th percentile row and shows a likely increase in temperature. Current and business as usual emissions are high.

RAINFALL

South Australian rainfall is variable on annual and decadal time frames as a result of influences from a number of global and regional climate systems. Mean annual rainfall ranges from less than 10 mm/year in the north to up to 400 mm/year in the south (Figure A1.6, Figure A1.7).

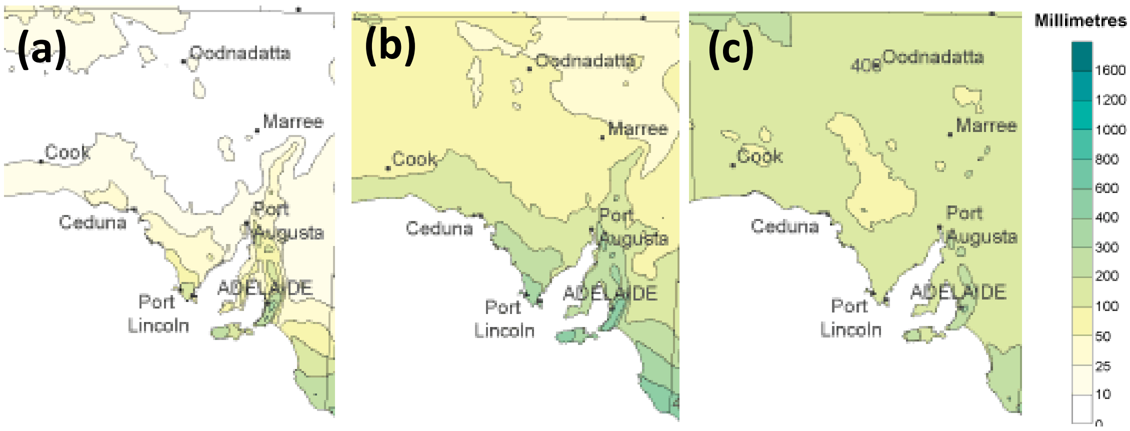

Figure A1.6: Mean rainfall for South Australia: (a) Annual; (b) May – September; and (c) October to April. Values are based on the standard 30 year period from 1961-1990 (Source: Bureau of Meteorology 2013).

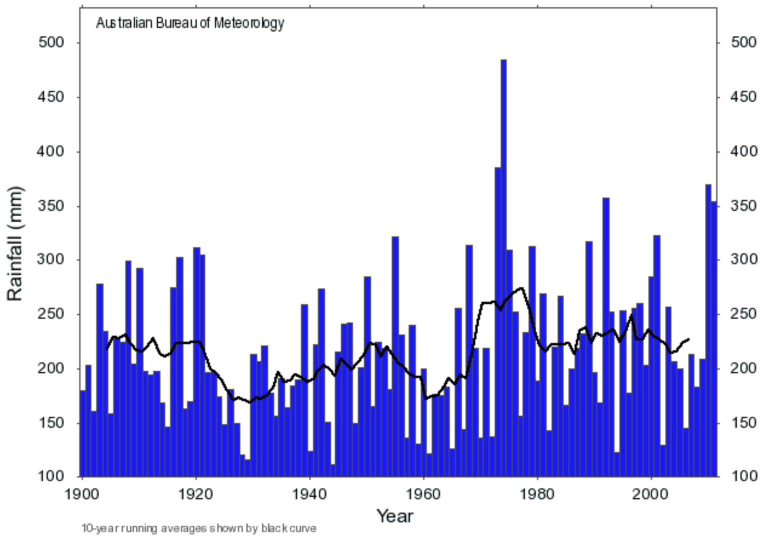

Figure A1.7: Total annual rainfall for South Australia from 1900 – 2011 (mm per decade) (Bureau of Meteorology 2014b). The black line shows the 10 year running mean rainfall for the state. Note the high interannual variability in rainfall in SA.

Records show that rainfall across the State has decreased since 1900, most notably in the second half of the century (Suppiah, Preston et al. 2006). Annual rainfall since 1970 has decreased by 10 – 40 mm/decade – most dramatically across the north-east of the state (Figure A1.8). It should be noted that rainfall in the 1970s was relatively high compared to other decades.

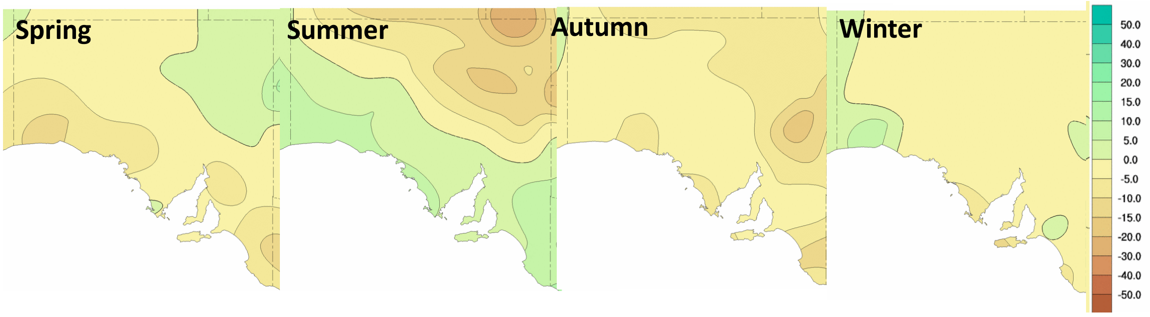

Figure A1.8: Total seasonal rainfall trend for South Australia from 1970 – 2011 (mm per decade) (Bureau of Meteorology 2014b).

As for temperature, projections for future rainfall have been undertaken by CSIRO for South Australia (Suppiah, Preston et al. 2006). Because of the complexity of the climate system and number of climate systems that bring rain to the State, projected changes in annual rainfall for South Australia are more difficult to model than changes in temperature. By 2030, annual average rainfall is expected to change by between -20% and +10% and by 2070 by –60% and +20% compared to 1990 levels (CSIRO and BoM 2007) (Figure A1.9).

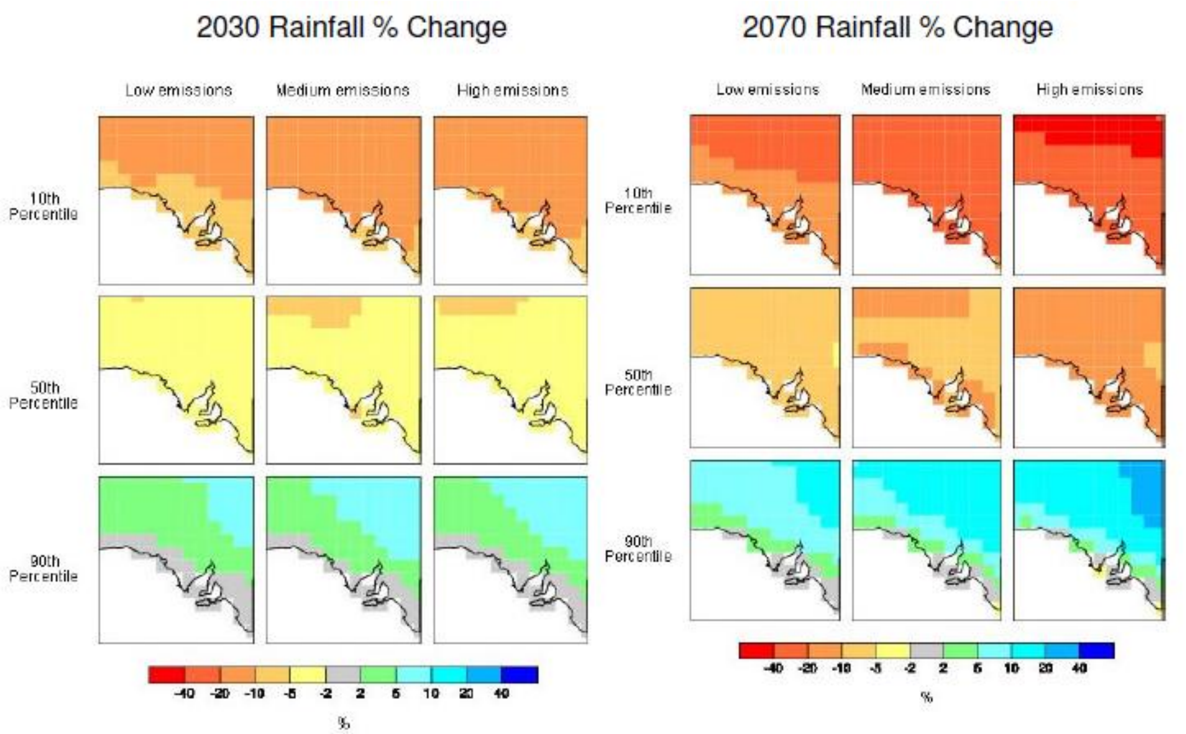

Figure A1.9: Expected range of changes to annual rainfall (%) for South Australia as predicted by a suite of Global Climate Models under low medium and high greenhouse gas emissions scenarios for the year 2030 (left) and 2070 (right) compared to the 1990 baseline (1980-1999) (Source: CSIRO and BoM 2007). The median expected change across all models is shown in the 50th percentile row and shows a likely decrease in rainfall. Current and business as usual emissions are high.

EVAPORATION

As would be expected in a warming environment where the atmosphere is able to hold more water vapour, pan evaporation (the amount of water evaporating from an open pan of water) has increased for most parts of Australia (Gifford, Farquhar et al. 2004; Wild 2004). Recorded evaporation trends for South Australia are the result of changes to a number of climate variables including temperature and wind at the local level (Bureau of Meteorology 2009) (Figure A1.10).

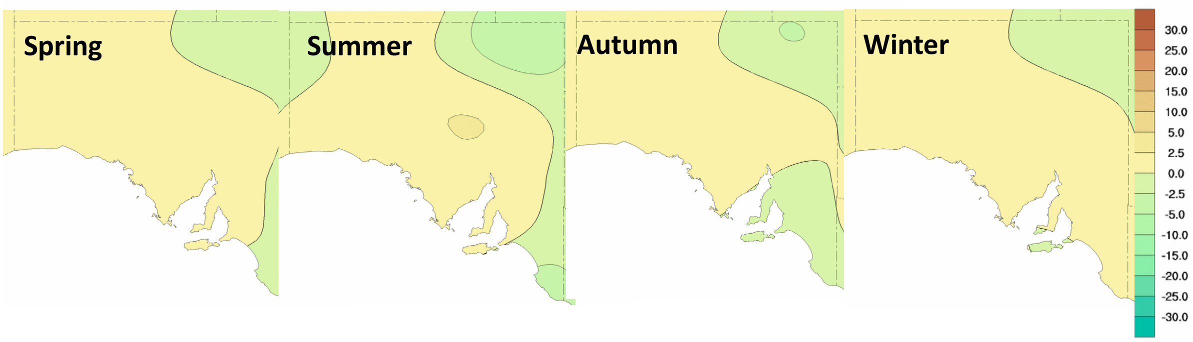

Figure A1.10: Trend in total seasonal pan evaporation 1970 – 2011 (mm/year) (Source: Bureau of Meteorology 2014b).

Projections for future changes in evaporation were also undertaken by CSIRO for South Australia (Suppiah *et.al.* 2006) (Figure A1.11).

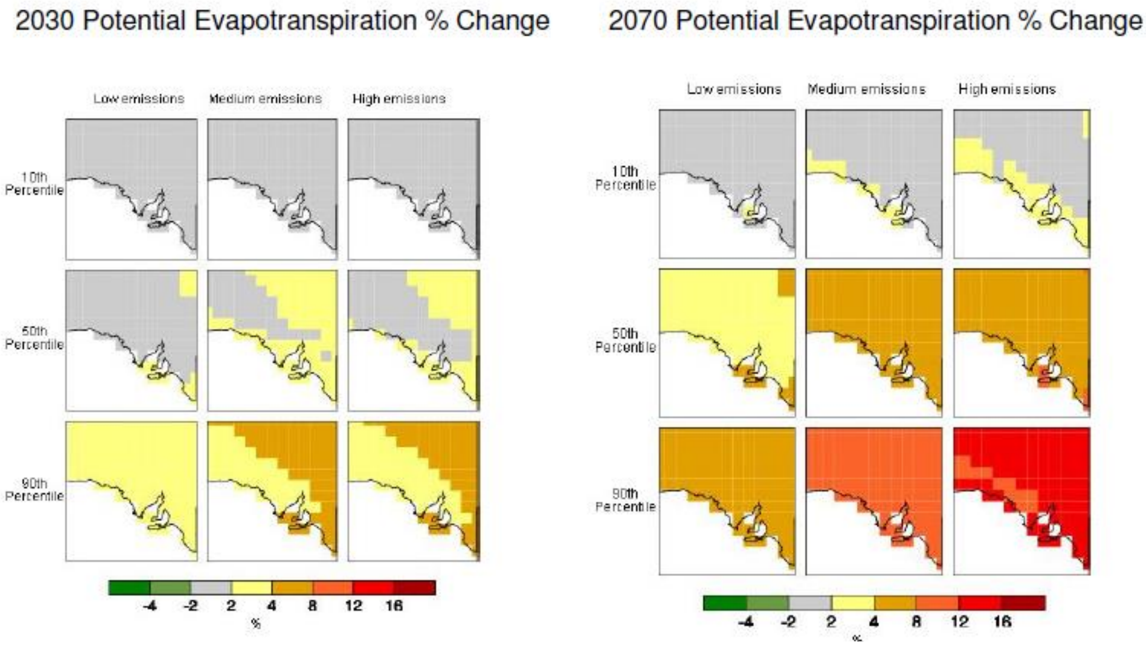

Figure A1.11: Expected range of changes to annual pan evaporation (%) for South Australia as predicted by a suite of Global Climate Models under low medium and high greenhouse gas emissions scenarios for the year 2030 (left) and 2070 (right) compared to the 1990 baseline (1980-1999) (Source: CSIRO and BoM 2007). The median expected change across all models is shown in the 50th percentile row and shows a likely increase in evaporation. Current and business as usual emissions are high.

WIND

Across Australia between 1975 and 2006 there has been a recorded widespread stilling in daily wind run of 0.009 m/s per year (McVicar, Van Niel et al. 2008).

Projections for future wind are calculated for 10 m above the ground and have only been undertaken at the continent scale (CSIRO BOM 2007). Average wind speed in South Australia is expected to increase in coastal regions by 2% to10% by 2030 in summer and increase or decrease by 2% in winter. By 2050, the magnitude of the change increases depending on the emissions scenario used (Figure A1.12).

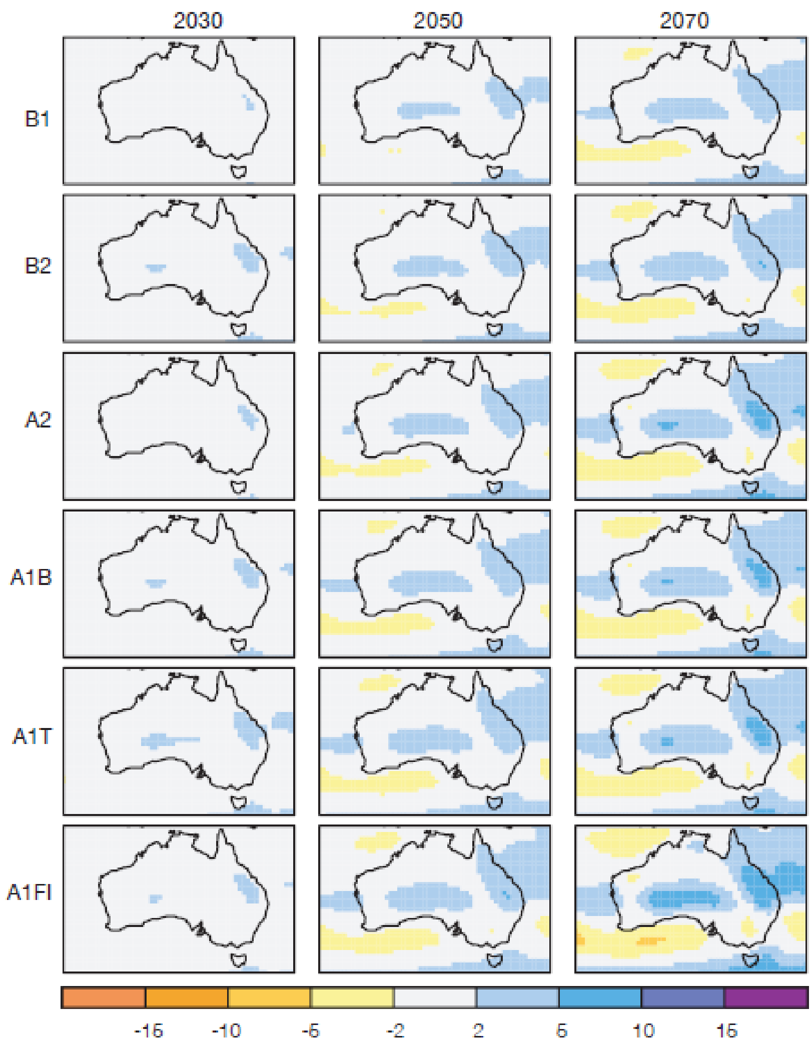

Figure A1.12: Best estimate (50th percentile) of the projected percent change in mean 10 m wind speed by 2030 (left column), 2050 (middle column) and 2070 (right column) for all six SRES emission scenarios tested (CSIRO and BoM 2007).

A1.6 GLOBAL BUSHFIRE STUDIES

As changes occur to each of the relevant climate parameters that influence bushfire, a number of studies have attempted to model the likely past and future changes to fire weather and fire frequency and intensity.

The IPCC Fourth Assessment Report noted that "trends in disturbance resulting from forest fires remains a subject of controversy" and that "there has been a decrease in fire frequency over some regions, including the USA and Europe, and an increase in others, including Amazonia, Southeast Asia, and Canada". They note that "the reasons for these regional differences are complex; in some cases climate change is a contributing factor, but other factors such as changes to forest management can also be important" (IPCC 2007).

A follow up study by Caesar and Golding (2011) used the Hadley Centre Global Environment Model version 2 to calculate the current global average FFDI (14) and future FFDI by the years 2100 for a number of A1B scenarios (average 20) (example output in Figure A1.13). The authors identify that the "primary meteorological driver of projected changes in forest fire danger on the global scale is temperature, followed by relative humidity which itself is strongly influenced by temperature". They also note that "in terms of global and regional climate projections, we have more confidence in the direction and magnitude of these projected changes compared to changes in precipitation and wind speed, which make less of a contribution to the results" (Caesar and Golding 2011).

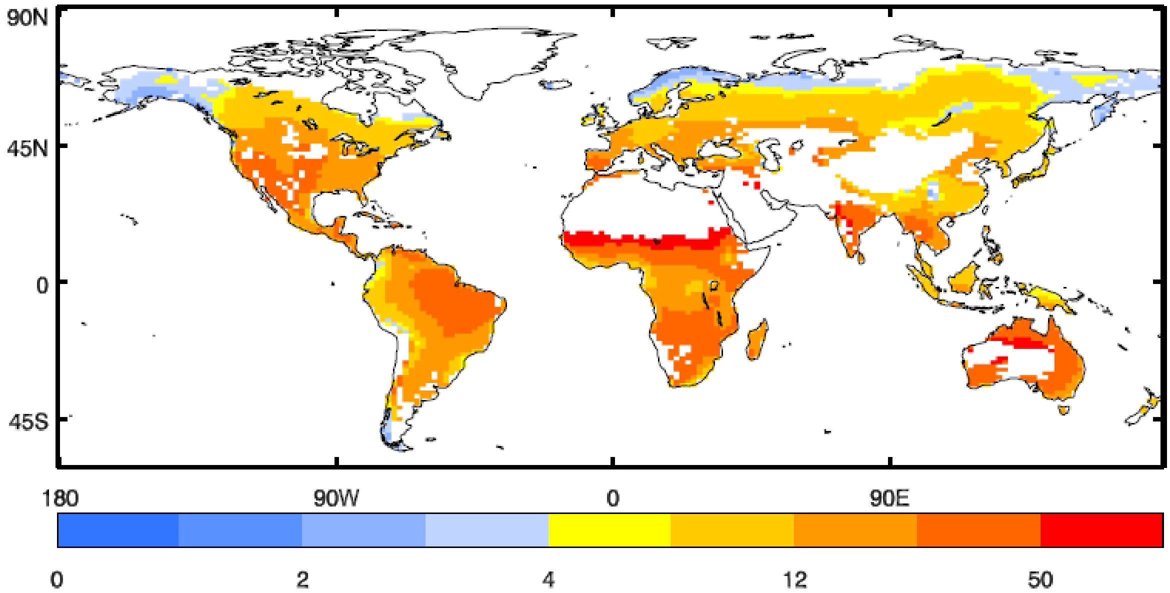

Figure A 1.13: Percentage change in Global Forest Fire Danger Index for the period 2090-2099 relative to 1971-2000 (Source: Caesar and Golding 2011).

A1.7 AUSTRALIAN BUSHFIRE STUDIES

As identified earlier, bushfire intensity is a function of the four switches of bushfire: biomass production; availability of fuel to burn; fire weather; and ignition (Bradstock 2010). As the climate changes it is expected that increasing dryness in woodland communities will decrease potential fire frequency as fuel loads diminish, while the opposite will apply in forests where fire is driven by fuel moisture and fire weather (Bradstock 2010). For these reasons, increasing dryness may diminish fire activity over much of Australia (dry woodlands), but increase in temperate forests. Elevated CO_2 and its impact on vegetation growth via carbon fertilisation and changes to plant water efficiency may confound or reinforce these trends (Bradstock 2010).

Because the monitoring of fuel loads for each of the fire danger indices is a complex process that may need to take into account a range of fuel types and characteristics, most previous studies that have considered the changes in past and future bushfire intensity and frequency have assessed the changes in bushfire weather alone (Bradstock 2010). Fire danger weather has increased in many areas by 10% to 40% from 2001 – 2007 compared to the 1980 – 2000 period (Steffen 2009). Four of the last five fire seasons (to 2007) were among the longest on record since 1942, a trend that has increased since the early 1990s (Lucas, Hennessy et al. 2007). Conditions recorded in the 2009 "Black Saturday" fires in Victoria were among the worst bushfire conditions ever recorded and included a drought of below average rainfall for a period of 12 years prior to the fire, wind speeds in excess of 100 km/hr and temperatures in the mid- to high 40 degrees Celsius (CSIRO 2011).

An early study of bushfire weather and climate change by Williams, Karoly et al. (2001) quantified "the possible impact of climate change on fire regimes by estimating changes in fire weather and the McArthur Forest Fire Danger Index". They used the CSIRO 9-level general circulation model (CSIRO9 GCM) to "simulate daily and seasonal fire danger for the present Australian climate and for a doubled- CO_2 climate". The results showed that the impact of doubling CO_2 levels significantly increased the FFDI at levels that were dependant on the site. "In the fire season control scenario at Sale and Hobart approximately 5% of daily FFDIs are in the 'very high' (FFDI between 24 and 50) and 'extreme' (FFDI greater than 50) categories. This rate of occurrence in the doubled CO_2 scenario increases slightly to 7% at Hobart but triples to 15% at Sale" (Williams, Karoly et al. 2001).

Following this initial study, an assessment of the impacts of climate change on fire weather in south eastern Australia was then undertaken by Hennessy, Lucas et al. (2005). Fire danger indices were calculated for "present conditions" using historical weather records from 1974-2003 for 17 sites in New South Wales, the Australian Capital Territory, Victoria and Tasmania. Two CSIRO global climate models (Mark 2 and Mark 3 downscalled to 50 km grids using the CCAM Mark 2 model) were then used to generate climate change scenarios for 2020 and 2050, including changes in average climate and daily weather variability that were then applied to the historical data sets. Fire danger indices are then calculated for 2020 and 2050. A key finding of the study was that "an increase in fire-weather risk is likely at most sites in 2020 and 2050, including the average number of days when the FFDI rating is very high or extreme. The combined frequencies of days with very high and extreme FFDI ratings are likely to increase 4-25% by 2020 and 15-70% by 2050" (Hennessy, Lucas et al. 2005).

Pitman, Narisma et al. (2007) assessed the impact of climate change on the risk of forest and grassland fires in Australia for January. They used a high resolution regional climate model, driven at the boundaries by data from a transitory coupled climate model. Two future emission scenarios (relatively high and relatively low) were used for 2050 and 2100. Results showed that there was a "consistent increase in regional-scale fire risk over Australia driven principally by warming and reductions in relative humidity in all simulations, under all emission scenarios and at all time periods" (Pitman, Narisma et al. 2007).

Hasson, Mills et al. (2009) also assessed the impacts of climate change on extreme bushfire in the south east of the continent. "A retrospective study of the meteorology of the Ash Wednesday 1983 fires, Mills (2005a) showed that many of the most extreme fire events in south eastern Australia over the 40 yr to the end of the 2003 summer, and ~80% of the bushfire-related deaths during that period, occurred on days on which the magnitude of the east–west 850 hPa temperature gradient in a small rectangle over south eastern Australia was in the highest 0.3% of its distribution… As these fronts intensify, the development of a northerly pre-frontal jet advects hot, dry gusty winds southwards—all the ingredients for extreme fire weather. In addition, the wind-shift associated with these fronts can cause the flank of a fire to become a much longer head-fire, and this effect is exacerbated if there is sufficient depth of cold air following these fronts to maintain strong, gusty, post-frontal winds that can greatly enhance fire spread" (Hasson, Mills et al. 2009). Using this knowledge, Hasson, Mills et al. analysed the 850 hPa temperature gradient from ten GCMs from the Coupled Model Intercomparison Project to estimate the frequency of these cold front events at the middle and end of the 21st Century for low and high greenhouse gas emissions scenarios. The results "suggested that the frequency of such events will increase from around 1 event every 2 yr during the late 20th century to around 1 event per year in the middle of the 21st century and 1 to 2 events per year by the end of the 21st century; however, there is a great degree of variation between models" (Hasson, Mills et al. 2009).

In a study of fire occurrence in Victoria (Dowdy and Mills 2009) identify that lightning fires accounted for 90% of the total area burnt by all fires, despite the fact that only 30% of the fires were caused by lightning. This imbalance was partly attributed to the Victorian alpine fires of January to March 2003 that burnt over one million hectares. However, even without this event, lightning fires still account for approximately 55% of the total area burnt by all fires. Little research has been done to determine how the changes in the climate might affect lightening and hence natural ignition events. On short time scales, lightning is correlated to surface temperatures and upper tropospheric moisture. Climate modelling studies show that in a future warmer climate we may have less thunderstorms overall, but more intense thunderstorms (Price 2009). Price and Rind (1994) suggest that there will be an increase of about 5% to 6% in global lightning frequencies for every 1°C global warming.

A study by Douglas (2011) examined the influence of climate change on bushfire in New South Wales. Thirty locations were selected to represent the 21 fire weather districts across NSW. The analysis used the Bureau of Meteorology 1976 to 2009 FFDI data set and Lucas (2009) GFDI data for 16 stations. The final report from the study is not available but was submitted to the Country Fire Authority of NSW with recommendations for defensible spaces and BAL levels for planning and building homes in bushfire prone regions.

A study by Clarke, Smith et al. (2011) used “skill-selected global climate models … to explore the effect of future climate change on regional bushfire weather in eastern Australia”. The daily FFDI was calculated for four regions in Eastern Australia for the years 2050 and 2100 using the A2 scenario: Central Queensland; southern Queensland / northern New South Wales; southern New South Wales; and Victoria (Figure A1.14 left).

Results showed that the projected changes in FFDI varied along a latitudinal gradient. “In summer rainfall-dominated tropical north-east Australia, mean and extreme FFDI are projected to decrease or remain close to 20th century levels. In the uniform and winter rainfall regions, which occupy south-east continental Australia, FFDI is projected to increase strongly by 2100” (Figure A1.14 right). For Victoria winter forest fire season area that would be comparable to those in south-eastern South Australia, results showed that small decreases might be expected in the FFDI by 2050 but that by 2100 all models projected an earlier start to the fire season and higher FFDI values (25-75% increase depending on the model used). These changes in the FFDI were shown to be linked to increases in temperature for the Victorian winter region and that changes in wind speed contributed very little to the projected changes. However, the authors note that, only daily average (rather than 1500 hours) values of relative humidity and wind speed were available” (Clarke, Smith et al. 2011).

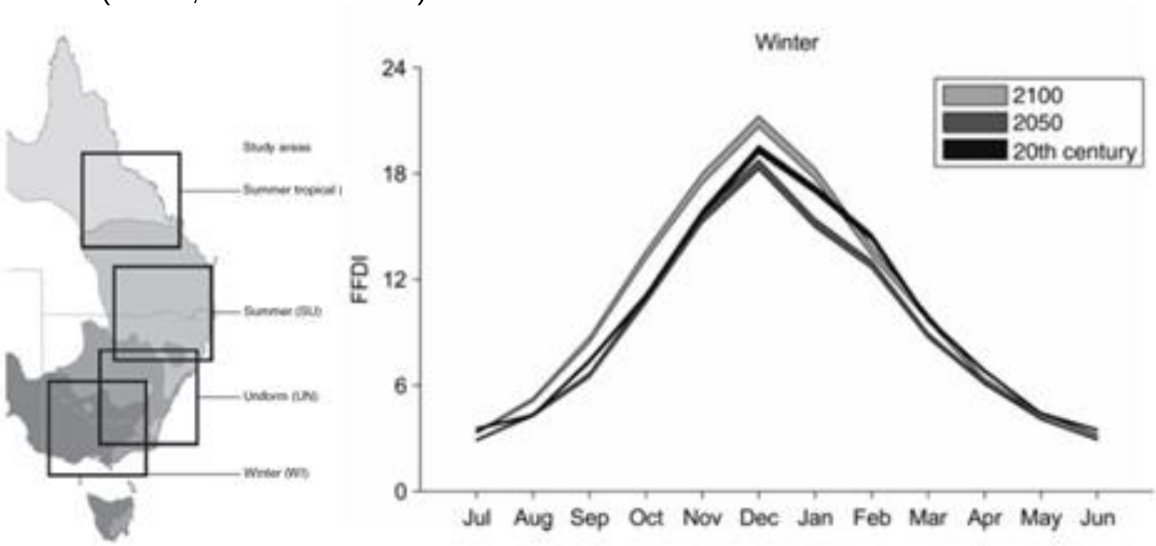

Figure A1.14: A study of the likely changes to the FFDI in eastern Australia by Clarke et al (2011). (Left) The study areas used in the assessment; (Right) The mean monthly forest fire danger index (FFDI) for each scenario from the CSIRO model in the Victorian winter forest fire seasonality area– winter wet and low summer rainfall. The width of each line provides a 95% confidence interval (Source: Clarke, Smith et al 2011).

Finally, a study by King, Cary et al. (2012) considered the effect of both a changing climate and atmospheric CO_2 combinations on grass curing, fuel load, and thus GFDI and potential fire-line intensity for an A1B emissions scenario for 2030, B1 for 2070 and A1FI for 2070 for three sites in south eastern Australia near Canberra, Sydney and Melbourne. Earlier studies had assumed maximum grassland fuel curing (100%) and average fuel load (4.5 t/ha) despite the fact that changes in the climate are likely to affect these qualities of the fuel as well. To overcome the absence of archived grass fuel and curing records, the agricultural pasture model GRAZPLAN was used to simulate historic and future daily changes for a native perennial grass, an exotic perennial grass and an exotic annual grass.

Results showed that “for each location, large differences were evident between distributions of monthly median GFDI that were determined from variable (GRAZPLAN-derived) and constant curing. Monthly median GFDI calculated with constant curing was always higher than GFDI derived from GRAZPLAN-derived curing, particularly in cooler months (May to November) when curing is normally at a minimum. At all locations, assuming variable curing and fuel load (GRAZPLAN-derived), peak monthly median GFDI values occurred later for native perennial grasslands, and earlier for both exotic grasslands” (King, Cary et al. 2012). In addition, “for each grassland and location, changes in temperature and moisture determined curing, with atmospheric CO_2 concentration having no significant effect… and … projected shifts in GFDI and potential fire-line intensity arising from future climate–CO_2 combinations were small compared with initial difference arising from using realistic GRAZPLAN-derived curing and fuel load values (compared with constant curing and fuel load) for grass dynamics. Monthly 50th and 95th percentile curing was generally predicted to increase as climates became warmer and drier (2030 A1B, 2070 B1 and 2070 A1FI), compared with the historical climate, particularly during spring and early summer (September–January) in Canberra and Melbourne, and during autumn (February–May) in Sydney…. and… monthly 95th percentile GFDI was generally predicted to increase as climates became warmer and drier (2030 A1B, 2070 B1 and 2070 A1FI), compared with the historical climate, particularly in the warmer months (November to March)” (King, Cary et al. 2012).

It is also interesting to note that “for the exotic annual grasslands at all locations and the exotic perennial grasslands in Canberra and Melbourne, the mean fuel load between October and April, when the majority of fire activity occurs, was a good approximation for the assumed mean fuel load of 4.5 t/ha used in earlier studies, whereas it was consistently lower for the native perennial grasslands in all locations and the exotic perennial grasslands in Sydney”. In summary, “the general trend in our study was for curing and GFDI to increase under the influence of warmer, drier future climates. This represents reduced fire-suppression potential and more days on which ignition will likely occur… however… the combined effects of generally higher GFDI and generally lower fuel loads modelled for future climate and atmospheric CO_2 combinations resulted in relatively small changes in modelled future potential fire-line intensity for the majority of grassland types, months and study locations” (King, Cary et al. 2012).

A1.8 SOUTH AUSTRALIAN BUSHFIRE STUDIES

In 2010, Lucas developed a national historical FFDI fire weather data-set, extending from 1973 to 2008. To create the data-set, meteorological measurements of air temperature, relative humidity, wind speed and rainfall were sourced for 77 stations are used. The data set created “has daily resolution and uses the observations at 3 pm for relative humidity and 10-minute averaged wind speed, rainfall for the previous 24 hours reported daily at 9 am and daily maximum temperature, which is generally observed in the mid-to-late afternoon.

This selection of variables is consistent with the original intent of the FFDI – a daily estimate of the fire weather danger centred on the time of maximum temperature. Under normal circumstances at most locations, the air temperature reaches its maximum in the mid-to-late afternoon and the 3 pm observations represents those which are closest to the desired time” (Lucas 2010). Stations in South Australia included in the data set were: Adelaide, Ceduna, Mt. Gambier, Port Lincoln, Renmark, Snowtown and Woomera. No assessment of the impact of climate change on bushfire weather was undertaken in this study.

An analysis of climate change impacts on bushfire by Lucas, Hennessy et al. (2007) assessed 28 stations across south east Australia. Stations in South Australia in the study included Adelaide, Ceduna, Woomera and Mt. Gambier. Historical data were analysed to determine trends and the current number of days when the fire danger rating exceeded high, very high, severe, extreme and catastrophic. Data for Adelaide shows that the average number of days each year when the FFDI score went above 25 (very high) was 17.3 and the average number of days each year when the FFDI score went above 50 (severe) was 10.9 (Figure A1.15). To 2007 there had been no days when the FFDI exceeded 75 (extreme) or 100 (catastrophic) in Adelaide.

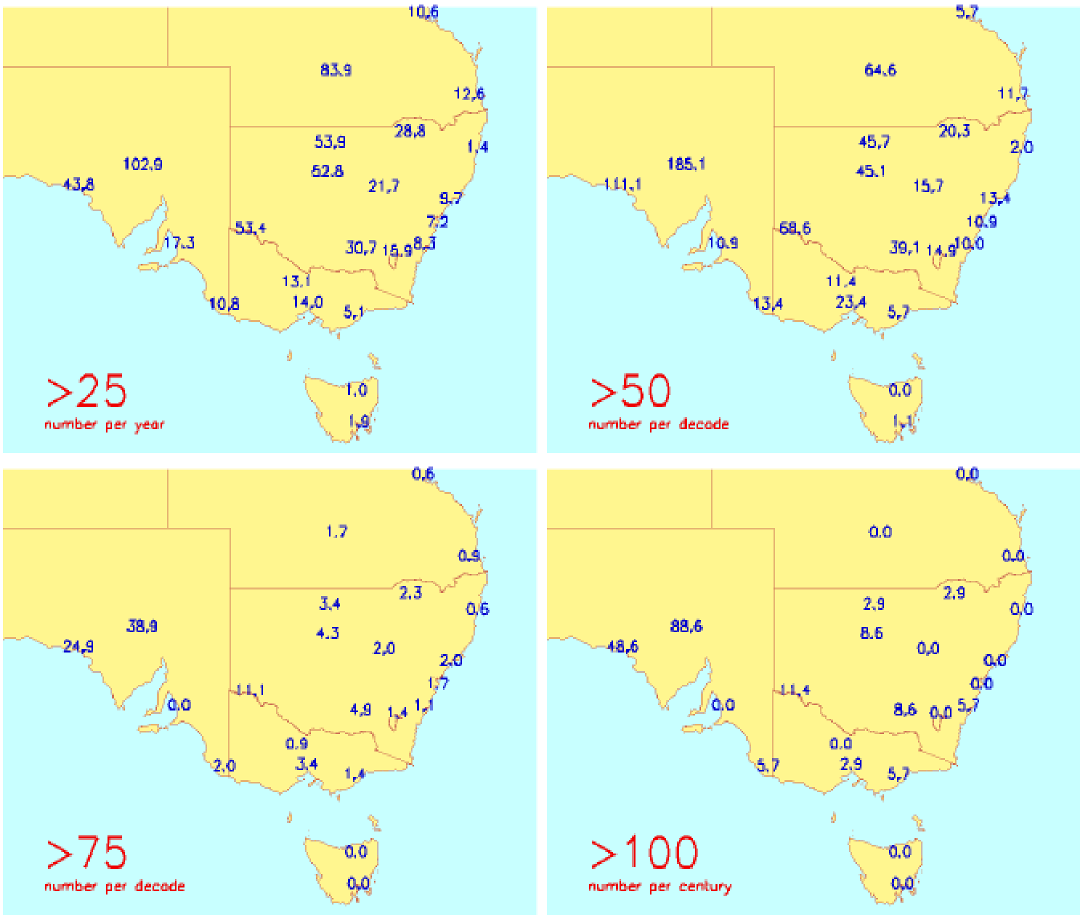

Figure A1.15: Average number of days exceeding a given FFDI/FDR threshold (red). FFDI values correspond to very high (>25), severe (>50), extreme (>75) and catastrophic (>100). Note the change in the time intervals. Based on data from 1973-2007 (Lucas, Hennessy et al. 2007).

Time series simulation output of cumulative FFDI for Adelaide shows the annual variation and the increasing trend over the time period assessed (Figure A1.16).

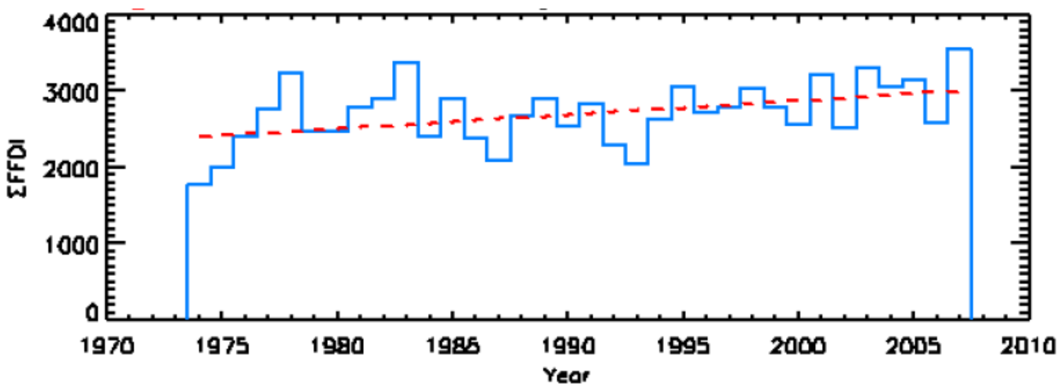

Figure A1.16: Increasing trend in the annual cumulative forest fire index (FFDI) for Adelaide from 1973 – 2007 (Lucas, Hennessy et al. 2007).

Assessments of future climate changes used two CSIRO global climate models (CCAM Mark 2 and Mark 3) to calculate daily values for temperature, humidity, wind and rainfall for the years 2020 and 2050, relative to 1990. The modelled changes from the various scenarios were then projected onto the observed daily time series of temperature, rainfall, wind and relative humidity from 1973 to early 2007. Results showed that in the future a mean temperature increase of up to 1.0^{o}C would lead to a 10 - 30% increase in the average number of very high fire days across southern Australia, and the average number of extreme fire days would rise by 15 - 65% depending on location (Figure A1.17). In addition, it is expected that fire seasons will start earlier, end later and be "generally more intense throughout their length".

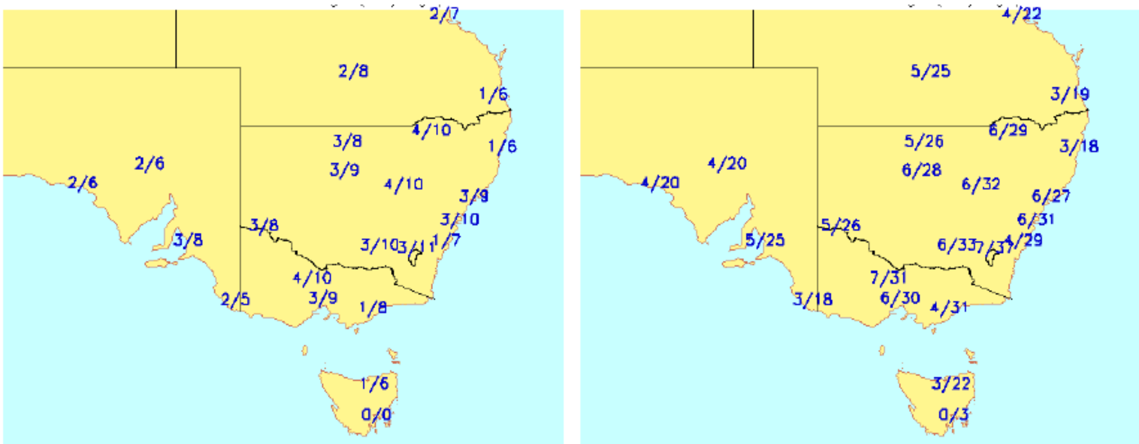

Figure A1.17: Percentage change in cumulative FFDI using results from the CCAM (Mark3) simulations for (left) 2020 and (right) 2050. At each location the low global warming scenario is on the left and the high global warming scenario on the right (Lucas, Hennessy et al. 2007).

For Adelaide, a high greenhouse gas emissions scenario would result in an estimated increase of four days each year when the FFDI was above 25 by 2020 and an additional twelve days by 2050 (Table A1.2). In addition, the annual cumulative FFDI was likely to increase by between 5% and 8% and 16% to 25% for high emission scenarios for the years 2020 and 2050 respectively (Lucas, Hennessy et al. 2007).

Table A1.2: Expected change in the number of days when the forest fire danger index (FFDI) exceeds 25 and 50 for the year 2020 and 2050 for Adelaide, Ceduna and Mt Gambier under low and high greenhouse gas emissions scenarios (Source: Lucas, Hennessy et al. 2007). Calculations are all compared to the 1973-2007 period. Current and business as usual emissions are high.

Location	Now	2020		2050	
		Low	High	Low	High
Number of days when the FFDI>25					
Adelaide	18.3	19.8	22.3	20.8	30.2
Ceduna	46.4	48	50.5	49	58.6
Mt Gambier	11.5	11.8	12.8	12.3	15.4
Number of days when the FFDI>50					
Adelaide	1.2	1.5	1.8	1.5	3.8
Ceduna	11.8	12.3	13.8	13.1	18.5
Mt Gambier	1.4	1.6	1.8	1.7	2.9

A follow up study by Clarke, Lucas et al (2012) examined changes in Australian fire weather as measured by the FFDI between 1973 and 2010 and included four South Australian locations. Annual cumulative FFDI increased significantly at 16 of the 38 stations tested, mostly those in the interior south-east of the continent and less along the coast. None of the stations showed a negative trend. The largest increases were shown to have happened in spring and autumn (Figure A1.18). The multi-station mean showed that on average across Australia, there had been an increase in annual cumulative FFDI since 1973 of 212 points per decade. Locations in the study in South Australia were Adelaide, Ceduna, Mt. Gambier and Woomera (Figure A1.18).

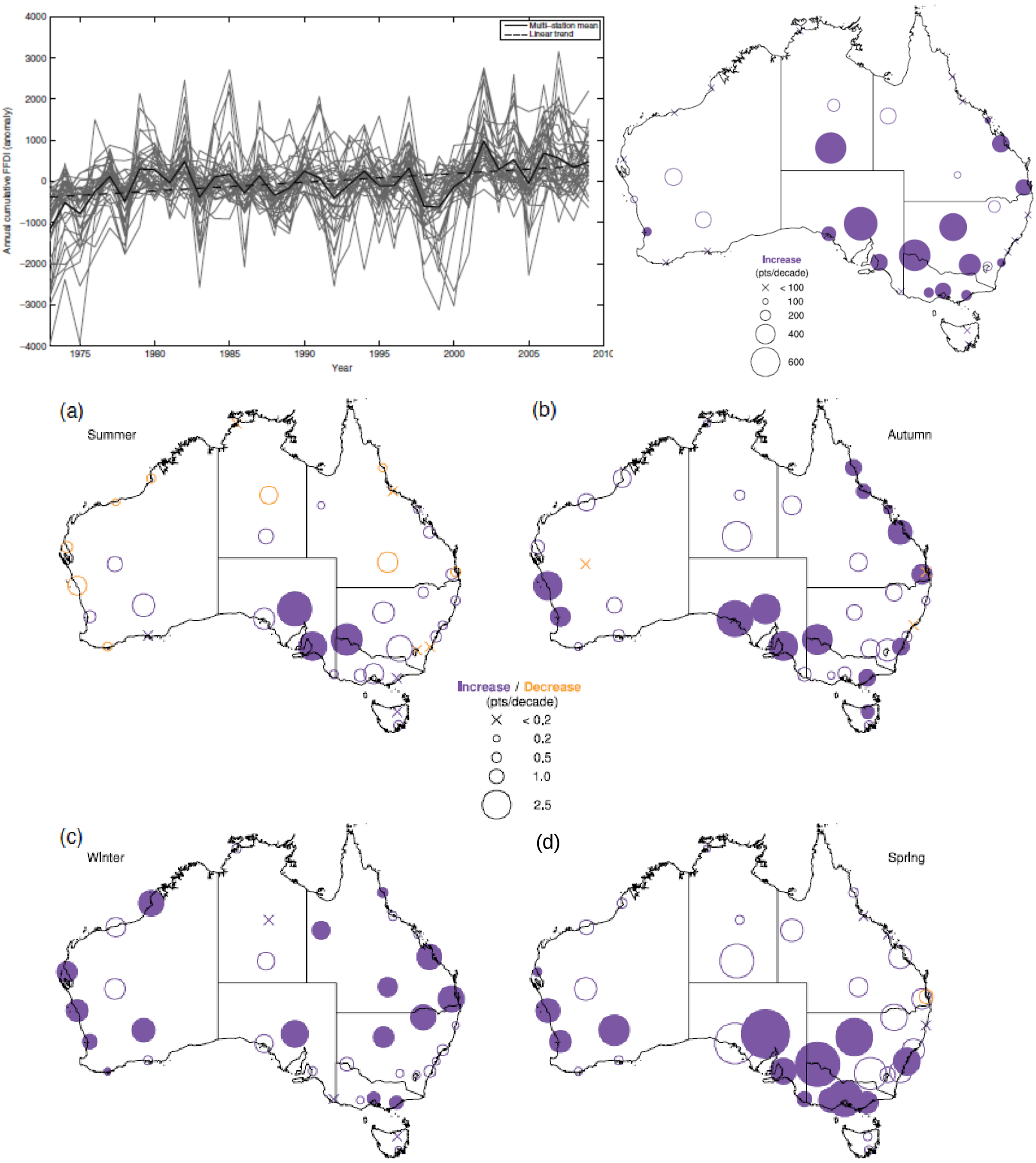

Figure A1.18: Increasing trend in the annual cumulative forest fire index (FFDI) across Australia from 1973 – 2010 shown as: (Top left) an annual total; (Top right) increase in points per decade (solid circles are statistically significant); and (a-d) increase in points per decade for each season decade (solid circles are statistically significant) (Source: Clarke, Lucas et al. 2012).

For South Australia, there were significant increases in both the annual FFDI and seasonal values – particularly in the spring and autumn. Trends were higher at the upper end of the distributions, an indication that the shape of the distribution is changing and not just the mean. Similar patterns of change were seen in the temperature and humidity data – particularly in the south east of the continent where the changes in FFDI were greatest (Clarke, Lucas 2012).

Most recently, a study by Kepert, Wain et al (2012) developed “nationally consistent fire danger index data set (the National Fire Danger Rating Project) for the FFDI, GFDI and Canadian FDI using the European Centre for Medium Range Weather Forecasting (ECMWF) Interim

Reanalysis Project ERA-1 at 75 km square resolution and using the drought index grid data set as per Finkele et al (2006)". This data set and others are reviewed in detail in the following section.

A1.9 LITERATURE REVIEW CONCLUDING SUMMARY

The incidence of bushfire within the landscape is controlled by four switches: rate of vegetation (fuel) growth; dryness of the fuel; occurrence of suitable weather for fire spread; and a source of ignition. Weather parameters that intensify potential bushfires are high maximum temperatures, strong winds and low relative humidity. Each of these weather parameters has been included with a measure of vegetation dryness in each of the two key fire hazard indices in use in Australia and South Australia – the Forest Fire Danger Index (FFDI) and the Grassland Fire Danger Index (GFDI). Recording and monitoring of these bushfire hazard indices provide some indication of the past trends in bushfire intensity and if combined with projections of future changes in the climate as a result of global warming can provide a guide as to how bushfire intensity may change in the future.

Bushfire weather in South Australia has been observed to have changed over the past 100 years: annual total rainfall has decreased although summer rainfall has increased in some areas; maximum temperatures have increased State wide; relative humidity has increased in some parts of the State and decreased in others; and wind speeds display mixed trends, increasing in some locations, decreasing in others. When included in the calculation of the historical FFDI for South Australia, there have been significant increases in both the annual FFDI and seasonal values – particularly in the spring and autumn. Trends were higher at the upper end of the distributions, an indication that the shape of the distribution is changing and not just the mean. In addition, at the locations considered, the length of the bushfire season has extended by 2.4 days per decade (Clarke, Lucas et al. 2012).

The one study that considered the impacts of climate change on South Australian bushfire weather included Adelaide, Ceduna, Mt. Gambier and Woomera. For Adelaide, a high greenhouse gas emissions scenario would result in an estimated increase of four days each year when the FFDI was above 25 by 2020 and an additional twelve days by 2050 (Lucas, Hennessy et al. 2007). In addition, the annual cumulative FFDI was likely to increase by between 5% and 8% and 16% to 25% for high emission scenarios for the years 2020 and 2050 respectively (Lucas, Hennessy et al. 2007).

APPENDIX 2 – DETAILED DESCRIPTION OF THE DATA AND METHODOLOGY

This Appendix 2 summarises the review of data and methodologies used in previous studies and then describes the options available for a methodology that would work for regional South Australia that takes into account the data sets available. The methodology selected is then described.

Using the existing model of fire danger (FFDI), analyses were then performed to determine both the observed fire risk and the likely future changes to bushfire weather as a result of global warming. The analyses were undertaken for two pilot areas where no assessment of climate change impacts on fire danger had previously been undertaken: Spring Gully Conservation Park (SGCP) within the Central LGA Region and the Mt Bold Reserve (MBR) in the Adelaide Hills.

The logic in undertaking this process is perhaps best followed via a series of questions and answers.

A2.1 QUESTION 1: IS THERE DATA FOR THE REGIONAL AREAS OF SA TO SUPPORT THE CALCULATION OF THE FFDI AND GFDI?

To answer this question we needed a detailed understanding of the parameters required for each of the fire models that have been developed (the FFDI and GFDI). We then undertook a detailed review of the data sets available for regional SA to assess which parameters and time frames each covered so as to determine whether the data available would support the calculation of the FFDI and GFDI.

THE FOREST FIRE DANGER INDEX MODEL

As detailed in the literature review, the McArthur Mark 5 Forest Fire Danger Index (Luke and McArthur 1978) is a complex calculation involving a range of meteorological parameters:

$$FFDI = 1.275(DF)^{0.987} \times [\exp{(0.0338T - 0.0345H)}] \times exp(0.0234V)$$

Where *T* = maximum daily air temperature ^{o}C,
V = daily mean wind speed km/hr in the open at 10 m height,
H = daily minimum relative humidity %, and
DF is a drought factor that in turn is a function of the Soil Moisture Deficit.

Each of these parameters and the calculation of the index is described in detail in the following pages.

The first step in the process of calculating the FFDI is to calculate the Soil Moisture Deficit.

THE SOIL MOISTURE DEFICIT.

The Soil Moisture Deficit (SMD) is calculated at a daily time frame and reflects the amount of water in the soil. More precisely, it reflects the amount of rainfall, in mm, required to bring the soil moisture back to field capacity.

$$SMD_i = SMD_{i-1} + ET_i - P_{eff_i}$$

Where: i is the current day;
i-1 is the previous day;
ET = evapotranspiration; and
Peff = effective precipitation.

In other words, the SMD describes the current soil moisture levels - the balance of the loss of moisture from evapotranspiration, and the gain of moisture from rainfall. A low SMD (for example 0 mm) reflects a saturated soil, and the highest value of the SMD reflects a dry soil.

Operationally in SA the SDI is used to calculate the FFDI. However, it has been shown that the SDI underestimates soil dryness in low rainfall areas. The SDI also requires an assessment of fuel type, and so does not allow for large scale studies that require a high level of automation in the calculations. For these reasons, previous climatological studies of bushfire danger have used the Keetch-Byram Drought Index (KBDI) (Keetch and Byram 1968). The KBDI is the most widely used measure of SMD, and so use of it allows for spatial consistency across large areas and comparison of results with previous studies. In this project we used the KBDI to calculate the SMD. The KBDI assumes a maximum soil moisture deficit of 200 mm and a minimum of 0 mm. Following Finkele et al (2006), we used the following estimations for KBDI:

$$KBDI_n = KBDI_{n-1} + ET - P_{eff}$$

Where: $KBDI_{n-1}$ = the previous days KBDI;
Peff = the daily effective rainfall as calculated below; and
ET = the daily evapotranspiration as calculated below.

$$P_{eff} = rain - (interception, runoff)$$

Where: rain is the previous 24-hour rainfall amount.

Note that the interception and runoff amount is approximated as the first 5 mm within consecutive non-zero rain days. This is the same approximation for both interception of vegetation cover or surface runoff.

$$ET = \frac{(203.2 - KBDO_{n-1})(0.968\, e^{0.0875Tmax+1.5552} - 8.3)}{1 + 10.88\, e^{-0.00173\, R_{an}}} 10^{-3}$$

Where: KBDI n-1 = the previous days SMD
Tmax = previous days maximum temperature
Rann = annual rainfall.

It is important to note that Finkele et al (2006) summarised five assumptions in the calculation of the KBDI from Sullivan (2001):

1. The rate of moisture loss from the soil is a function of vegetation cover, that itself is a function of annual rainfall;
2. The vegetation-rainfall function is approximated by an exponential curve and moisture loss is a function of mean annual rainfall;
3. The rate of moisture loss from the soil is determined by the evapotranspiration;
4. The rate of moisture loss from the soil is approximated by an exponential decay curve in which the wilting point is the lowest moisture level; and
5. The soil depth is such that it has a field capacity of 200 mm.

THE DROUGHT FACTOR

The drought factor (DF) is an estimate of the fire fuel moisture content. The factor is dimensionless and ranges between 0 and 10 and uses the KBDI in its calculation, following (Griffiths 1999), as:

$$DF = 10.5\left(1 - e^{-(SMD+30)/40}\right) \frac{41x^2 + x}{40\,x^2 + x + 1}$$

Where: *X* expresses the influence on the drought factor of past rainfall over the past 20 days.

X is defined as:

$$X = N^{1.3} / (N^{1.3} + p - 2) \qquad \text{for } N \geq 1 \text{ and } p > 2$$

$$X = 1 \qquad \text{for } p \leq 2$$

Where: P = the past rainfall amount. More specifically, the sum of the rainfall of the rainfall event defined as consecutive days with p > 2 mm; and
N = days since rain. More specifically, the number of days since the day with the largest daily rainfall amount.

THE FOREST FIRE DANGER INDEX (FFDI)

Finally, the FFDI is determined by the following algorithm that includes the drought factor:

$$FFDI = 1.275(DF)^{0.987} \times [\exp(0.0338T - 0.0345H)] \times exp(0.0234V)$$

Where: *T* = maximum daily air temperature °C,
V = daily mean wind speed km/hr in the open at 10 m height,
H = daily minimum relative humidity %, and
DF = a drought factor.

Additional algorithms that might be needed in the calculations include the conversion of Vapour Pressure Deficit (VPD) to Relative Humidity (RH):

$$\text{VPD} = e_s - e$$

$$RH = \frac{e}{e_s} \times 100 \quad = \frac{(e_s - VPD)}{e_s}$$

$$e_s = 6.11 \times 10^{\left(\frac{7.5 \times T}{237.3 + T}\right)}$$

Where: e_s = saturated vapour pressure;
T = temperature (^oC);
RH = relative humidity; and
VPD = vapour pressure deficit.

Where maximum daily vales are not available 3 pm recordings from BOM observing stations are usually used.

In summary, the steps to calculate the FFDI are:

1. Determine the Soil Moisture Deficit (SMD), a measure of how dry the soil is and the degree of drought;

2. Calculate the Drought Factor: this combines the SMD and recent rainfall; and then

3. Calculate the FFDI.

In addition to the caveats identified by Finkele (2006) for the calculation of the SMD, other assumptions that need to be considered when using the FFDI include that the model was based on fires in low to medium quality dry sclerophyll forests with a fuel loading of 12 t/ha, in south-eastern Australia.

THE GRASSLAND FIRE DANGER INDEX MODEL

Similarly to the FFDI, the McArthur Mark 4 Grassland Fire Danger Meter (GFDI) (McArthur 1966) is used operationally to assess fire weather conditions relevant to grasslands. Purton (1982) developed the GFDI algorithm:

$$GFDI = \exp(-1.523 + 1.027\ln(Q) - 0.009432(100 - C)^{1.536} + 0.02764T - 0.22005\sqrt{H} + 0.6422\sqrt{U})$$

Where: *T* = maximum daily air temperature ^oC,
V = daily mean wind speed km/hr in the open at 10 m height (km/h),
H = daily minimum relative humidity %, and
Q = the quantity of fuel (t/ha)
C = the degree of grass curing (%)

The GFDI is similar to the FFDI, except there is a quantity of fuel component and the SMD and Drought Factor are replaced by a curing index. Curing is the proportion of the dry weight of dead grass to total grass biomass. For example, a curing factor of 70% means that 70% of the grass is dead. To analyse the climatology of the GFDI, a historical and future curing dataset is required. Archives of the historic curing index as assessed on-ground are available for areas across South Australia but not in digital form. Data from satellite imagery can be retrieved retrospectively but are expensive and extend back to the maximum of about 20 years.

Where historical data is not available, pasture growth models such as GRAZPLAN (Donnelly et al 2002) have been used (e.g. King et al 2012). Calculations of monthly pasture biomass, pasture growth, curing and grass fire risk are provided at a monthly resolution by the Queensland Government for all of Australia as a map from the 1890s to the present. Grass growth and curing uses the Aussie GRASS pasture simulation model and takes into account the total amount of pasture growth over any consecutive 12-month period. The maps use gridded climate data (daily rainfall, maximum and minimum temperatures, evaporation, solar radiation and vapour pressure) on a regular 0.05 degree grid extending from latitude 10° S to 44° S and longitude 112° E to 154° E as per Jeffery et al (2001). Maps are available via the SILO online portal (https://www.longpaddock.qld.gov.au/silo/). Rainfall data uses the Bureau of Meteorology official rainfall. The authors note that the most reliable output from the model at this stage is the 'Pasture Growth Relative to the Last 40 Years'. Other products from the GRASP model (including grass fire risk) generally require some further validation. For South Australia the model does contain local pasture species. However, to validate the model outputs, an historical curing dataset would be required.

Previously studies such as Henessey et al (2005) have dealt with this lack of ‘ground-truthed’ curing data by setting the curing and fuel load parameters of the GFDI to a constant, and Lucas et al (2007) opted to not utilise the GFDI at all.

For future calculations of grass growth and curing a grass model would need to be run using future climate scenario data. Projections of future pasture biomass have been undertaken for some point locations in South Australia by SARDI (*Melissa Truscott, Pasture modeller, SARDI pers. comm. 12 November 2014*) but not curing. If funding were available it would be possible to undertake the calculations.

An accurate estimation of curing is essential if using the GFDI as the effects of uncertainty of curing percentage are greater than those from weather related components, especially local variations in wind speed (King et al. 2012, Hicks 2012). Given that the output GFDI is highly sensitive to the uncertainties in the input data, especially curing (Hicks 2012), and the lack of reliable pasture curing data for both historical and future climates, the analysis in the following sections of this project was devoted to the FFDI only.

AVAILABLE WEATHER DATA SETS

As noted in the review of previous studies of fire danger, there have been a number of different datasets used for input to the FFDI and GFDI. The differences between these data sets involve aspects of data quality, observing station location, and data resolution. The conclusions that can be drawn from the analysis will be partially dependant on the quality of the fire weather data used. To use real observed data requires the close proximity of a long-term high quality observing station run by the Bureau of Meteorology or other agency that collects data for each of the parameters needed. Where observed data is not available an interpolated (gridded) dataset may be used (this is estimated data calculated using real data from nearby observing stations). The capacity of gridded data to accurately represent real weather events across a landscape is affected by the topography of the land, distance from the sea, distance from a high quality observing station, the equations used to interpolate between the gaps, size of the grids and length of record. Some of these limitations also apply to the observing station data: that is, results can only be extrapolated to other nearby locations with caution.

Details of the synthetic data sets and global climate model output data sets are described in Table A2.1 on the following page. Each of these data sets would be available for regional South Australia including the two pilot locations identified.

Table A2.1: Review of data sets used in previous studies of bushfire in Australia and South Australia.

	Data set	Source	Spatial scale	Temporal scale	Temp	Precip.	Humidity	Wind (10 m)	VP	Strengths	Weaknesses	Notes
Climate change data	CSIRO Mark 3	CSIRO, Australia	200kms	1 hourly. Depends on storage space, download time, analysis requirements.	√	√	√	√	√	A 'hot dry' model: allows us to assess a worst case scenario.	There are GCMs in terms of ability to simulate ENSO and other key features of Australia's climate.	
	CCAM (McGregor and Dix 2008)	BOM, Australia	60kms (0.5deg).	As above	√	√	√	√	√	Good spatial resolution.	Not freely available.	Bertrand Timbal did model runs for SA.
	SILO Consistent Climate Change Scenarios. CMIP 3 Multi-model	Queensland Government	Station locations	Daily	√	√	x	x	√	Easy access to climate change scenarios that are all in a consistent form.	Change factor methodology.	ALL SRES scenarios for 2030. Patched point data locations as per SILO.
Synthetic and observed historical data	**Point datasets**											
	BoM station data	BOM, Australia	Point	n/a	√	√	√	√	√	This is observed data.	Data quality may be poor.	Check: The use of 3 pm values (cf daily mins or maxs, eg as in Hennessy et al 2005) decreases extreme FFDI by approx 20%.
	Gridded data sets											
	AWAP (Jones et al. 2009)	BOM, Australia	Gridded	Daily	√	√	x	x	√	Gridded dataset allow for greater spatial consistency. Gridded datasets aim to produce a representation of the area-average rainfall, not rainfall at individual points.	(1) The differences in the rainfall amount between the value representing a grid cell and a point location can be large, such as in complex terrain or in convective small-scale rain events. Extreme rainfall events are not well captured. Gridded datasets tend to underestimate wet events and overestimate dry events. (2) The difference in maximum temperature between grid value and point value is generally rather smaller due to the greater spatial homogeneity (and perhaps also to the less-dense observation network) of the maximum temperature observations.	Observed data is decomposed into averages and anomalies (anomalies are weakly related to topography). The averages are interpolated using 3-dimensional smoothing splines, and the anomalies are interpolated using the Barnes successive correction technique. Similar to SILO, but different algorithms.
	SILO (Jefferies et al 2001)	QCCCE	Gridded 0.01 deg.	Daily	√	√	x	x	√	As above	As above	Observed data is interpolated using kriging. The process is designed to accurately reproduce the observed data.
	Daily near-surface wind speed. (McVicar et al. 2008)	CSIRO DOI:10.4225/08/510B50F8DBB30	Gridded (from BoM point data) 0.01 deg.	Daily 1975-2012	x	x	x	√	x	Good spatial resolution of wind speed.	This is daily mean WS that will underestimate FFDI. We need daily max WS or 3 pm WS. Use Guo 2013 to convert. Or ECMWF to compare, or nearby point stations.	
	Drought Factor (Finkele et al. 2006)	BOM, Australia	Gridded 0.01 deg and 0.25 deg.	Daily (1965-2005)	x	x	x	x	x	Fine spatial resolution.	Derived from BOM NCC gridded Tmax and P (Weymouth et al 1999, Jones 1999). These are different datasets to SILO and AWAP.	
	Modelled data											
	BoM MESOLAPS forecast data (Puri et al. 1998)	BOM, Australia	0.125 deg lat/long	2000 til present. 3 hrly	0600UTC unless 0300 is greater	KBDI	√	√		Fine spatial and temporal resolution.	Only available since 2006. (2) Forecast data: less reliable than reanalysis.(3) An FFDI derived from gridded forecast field will differ to single station analysis.	BoM MESOLAPS (as per Dowdy et al 2010).Used for daily FFDI forecasts since 2006.
	ECMWF (as per Kepert et al. 2012)	United Kingdom Met. Office	Gridded 75 km.	3 hourly	√	x Keppert uses Finkele SMD/KBDI (BoM)	√	√	√	(1) Data is available every 3 hours.(2) Data is available every 75kms (3) There are many more variables available cf BoM observing stations, such as measures of atmospheric instability that have been shown to relate to fire danger.	(1) Rainfall is hard to estimate in reanalysis, therefore use other source such as BoM. (2) 75 km is relatively coarse resolution.	
	Datasets that could be used for validating other datasets											
	FFDI (derived by Lucas et al. 2010)	BOM, Australia	Point (77 BoM stations)	Daily FFDI	Daily Tmax	KBDI	3:00 PM	10 min average	x	The input data have been highly scrutinised.	There are only a few locations in SA. Despite the data being of the highest quality (relative to other data), in general the data is still not homogeneous due to the introduction of AWS in 1990s.	

A2.2 ANSWER TO QUESTION 1:

From the review of data the variables required for the calculation of the historical Forest Fire Danger Index shows that the data are available at point source and gridded format as shown in Table A2.2.

Table A2.2: Sources of data for the calculation of the historical FFDI available in South Australia.

Meteorological parameter	Sources			
Temperature (T)	BOM observing station	BOM gridded data set	SILO gridded data	AWAP gridded data
Precipitation (P)	As above	As above	As above	As above
Relative Humidity (RH)	As above	As above	As above (in the form of vapour pressure)	As above
Wind Speed (WS)		McVicar (CSIRO)		As above

A2.3 QUESTION 2: IF WE CAN USE GRIDDED DATA TO UNDERTAKE THE CALCULATIONS OF THE FFDI, WHICH ONE/S ARE SUITABLE TO USE IN REGIONAL SA?

Once the data sets had been identified we then undertook to identify which of the data sets would be best to use in regional SA.

A detailed review of observed and gridded rainfall data sets for South Australia was undertaken as part of the Goyder Project (www.goyderinstitute.org) to identify the differences between two gridded rainfall data sets and observed rainfall data for the state (Tozer et al 2012). The study compared Bureau of Meteorology observed data with synthetic gridded data sets developed by the Bureau of Meteorology (AWAP) and the Queensland Government (SILO data set). Although the AWAP and BOM rainfall grids have the same spatial resolution (0.05^o x 0.05^o, approximately 25 km^2), different methods were used to achieve the data and consequently there are differences between the two datasets (Figure A2.1).

Results of the comparisons across annual, seasonal and monthly time frames indicated that neither the AWAP or the SILO gridded rainfall accurately capture the spatial variability of rainfall within a grid cell, nor do they capture extreme events. However, SILO has a better fit to the BOM station data because the method used to create the grid enforces exact interpolation of the observed dataset (Jeffery et al 2001). The smoothing out of extreme rainfall events appears to be a common issue with gridded rainfall dataset (e.g. Beesley et al 2009, Silva et al 2007, Ensor and Robertson 2008).

Like rainfall, gridded temperature data is also different to point values. However, the difference is generally rather smaller due to the greater spatial homogeneity, and perhaps also to the less-dense observation network of the temperature observations (Finkele et al 2006). An example of the differences between gridded and point values for both rainfall and are shown in Figure A2.2 for Cranbourne, Victoria.

The difference between the FFDI calculated at observing stations and from gridded data is shown in Figure A2.3 (Lucas and Finkele 2006). Despite limitations in the gridded data set for rainfall, there is very good agreement between the two datasets for the FFDI. The authors state that “gridded FFDI may be used with confidence to identify high fire danger days”.

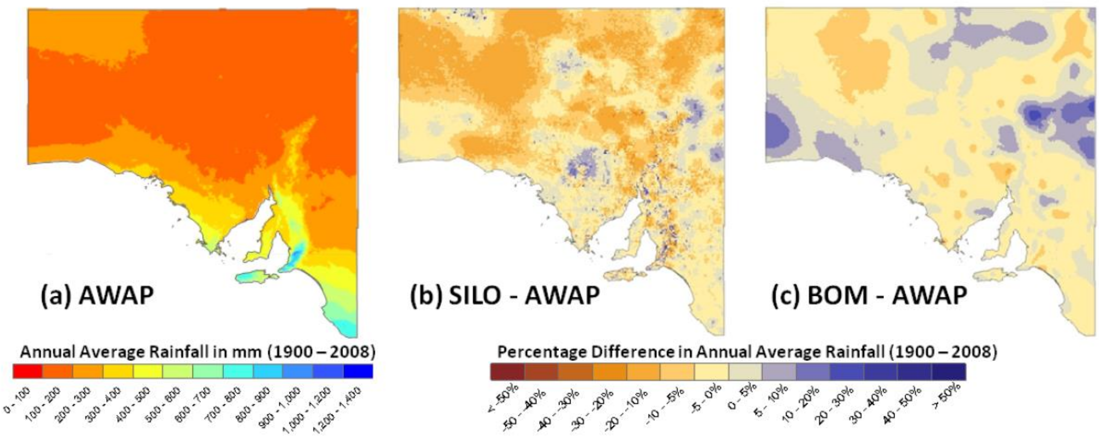

Figure A2.1: (a) Annual average rainfall for the AWAP gridded dataset; (b) percentage difference in annual average rainfall between the SILO and AWAP datasets;(c) percentage difference in annual average rainfall between the BOM and AWAP datasets (Source: Tozer et al et al 2012).

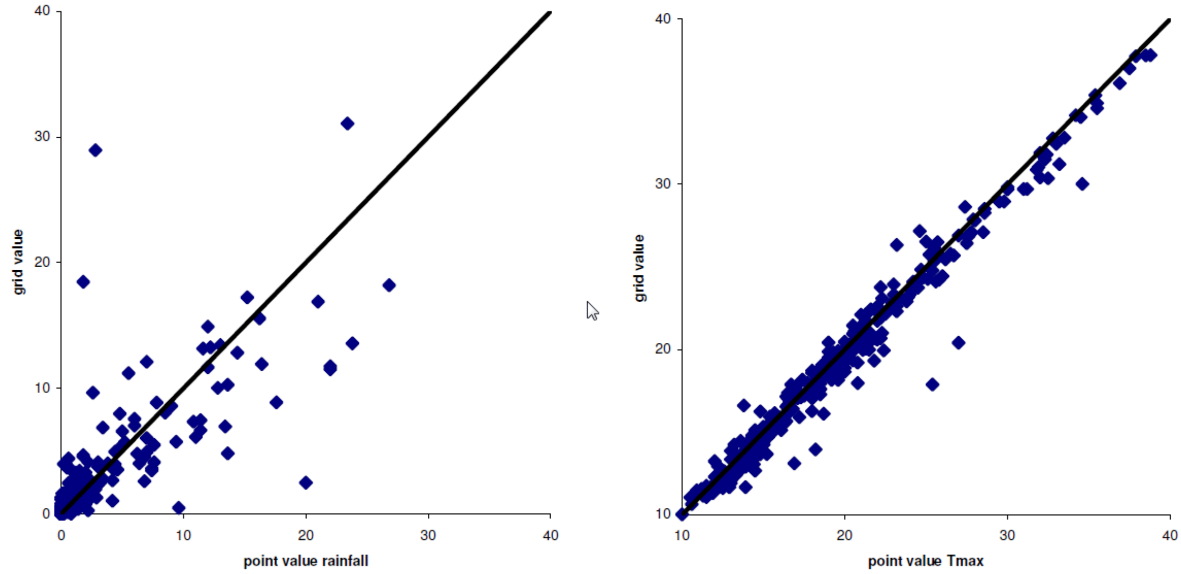

Figure A2.2: The difference between gridded and point values for daily rainfall (left) and daily maximum temperature (right) at Cranbourne, Victoria (Source: Finkele et al 2006).

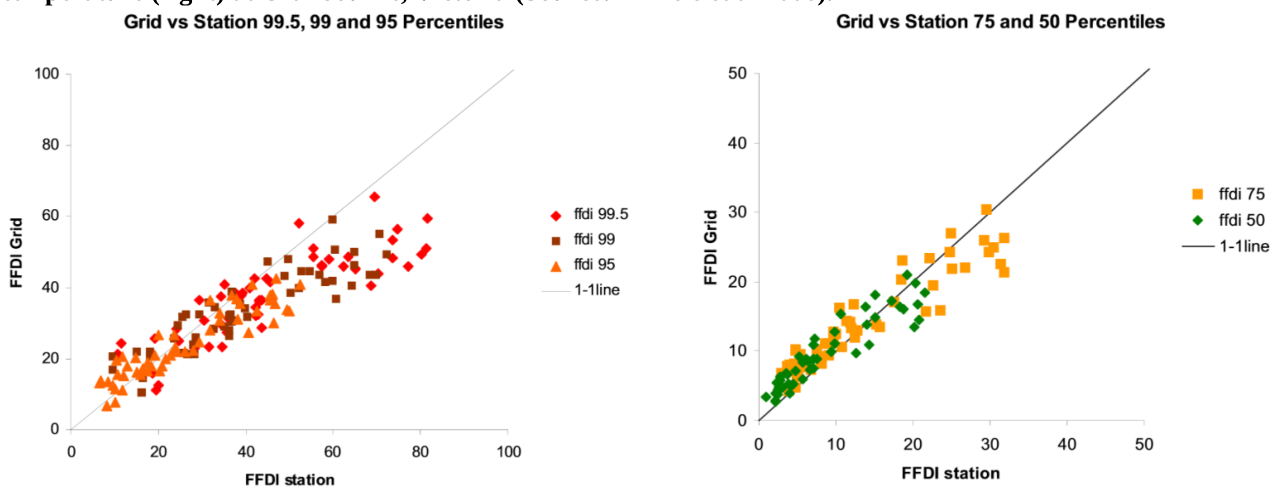

Figure A2.3: Scatterplots of FFDI calculated at 54 observing stations across Australia (1957-2003) and gridded FFDI at 25 km resolution (2000-2006) for the 99.5, 99 and 95 percentiles (left) and the 75 and 50 percentiles (right) (Source: Lucas and Finkele 2006).

A2.4 ANSWER TO QUESTION 2:

The answer to this question is that gridded datasets can be used as a proxy for observed point data (whether it is rainfall, temperature, or wind) although each are developed in slightly different ways and so have different strengths and weaknesses.

However, it is important to appreciate that gridded data is not observed data and may not be representative of the real situation, especially extreme rainfall events. This point is especially important if using gridded data for trend analysis. In this sense, there is no “best” gridded data set that can be used although some will be more useful than others in this assessment depending on the variables they include and their spatial and temporal resolution.

A2.5 QUESTION 3: IF THERE IS A RANGE OF DATA OPTIONS FOR USE IN THE ANALYSIS OF THE FFDI, WHICH METHODOLOGICAL APPROACH IS THE BEST FOR USE IN REGIONAL SA?

As would be expected from the number of studies that have examined the bushfire risk in Australia, a range of different methodological approaches were used. Studies were an assessment of either historical or future FFDI or GFDI and used either the historic observed or gridded data for analysis of past fire weather and global climate model outputs or modified historic data sets for future assessments.

Analysis considered a range of spatial scales from individual points, larger regions based on an average of points or a spatially gridded surface. Temporal scales also varied from the daily scale up to monthly, seasonal and even annual.

A summary of the methodological approaches used in each study is provided in the table on the following page (Table A2.3). Each of these approaches were considered and assessed for use in this study. A flowchart methodology was developed to map the various options (Figure A2.4) and the strengths and limitations of each were then assessed.

DATA AND METHODOLOGICAL OPTIONS TO ASSESS HISTORICAL FFDI FOR THIS STUDY

This section describes the methodological options for data selection for FFDI analysis. As identified in the review of previous studies, there are a number of datasets that have been used to calculate the historical FFDI and a number of options for their use. Figure A2.4 guides the reader through these options in the form of a flowchart methodology.

For the two study locations identified for this pilot study Spring Gully Conservation Park in the Clare Valley and the Mount bold reserve in the Adelaide Hills (See Chapter 4 of the main report), the closest Bureau of Meteorology observing stations are shown in Table A2.4. Spring Gully Conservation Park (SGCP) is at 33.9121^{o}S, 138.6125^{o}E and Mt Bold Reserve (MBR) is at 35.1176^{o}S,138.7055 ^{o}E. The two locations are approximately 135 km apart. The BOM stations shown in Table A2.4 have been selected because they have wind speed records. There may be observing stations closer to our study areas, however they have not recorded wind speed.

Table A2.3: Review of bushfire and climate studies in Australia and South Australia including methodology and data sets used.

Author/s	Date	Study locations	Historical	Future	Methodology	Data sets used	FFDI/GFDI	Outputs	Notes / Limitations
Williams, A.J. Karoly, D.J. Tapper, N.	2001	Eight GCM grids across northern and southern Australia.	√	√	Calculated changes in daily and seasonal fire weather and the McArthur FFDI using the CSIRO9 GCM to simulate current and double CO_2 climate. GCM outputs were validated using historical data at a number of point locations to compare GCM and observed daily FFDI distributions. Historical analysis used observed station data 1960-1992.	CSIRO-9 GCM forced for double CO_2	FFDI	Frequency distributions of daily fire weather and FFDI. Historical daily and seasonal fire danger and fire weather 1960-1992.	GCM outputs may underestimate extreme events in future climate. Temporal and spatial limitations of grid resolution for future climate projections. No sites in SA.
Hennessy, K.J. Lucas, C. Nicholls, N. Bathols, J. Suppiah, R. Ricketts, J.	2005	17 sites in NSW, ACT, VIC and TAS.	√	√	Fire danger indices were calculated for “present conditions” using historical weather records from 1974-2003. Two CSIRO global climate models (Mark 2 and Mark 3 downscalled to 50 km grids using the CCAM Mark 2 model) were then used to generate pojected changes in daily temperature, humidity, wind and rainfall for the years 2020 and 2050, relative to 1990. Changes were then applied to the historical data sets.	CSIRO Mark 2 GCM and CSIRO Mark 3 GCM.	FFDI	FFDI and GFDI for 2020 and 2050.	Temporal and spatial limitations of grid resolution for future climate projections. Use of historical data adjusted by GCM outputs retains observed distributions and so captures full variabiity but does not allow for shift in distribution shape. No sites in SA.
Pitman, A.J. Narisma, G.T. Mc Aneney, J.	2009	Across all Australia at a resolution of 56 km grids.		√	Assessed the impact of climate change on the risk FFDI and GFDI in Australia for January using a high resolution regional climate model (RAMS) driven at the boundaries by data from a transitory coupled climate model. Two future emission scenarios (relatively high and relatively low) were used for 2050 and 2100 and four realisations for each scenario were run.	AUSLIG data set to identify vegetation cover. CSIRO Mark 2 to force the boundaries of RAMS.	FFDI & GFDI	Probability density function for the fire risk for a single point in New South Wales for January 2050 and 2100. Mapped change in FFDI and GFDI for all Australia for January 2050 and 2100.	Analysis for January only. GCM outputs may underestimate extreme events in future climate. Change in probability distribution undertaken for one location only.
Hasson, A.E.A. Mills, G.A. Timbal, B. Walsh, K.	2009	850 hPa temperature gradient as indicator of cold front activity.		√	Analysed the 850 hPa temperature gradient from ten GCMs from the Coupled Model Intercomparison Project to estimate the frequency of cold front events at the middle and end of the 21st Century for low and high greenhouse gas emissions scenarios.	Ten GCMs from the Coupled Model Intercomparison Project.	Neither	The change in the frequency of cold fronts responsible for extreme fire weather across southern Australia.	Analysis of only one weather parameter.
Lucas, C.	2010	77 locations across southern Australia. In SA: Adelaide, Ceduna, Port Lincoln, Mt Gambier, Renmark, Snowtown, Woomera.	√		Development of a national historic fire weather data set. Calculated the FFDI for each location.	Bureau of Meteorology observing station data.	FFDI	Fire weather data set.	Development of data set only. Analysis of inhomogeneities in the data sets for temperature, rainfall, wind and humidity and impact of those on the FFDI. No analysis of the FFDI undertaken.
Douglas, G.	2011	30 locations in 21 fire regions in NSW.	√		Historical analysis of FFDI and GFDI for 16 stations across New South Wales using BOM data.	BOM station data.	FFDI & GFDI	Historical change in FFDI and GFDI.	Preliminary results only - find follow up report. No sites in SA.
Clarke, H.G. Smith, P.L. Pitman, A.J.	2011	Four 600,000 km^2 regions in eastern Aust: Central QLD; southern QLD /northern NSW; southern NSW; VIC.		√	World Climate Research Program’s (WCRP) Coupled Model Intercomparison Project phase 3 (CMIP3) multimodel dataset used to calculate daily FFDI for current climate (1961 to 2000), 2050 climate (2046 to 2065) and 2100 climate (2081 to 2100). Model runs used the A2 SRES future. Models selected had the highest skill score over Australia (Perkins et al. 2007). MRI ranked fifth but was included because daily data for all variables were not available for MIROC-m, which would otherwise have been used.	CMIP3 multi-model daily archive. CSIRO, ECHO-G, IPSL and MRI.	FFDI	FFDI distributions for current, 2050 and 2100 for each study region.	East coast regions only. The CMIP3 archive includes simulations of past, present and future climate so the same data set can be used for all analysis. However, no validation was made with observed FFDI. GCM outputs can underestimate future extreme events. No sites in SA.
King, K.J. Cary, G.J. Gill, A.M. Moore, A.D.	2012	Three sites in south eastern Australia near Canberra, Sydney and Melbourne.	√	√	Assessed effect of both a changing climate and atmospheric CO_2 combinations on grass curing, fuel load, and thus GFDI and potential fire-line intensity for an A1B emissions scenario for 2030, B1 for 2070 and A1FI for 2070. Patched point historical, daily weather datasets (Jeffrey et al. 2001) were used as input for GRAZPLAN modelling. Daily weather was derived for alternative future climates by applying the 50th percentile (median) projected seasonal changes in temperature, rainfall, wind speed, relative humidity and solar radiation to each historical daily weather value (1 January 1965 to 30 April 2011) for each location. Future climate scenarios were 2030 under the A1B SRES emissions scenario with 450 ppm CO_2; 2070 under the B1 emission scenario with 518 ppm CO_2 and 2070 under the A1FI emission scenario with 707 ppm CO_2.	GRAZPLAN model to calculate grass growth and curing rates. Suite of GCM output mean changes applied to historic weather data. Projected atmospheric CO_2 concentrations from the Bern Carbon Cycle model.	GFDI	Change in grass growth rates, curing and GFDI for each location for each future climate year.	Good assessment of GFDI. FFDI not included. Future climate a current climate mean shifted by GCM output average changes for each parameter - not a single model output and so might have issues about loss of model output integrity. No sites in SA.
Lucas, C. Hennessy, K. Mills, G. Bathols, J.	2007	28 stations across south east Australia. In SA: Adelaide, Ceduna, Woomera, Mt. Gambier.	√	√	Historical data were analysed to determine trends and the current number of days when the fire danger rating exceeded high, very high, severe, extreme and catastrophic. Future climate changes used two CSIRO global climate models to calculate daily values for temperature, humidity, wind and rainfall for the years 2020 and 2050, relative to 1990. The modelled changes from the various scenarios were then projected onto the observed daily time series of temperature, rainfall, wind and relative humidity from 1973 to early 2007.	Observed historic data set from BOM stations. CSIRO CCAM Mark 2 and Mark 3 for future simulations as per Hennessy et al. 2005.	FFDI	Change in the the annual cumulative FFDI and the number of high, very high, severe, and catastrophic fire days at each location.	Point locations only. Only four sites in SA. Change factor methodology.
Clarke, H. Lucas, C. Smith, P.	2012	38 stations across Australia, most in the south east. SA stations as above.	√		Examined changes in Australian fire weather as measured by the FFDI between 1973 and 2010. No future climate change considered.	Observed historic data set described in Lucas et al 2007.	FFDI	Observed change in FFDI for each location.	Historical study only. Point locations only. Only four sites in SA.

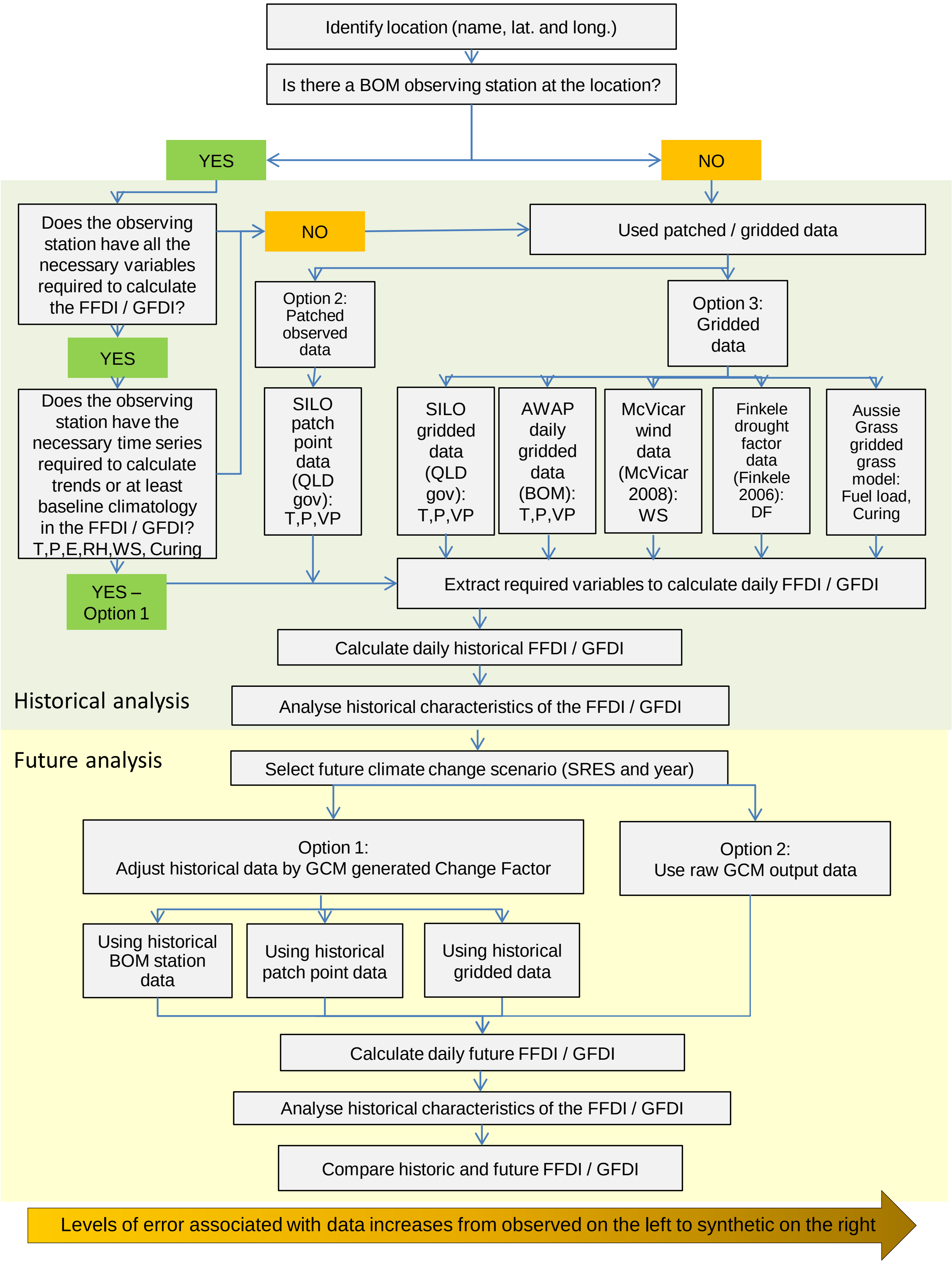

Figure A2.4: Flow chart of data and methodological approaches to the analysis of historical and future changes in the Forest Fire Danger Index (FFDI) and Grassland Fire Danger Index (GFDI). GCM refers to Global Climate Model data.

Table A2.4: Bureau of Meteorology recording stations close to the two pilot study areas at Spring Gully Conservation Park in the Clare Valley region and Mt. Bold Reserve in the Adelaide Hills. SILO PPD refers to the SILO Patched Point Dataset.

Station	Name	Coordinates	Distance from SPCP	Start	End	Available on SILO PPD
021014	Clare Post Office	33.84°S,138.61°E	8.22 km	1957 Jan	1994 Aug	Yes
021131	Clare High School	33.82°S, 138.59°E	9.68 km	1994 Apr	2014 Sept	No. Nearby locations include: Clare Hill River, Clare Calcannia, Clarendon
Station	**Name**	**Coordinates**	**Distance from MBR**	**Start**	**End**	**Available on SILO PPD**
023887	Kuitpo Forest Reserve	35.17°S, 138.68°E	6.4 km	1998	Present	No, Nearby location: Clarendon

Using the flowchart methodology developed for the selection of data, for the pilot study area Option 1 on the left side of the chart identifies the use of BOM observing station data using the stations available. Lucas (2010) calculated an FFDI at two locations relatively close to our pilot study areas: Snowtown (approximately 40 km away from SGCP) and Adelaide (approx. 25 km away from MBR).

The difference in topography and fire management strategies between our locations and those of Lucas is considered significant by fire managers. Consequently it is desirable to assess climate change impacts as close as possible to the selected study areas. However, previous studies (e.g. Dowdy et al, Lucas 2010, Clarke et al 2011) have identified that the limiting factor when using BOM stations is the quality and length of wind recordings – a necessary parameter for the calculation of the FFDI. Consequently the choice of station for FFDI analysis has been limited (Table A2.5).

Option 2 in the flowchart uses patch point data sets. Some, but not all, station data from BOM are in the SILO Patched Point Data set (Jefferies et al 2001). The Patched Point data set is observed data (from BOM observing stations) in which any missing or 'suspect' values are replaced ("patched") by interpolated values from nearby stations (Jeffery et al 2001). All patched stations extend back to 1910 using the interpolated data if observed data is not available. Of relevance to this study is data for the Clare Post Office (BOM Station Number 21014).

Option 3 in the flowchart uses gridded data sets. As described in earlier, interpolated (gridded) datasets are estimated data calculated using real data from nearby observing stations (Table A2.5). The primary limitation in using gridded data is that they do not necessarily represent accurately what happened at a particular location. The assessment by Tozer et al (2012) showed that in SA there are in some locations significant differences between the data at an observing station and that of the corresponding grid cell.

Table A2.5: A summary table of the two data options to assess historical FFDI.

<table>
<tr><th colspan="4">Option 1 and 2: BOM point location for SPCP and MBR</th></tr>
<tr><th>METHOD</th><th>STRENGTHS</th><th>LIMITATIONS</th><th>SOLUTIONS</th></tr>
<tr><td>Option 1: Obtain historical observed data from the closest BOM station. E.g. Clare (See Table 1.)

OR
Option 2: Use the patched point data from SILO in combination with this data.</td><td rowspan="2">This dataset is the easiest for clients to obtain, use, and understand.

Data is a record of actual observed events.

Data is checked and errors identified and fixed by the BOM.</td><td rowspan="2">Poor quality data and possible large temporal gaps for some locations.

Not all the required parameters are recorded at every location.

There are not enough years to undertake a trend analysis in many cases.</td><td rowspan="2">Compare data with that at a relatively close station that has been used before, e.g. Snowtown (as in Lucas 2007). See Table 3 for station specifics.

Using statistical relationships between the two locations extend the dataset for the necessary number of years.

OR simply do not do trend analysis, but rather limit analysis to distributions of monthly FFDI, number of days FFDI >50, etc for the period available.</td></tr>
<tr><td>Calculate input variables for FFDI. Calculate FFDI.</td></tr>
<tr><th colspan="4">Option 3: Gridded data sets for SPCP and MBR relevant grids</th></tr>
<tr><th>METHOD</th><th>STRENGTHS</th><th>LIMITATIONS</th><th>SOLUTIONS</th></tr>
<tr><td>Either AWAP or SILO: Obtain T, VP, and P.
Spatial resolution: 0.01^{o} grid</td><td rowspan="4">Provides high resolution coverage across regional areas that might not be near an observing station.</td><td rowspan="4">The data is not a record of actual observed events; it is interpolated and so values will not always be an accurate representation of what occurred at every location.

The grids of each of the different datasets may not align with one another.</td><td rowspan="4">Realignment of data can be undertaken using software such as ferret, or user simply drills down to a location and undertakes a point analysis instead.

Calculate the FFDI using both the observed and gridded data at a nearby point to determine the scale of difference between them.

Make user aware of the limitations of gridded data by providing caveats to the outputs whilst also explaining that use of interpolated data is common - interpolated data is used whenever any point data is used to create a map.</td></tr>
<tr><td>McVicar: Wind Speed.
Spatial resolution: 0.01^{o} grid</td></tr>
<tr><td>Finkele: Drought Factor:
Spatial resolution: 0.25^{o} grid</td></tr>
<tr><td>Calculate FFDI.
Spatial resolution: either 0.01^{o} or 0.25^{o} grid, depending on if the Finkele data is used.</td></tr>
</table>

DATA OPTIONS TO ASSESS FUTURE CHANGES TO FFDI FOR THIS STUDY

In the climate change literature, there are a range of methods used to create future climate scenarios. Examples from the fire-climate change literature include the following options:

1) direct GCMs output data is used as per that from a Regional Climate Model in Pitman et al 2007;
2) use of a monthly change factor derived from a GCM that is applied to historic FFDI input variables as in Lucas et al, (2007); and
3) the historical FFDI input weather variables are adjusted by an factor of choice as per Cary and Bank (1999).

Projections of changes to fire danger as a result of climate change have only been done for four point locations in South Australia – Adelaide, Ceduna, Mt. Gambier and Woomera in a single study by Lucas et al (2007). More options identified from the literature review are shown in Table A2.6.

Table A2.6: An example of studies that have used GCM future climate scenarios for future fire analyses.

STUDY	REGION	GCM	METHOD	OTHER
Lucas et al 2007	28 point locations across SE Australia.	CSIRO GCM with CCAM, 2020, 2050	Change factors on daily historical data (adjusted historical data)	
Pitman et al 2007	Across all Australia at 156 km grids	CSIRO GCM with RAMS, 2050, 2100, SRES: B2, A2	Used GCM direct output	DF was fixed at 10.
Hasson et al 2009	Synoptic over Australia	10 GCMS, 2050, 2100, B1, A2	Assessed the 850 hPa temperature gradient as a proxy for significant frontal events	
Clarke et al 2011	38 stations across eastern Australia in four areas based on rainfall seasonality.	CSIRO, ECHO-G, IPSL, MRI (as selected by Perkins et al 2007), 2050,2100. A2. Resolution ranges between 1.9o & 3.9o.	Direct GCM output. Significant differences between GCMs in baseline simulation of FFDI. No comparison with historical.	DF: uses the Finkele et al 2006 correction. Uses daily averages of WS & RH, not 3 pm.

To create a future climate scenario for the two locations identified for this study, and to meet the project partner requirements for high spatial resolution, we identified three possible data approaches for the assessment of future changes to the FFDI. The options are detailed in Table A2.7. There is often a perceived need for downscaled GCMs. The CSIRO downscaling model (CCAM) and the BOM SDM have been applied to only a few GCMs and only for temperature and precipitation. In addition, we emphasise that downscaled GCMs may not provide any added utility as there may be no extra information about the climate change at the finer resolution.

Table A2.7: A summary table of the data options to assess FFDI climate change scenarios.

<table>
<tr><th colspan="4">Option 1: Use the Patterns of Changes statistically downscaled GCM output (Ricketts and Page 2007): adjusted historical data (SILO Consistent Climate Change Scenarios).</th></tr>
<tr><th>METHOD</th><th>STRENGTHS</th><th>LIMITATIONS</th><th>SOLUTIONS</th></tr>
<tr><td>SILO Consistent climate change scenarios database (CCCS): Obtain T, VP, and P.</td><td rowspan="4">VP is available – this is not found in many GCMs (as commented by Clarke et al 2011)</td><td rowspan="4">Adjusting historical time series captures the bias of a GCM.

Assumes a linear relationship between annual mean global warming and regional climate (i.e. temperature, precipitation, humidity and wind speed).</td><td rowspan="4">In terms of using WS data from another GCM data set, it is helpful to consider that Clarke et al 2011 conclude that changes in WS did not contribute to the changes in FFDI.</td></tr>
<tr><td>Wind speed: change observed data according to estimates from GCMS.</td></tr>
<tr><td>Calculate daily FFDI.</td></tr>
<tr><td>Analyse future characteristics of the FFDI and compare with historical.</td></tr>
<tr><th colspan="4">Option2: Use direct downscaled GCM output: (CCAM, Bertrand Timbal data sets)</th></tr>
<tr><th>METHOD</th><th>STRENGTHS</th><th>LIMITATIONS</th><th>SOLUTIONS</th></tr>
<tr><td>Obtain GCM data: CSIRO3.5</td><td rowspan="3">State of the art climate representation at a regional scale.</td><td rowspan="3">The GCMs still have biases in them (a problem with all models and datasets).

Still a fairly coarse grid scale.

Relatively hard for a non-programmer to access.

Historical 20th century runs are not actual observed or interpolated data sets – purely synthetic and so can't be compared directly with historical data.</td><td rowspan="3">Don't compare outputs from the GCM analysis with the historical baseline assessments - just describe change. Approach doesn't allow for the use of some metrics e.g. Probability Distribution Functions (PDFs).</td></tr>
<tr><td>Calculate daily FFDI</td></tr>
<tr><td>Analyse future characteristics of the FFDI and compare with historical.</td></tr>
</table>

A2.6 ANSWER TO QUESTION 3:

On the basis of the detailed review of data and methodological options assessed above, and discussion with Darren Ray (Climatologist, Bureau of Meteorology), the following approach for assessing historical and future bushfire changes for this study were developed.

HISTORICAL FFDI CALCULATIONS FOR THIS STUDY

The historical data is selected as follows:

1. Source observed BOM station data for Clare and Kuitpo Forest Reserve through the SILO patched point database and the BOM observed records. The SILO dataset contains the BOM observed records for rainfall, temperature, and vapour pressure with the gaps patched, and the

data from BOM contains the wind speed. The advantage of using SILO rather than BOM directly is twofold: (1) missing data have already been in-filled, and (2) the future climate scenario Change Factors have already been calculated for those locations for use in the climate change step.

FUTURE CLIMATE CHANGE FFDI CALCULATIONS FOR THIS STUDY

For the assessment of future changes to the FFDI, Option 2 from the flowchart and Table A2.5 (the SILO change factors data set) was used as it allowed for a comparison of historic and future changes in the FFDI using the same data set but with the added value of GCM data adjustments that have already been calculated:

1. Use data from SILO's Consistent Climate Change Scenarios (CCCS) for the two locations stations for rainfall, temperature, and vapour pressure for four GCMs. These data have already been perturbed using the Change Factors provided in the relevant SILO metadata files. Change Factors for wind speed are also provided and we applied them to the observed wind speed from the observing stations.
2. Based on previous studies and expert opinion, outputs from the following GCMs were used: HADGEM1, GFDL2.1, and MIROC3.3.

This approach is shown on the methodological flowchart developed on the following page as a pathway highlighted in red (Figure A2.5).

A2.7 QUESTION 4: ONCE A METHODOLOGICAL APPROACH HAS BEEN DETERMINED, WHAT ANALYSIS OF THE DATA NEEDS TO BE DONE TO DESCRIBE THE HISTORICAL AND FUTURE CHARACTERISTICS AND TRENDS IN THE FFDI?

The analysis of historic and future changes in the FFDI can be calculated in a number of ways and at a number of temporal scales.

A2.8 ANSWER TO QUESTION 4:

Based on previous studies we proposed the following calculations so as to allow for comparison with Lucas et al (2007):

- Change in the annual cumulative FFDI (∑FFDI, as per (Beer and Williams 1995)). This value is the sum of the daily FFDI for each year;
- The monthly ∑FFDI was also examined – the sum of the daily FFDI for each month;
- Changes in number of days the FFDI exceeds a particular threshold; and
- Changes in the frequency of certain threshold events. Lucas et. al. (2007) used the number of 'very high' and 'extreme' days - the number of days where the FFDI >25. We also examined the number of days of the FFDI >40 (as per Blanchi, Lucas et al. 2010), and FFDI > 50 (as per Bradstock and Gill 2001).

In a study in the Sydney region Bradstock and Gill (2001, 2010) found the probability of property destruction approached 100% when the FFDI exceeded 40 (50 in forested areas), given a fire is burning at the time.

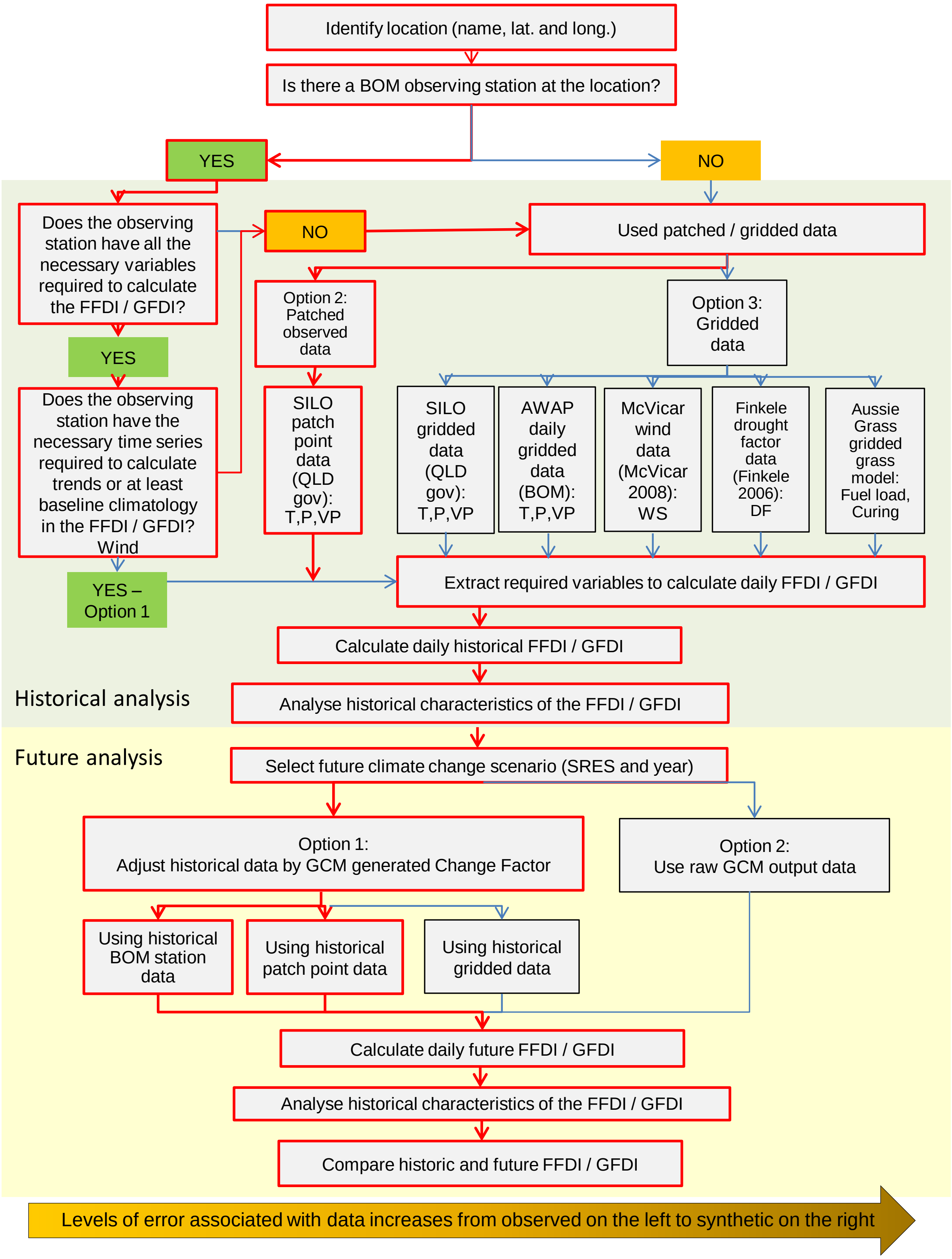

Figure A2.5: Pathway through the methodological flow chart developed that was used for the analysis of historical and future changes in the Forest Fire Danger Index (FFDI) and Grassland Fire Danger Index (GFDI) in this study. GCM refers to Global Climate Model data.

APPENDIX 3 – ANALYSIS AND RESULTS

A3.1 INTRODUCTION

For the two study areas, Spring Gully Conservation Park (SGCP) and Mt Bold Reservoir (MBR) a range of metrics were used to assess the possible change to fire danger climatology that may occur with global climate change. Historical fire danger was assessed using the FFDI model with daily historical observed data. The FFDI was then calculated using daily data modified by a climate change scenarios to integrate projected changes into precipitation, temperature, relative humidity, and wind speed. The observed historical fire danger was then compared with that of the period 2046 to 2065 ("2050").

Appendix 2 discussed in detail the process by which we arrived at this choice of data and method. We further discuss the data and methodology as applies to this analysis in more detail below.

A3.2 DATA

The FFDI requires daily 3pm temperature, relative humidity, precipitation, and wind speed. These variables were described in detail in Appendix 2 including the accepted use of 3 pm values rather than daily maximum/minimum values. A detailed assessment of appropriate data for this assessment followed the methodology developed in Appendix 2 and considered all available data sets for the two chosen study locations.

The key selection criteria when deciding on a data set for the historical analysis is whether it has the required climate parameters and if the data set spans a time period that is long enough to capture a significant proportion of the natural year to year variability. In their assessment of fire weather across Southern Australia, Lucas et al (2007) only used data sets that met certain criteria. One criterion was simply the location of the station; a national data-set was sought, ideally with a spatial scale of several hundred kilometres between stations. A second criterion was the presence of a generally complete record of observations during the time period chosen from 1971-2007. Finally, stations that are representative of the broader area were sought, so that the value at a given station can be confidently applied outside the immediate locale of the station. Consequently they only chose seven locations in SA. In choosing these seven observing stations they still had missing data to contend with.

There are, however, other observing stations that, in addition to those in Lucas et al (2007), can be used. We investigated the availability of the BOM observing stations available from the Patched Point Dataset in SILO rather than BOM itself (Queensland Government SILO database at http://www.longpaddock.qld.gov.au/silo, Jeffrey et al. 2001). This approach has the advantage of using a data set that has no missing data as in the BOM observed data because SILO uses an "infilling" process to ensure the data are both rigorous and complete (Jeffrey et al 2001). The other added advantage in using SILO, is that the Consistent Climate Change Scenarios dataset of future climate for a range of GCM outputs have already been created based on the SILO historical dataset. In addition, to use both the SILO historical and the SILO CCCA data provides some consistency.

The BOM high quality gridded data set (AWAP) would provide continuous spatial coverage of the State. However, it contains only rainfall and temperature data and so for this analysis did not provide all the required variables. In addition, the technique used to fill gaps in the spatial extent of the dataset does not force the synthetic surface to match the observed historical records for the grids that overlap a recording station. So, rainfall and temperature records from an AWAP grid that correspond with an observed observing site may be different to the observed values and may be disconnected to other parameters such as wind or evaporation that would have been observed at the site.

On the basis of the detailed assessment of data for the historical analysis and flow chart methodology developed, we used a slightly different approach for SGCP than for MBR, described as follows. Neither of the two study areas, SGCP and MBR are within the BOM observing network and so are not in the SILO Patch Point database either. As use of observed data is preferable to gridded data where it is available we selected the nearest stations with **all** of the required data as proxy locations for SGCP and MBR. The observing stations closest to SGCP and MBR are the Clare Post Office and Kuitpo (Bureau of Meteorology site numbers: 021014 and 023887 respectively). The benefits of using the observed data from the SILO Patch Point data base have been explained (in summary in Section 3 and in detail in Appendix 2) and so we examined data availability for the Clare Post Office and Kuitpo. Clare Post Office is in the SILO Patch Point Database, however, Kuitpo is not. Therefore, for Clare Post Office we obtained historical daily maximum temperature, rainfall data and vapour pressure data from 1960 to 2010 from SILO, and for Kuitpo we obtained the data from BOM historical records from 1998-2014.

Wind speed data is not available in the SILO database, as discussed in Appendix 2. As Lucas et al. 2007 identified, the poor quality of wind data in the observing station network is the primary reason why long term studies of FFDI have only been done for a very limited number of locations. Examining the BOM observing station network, the closest stations to SGCP and MBR that recorded daily wind speed (at 3 pm and 10 meters height) were Clare Post Office (site number 021014) and Kuitpo (site number 023887). Years of availability (between 1960 and 2010) are 1960 to 1994 for Clare PO, and 1998 to 2010 for Kuitpo. There were some missing data and these have been in-filled using the long term median value. An analysis of the differences in wind speeds in the study area was undertaken and results provided here (Figure A3.1).

A range of climate parameters have also been recorded by the SA Water observation station at Mt. Bold Reservoir. However, the recording station is situated over water and only extends from 2007 – 2012. This is not a sufficient time period to perturb when producing a future climate scenario. After examination of the data set it was not used in this study.

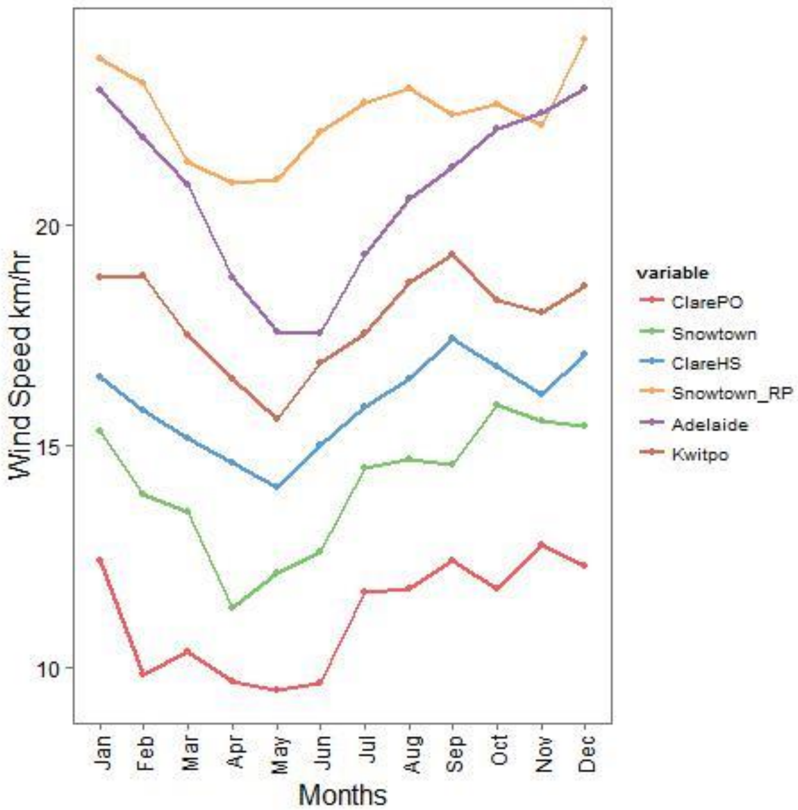

Figure A3.1: Monthly mean 3 pm wind speed for key observing stations near the SGCP and MBR sites.

CLIMATE CHANGE SCENARIOS

For the climate change analysis, future climate scenarios for the 30 year period around 2050 were obtained from the SILO Consistent Climate Change Scenarios (CCCS) database (Burgess, Ricketts et al. 2012). As per the historical data, the key variables required for the fire danger model are future projections of maximum temperature, relative humidity, rainfall, and wind speed data. Initially we explored both the A1FI and A1B SRES scenarios (Special Report on Emission Scenarios) to capture a high emissions scenario (A1FI) and a moderate emissions scenario (A1B) (Nakicenovic and Swat 2000). However, given the current trajectory of emissions (Fuss, Canadell et al. 2014), we have used the A1FI scenario as the most likely, albeit worst-case, scenario.

There are many methods available to generate future climate projections from GCMs (Solomon, Qin et al. 2007). The climate data used in this study was obtained from the CCCS using the Change Factor methodology developed by the CSIRO (Whetton, Katzfey et al. 2001). The Change Factor technique changes the climatological mean of a specific climate variable from its historical value to a future value. The resolution of the final climate change scenario data is the same as the historical data set. The CCCS has utilised the OZCLIM methodology (Page and Jones 2001) to transform the 1975 to 2004 baseline climatology SILO historical daily climate data into monthly climate scenarios for the year 2050. The Change Factor is calculated on a monthly basis for each grid cell, an example of which is shown in Figure A3.2. Despite the limitations of the CF methodology (the main limitation is there is no change in daily frequencies), this 'patterns of change' concept is widely used and described by (Hennessy, Lucas et al. 2005; Whetton, McInnes et al. 2005; Ricketts 2009).

Three Global Climate Models (GCMs) were selected from the CMIP3 collection of climate models: MIROC-H; HADGEM1; and GFDL-21. The websites that contain the documentation for each GCM and a wealth of additional information are as follows:

MIROCH (http://www.ccsr.u-tokyo.ac.jp/kyosei/hasumi/MIROC/tech-repo.pdf),
GFDL2.1 http://nomads.gfdl.noaa.gov/CM2.X/references/
HADGEM http://www-pcmdi.llnl.gov/ipcc/model_documentation/HadGEM1.htm

This choice of GCMs was based on four criteria:

1. The GCM has good atmospheric chemistry, including ozone that is important for the simulation of changes in higher latitude circulation systems;
2. The GCM has an 'ENSO-like' oscillation of ocean temperatures that are a driver of some of the climate variability in Australia;
3. The GCMs ranked highly in the reviews of CMIP3 GCMs by Watterson (2012), Smith and Chandler (2010), and Suppiah et al. (2007); and
4. The GCMs represented a range of climate futures.

In summary, the projected changes in daily temperature, humidity, wind and rainfall were generated by the GCMs for the year 2050, relative to 1990 (the reference year used by the IPCC). These projections can also be expressed as a pattern of change per degree of global warming. The patterns were scaled for the year 2050 using estimates of global warming for those years. We used 'medium' levels of global warming sensitivity. Note that although the SILO CCCS database does not contain a wind speed time-series, it does contain the monthly Change Factors for wind speed. These Change Factors were applied to the wind speed data from our historical observing stations. Note that as Kuitpo is not in the SILO Patch Point database we obtained the Change Factors for Clarendon which is in the same GCM gridbox (Figure A3.2).

The modelled changes from the various scenarios are then projected onto the observed time series of temperature, rainfall, wind and relative humidity from 1960-1994 for Clare PO, and 1998-2010 for Kuitpo. This methodology provides an estimate, based on the observed historical weather, of what a realistic time series affected by climate change may look like. By using this procedure, the natural inter-relationships between the variables that make up the FFDI are maintained.

The length of time-series in the future analyses is the same as that for the historical analysis. That is, for SGCP the historical data extends from 1960-1994 (34 years) and the 2050 dataset is therefore also 34 years long. The MBR data as represented by the Kuitpo wind data extends from 1998 to 2010 (12 years) and therefore the 2050 dataset also extends for 12 years.

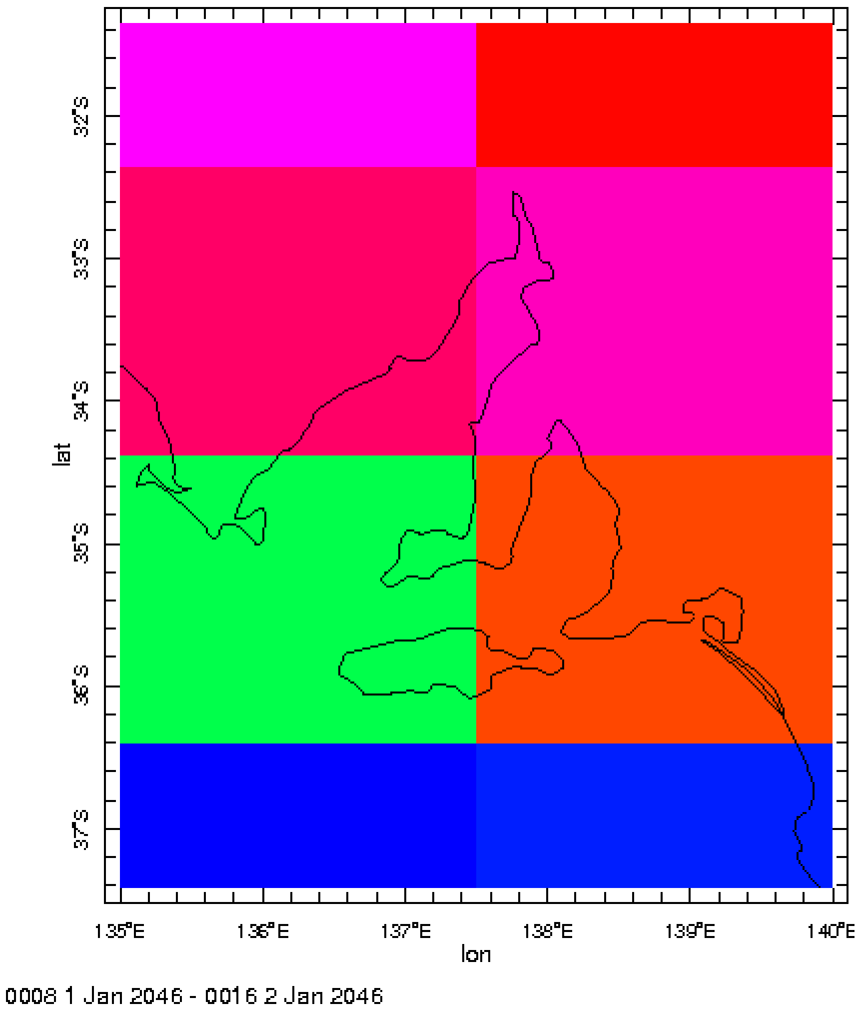

Figure A3.2: The grid resolution of the GFDL-21 GCM.

A3.3 METHODOLOGY USED AT THE PILOT STUDY AREAS

For both the historical and future climates the following was calculated:

- Change in the annual cumulative FFDI (∑FFDI, as per Beer and Williams 1995). This value is the sum of the daily FFDI for each year;
- The monthly ∑FFDI was also examined – the sum of the daily FFDI for each month;
- Changes in number of days the FFDI exceeds a particular threshold;
- Changes in the frequency of certain threshold events. Lucas et. al. used the number of ‘very high’ and ‘extreme’ days - the number of days where the FFDI >25. We also examined the number of days of the FFDI >40 (as per Blanchi et. al. 2010), and FFDI > 50 (as per Bradstock and Gill 2001).

Note: In this study, historical trends were not computed because of the limited availability of long-term daily data. The SGCP analysis extends from 1960 to 1998, and the MBR analysis extend from 1998 to 2010, neither of which is long enough to accurately identify historical trends.

A3.4 ANALYSIS

As per the methodology outlined in Appendix 2, metrics were calculated using the historical data sets. Next the metrics were calculated using the Change Factor adjusted historical data sets for each of the three GCM projections for the year 2050. Then, each of the fire weather parameters of the FFDI calculated using the historical data were compared with the 2050 projections. This was followed by a comparison of historical and future FFDI metrics.

STATISTICS

The results from this analysis are displayed below using cumulative distribution functions (CDF), kernel density estimates and box and whisker plots.

The CDF is a technique for clearly displaying the median (50th percentile), and any other percentile. For example what is the likelihood of a year with a ∑FFDI greater than or less than 3000.

The kernel density estimate is a non-parametric way to estimate the probability density function of a variablehttp://en.wikipedia.org/wiki/Random_variable. The kernel density estimate is similar to a histogram except there is no dependence on the end points of the bins (Hwang, Lay et al. 1994).

The box and whisker plots display variations of the data and are non-parametric. The spacing between the different parts of the box indicates the degree of dispersion (spread) and skewness in the data, and shows outliers. The bottom and top of the box are the first and third quartiles, and the band inside the box is the second quartile (the median). The vertical lines (whiskers) indicate the variability outside the upper and lower quartiles and show the data within 1.5 inter-quartile range of the lower and upper quartiles. The individual points are the outliers.

ANALYSIS OF CHANGES IN KEY METEOROLOGICAL VARIABLES

Mean total monthly rainfall (Figure A3.3) is slightly different at the two sites. Although they both have peak winter rainfall and the driest months in summer, at MBR the wettest months are June-July whereas at SGCP the wettest months are July-August. The driest months also occur a month earlier at the southern site as January-February at MBR is equivalent to February-March at SGCP.

The 2050 projections for rainfall are similar between the three GCMs: Miroc-H shows little change in rainfall (slightly drier in the spring months); GFDL-21 is significantly drier especially in winter-spring; and HADGEM1 is midway between the other two GCMs and shows the greatest decrease in autumn. At both locations, in all GCMs, the March rainfall has a greatest percentage decrease compared with January-February and has the effect of extending the dryness of summer. In terms of the possible rainfall seasonality in 2050 there is significant difference between the projections, more so than for any other variable (Figure A3.3).

Both locations have a similar annual cycle of mean daily wind speed (Figure A3.4), although at different magnitudes: MBR generally has higher wind speeds. Mean daily wind speed is greatest in spring/summer and lowest in early winter. This annual cycle is projected by all GCMs to continue in 2050 and become more pronounced with a greater difference between the May minimums and spring/summer maximums. Although all three GCMs project a large decrease in May wind speeds, and an increase in late summer wind speeds, there is a range of projections for the other months of the year. MIROC-H projects a decrease in winter/spring wind speeds at both locations, and HADGEM1 projects an increase.

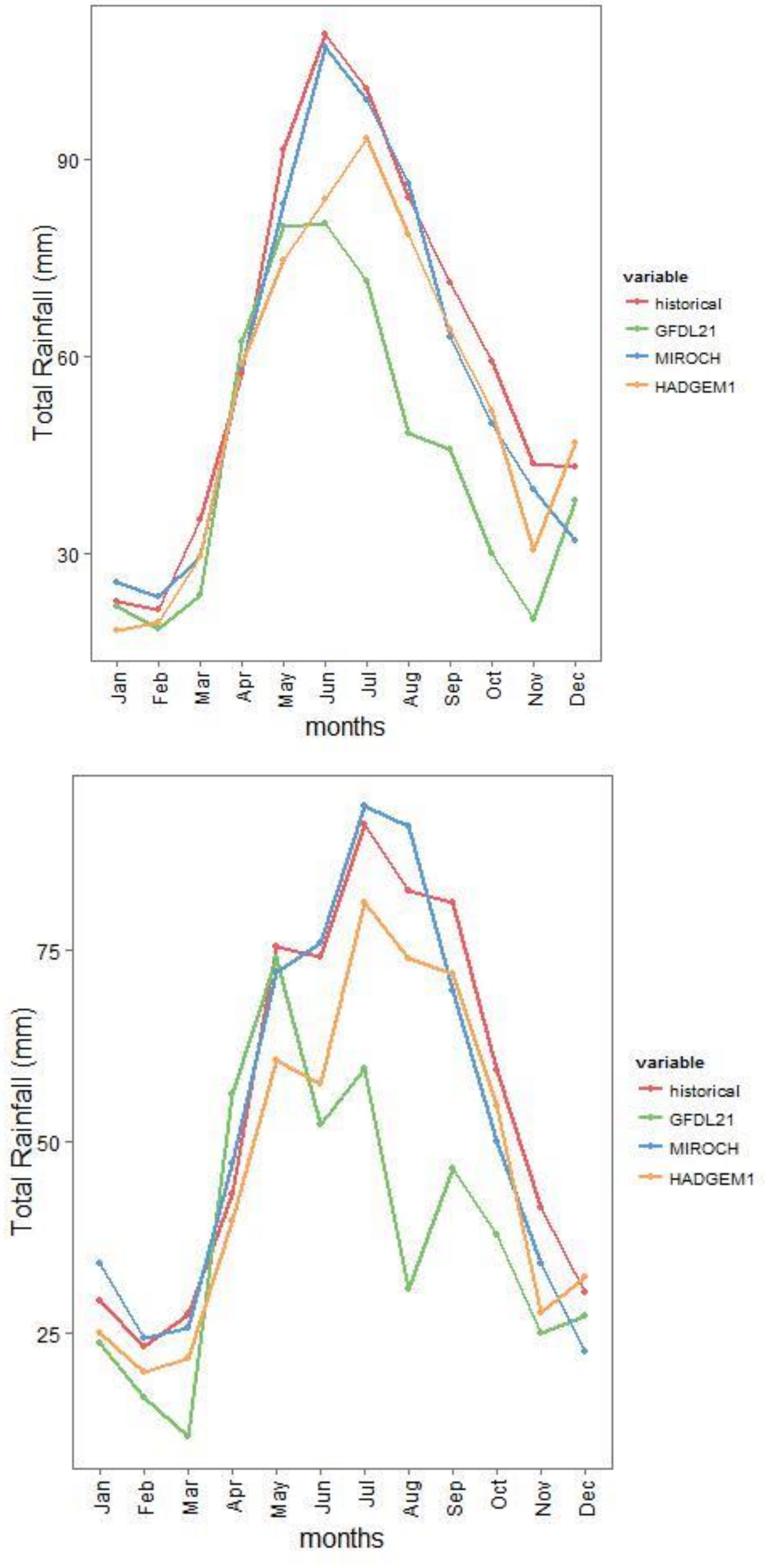

Figure A3.3: The cycle of mean monthly total rainfall for MBR (top) and SGCP (bottom) for the historical climate (red) and three possible future climates in 2050 as modelled by GFDL -21(green), MIROC-H (blue), and HADGEM1 (orange) using the A1FI high emissions SRES scenario.

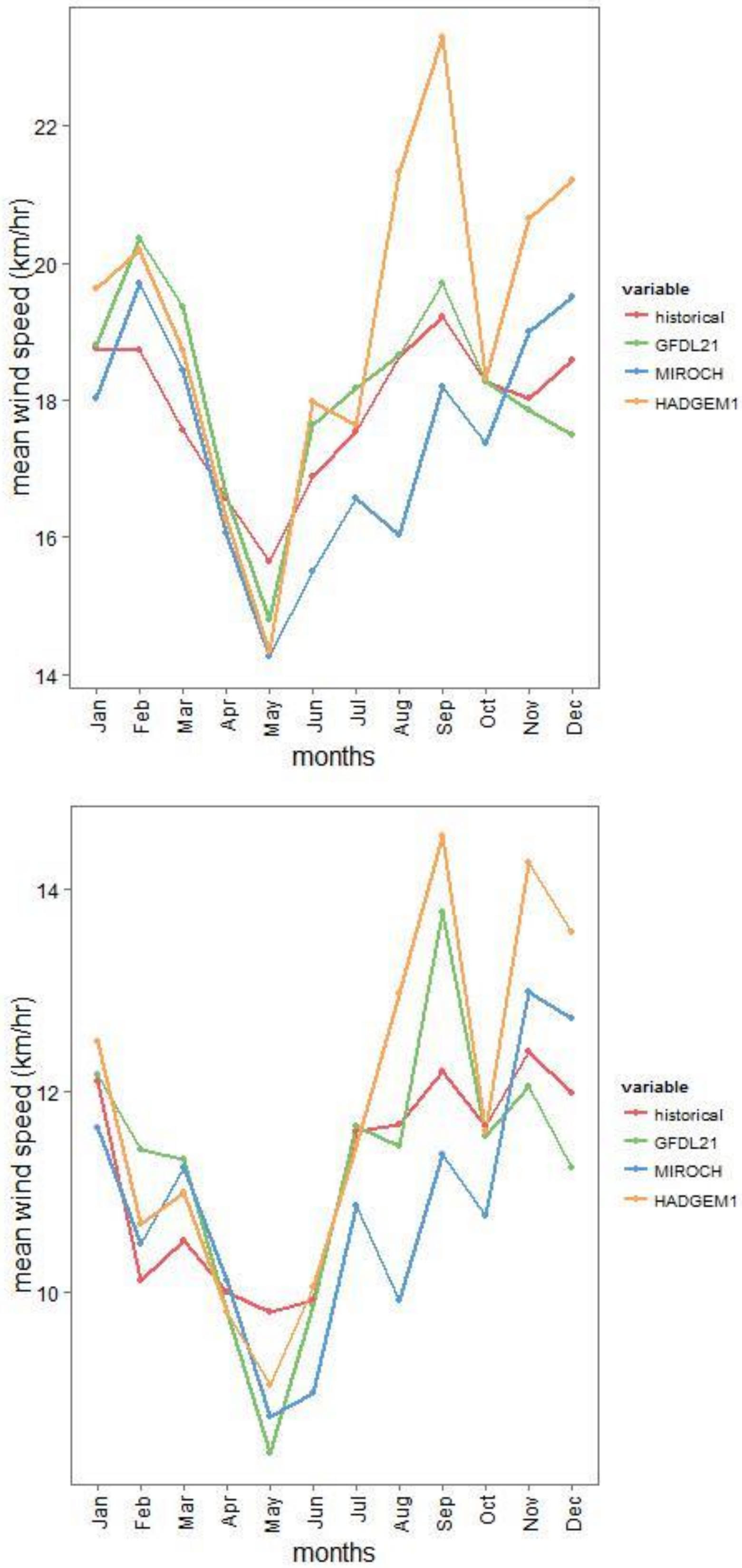

Figure A3.4: The cycle of mean monthly wind speed for MBR (top) and SGCP (bottom) for the historical climate (red) and three possible future climates in 2050 as modelled by GFDL -21(green), MIROC-H (blue), and HADGEM1 (orange) using the A1FI high emissions SRES scenario.

The historical relative humidity data show a similar annual cycle at both locations (Figure A3.5) with a winter maximum (June-July) and a summer minimum. MBR has slightly higher levels than SGCP all year round.

Although there is a range of 2050 projections from the three GCMs (Figure A3.5), they all project a decrease in relative humidity in the fire season. At both locations the greatest differences in humidity between models occurs in winter. At SGCP the GFDL-21 has the greatest decreases. We advise interpreting the GFDL-21 data at MBR with caution. The change factor values for GFDL-21 in the SILO CCCS dataset for the Clarendon location are zero for all months. This lack of change may be due to various reasons: 1) the raw GFDL-21 output may not be available, 2) it may be a reflection of the change factor methodology, 3) or it may be that the change as modelled by GFLD-21 is actually zero, although we consider this the least likely option. Because the GFDL-21 relative humidity change factor is zero, the values of 2050 relative humidity will be the same as the historical values (i.e. no change to baseline data).

Of all the meteorological variables considered, there is most agreement between the GCMs of the 2050 projections in maximum temperature (Figure A3.6). At each location there is approximately a 2°C increase in temperature. Mean monthly maximum temperature seasonality changes slightly at SGCP with a proportionally greater increase in December.

CHANGES IN THE ANNUAL CUMULATIVE FFDI

The effects of climate change as projected by the three GCMs on the mean annual cumulative FFDI (∑FFDI) for both SGCP and MBR are shown in Figure A3.8 as cumulative probability distribution plots.

At MBR the median of the historical annual ∑FFDI is approximately 2200; the maximum recorded was approximately 3000 and the minimum 1800. At SGCP, the historical annual ∑FFDI ranges from a minimum of about 1800 to a maximum of 3800. At MBR the three GCMs have similar projections of ∑FFDI for 2050. That is, the median increases to about 2500 in the MIROC-H projection and 2700 in the GFDL-21 projection. There is a greater range between the GCM in the 2050 projections for SGCP (shown in Figure A3.8 bottom graph). At this location, the MIROC-H GCM is also projecting the lower change (median 3100) and GFDL-21 is projecting a high FFDI future (median 3400).

Another useful way of interpreting the CDF plots is to assess the risk of a certain event. For example, at SGCP the historical risk of having an annual ∑FFDI of less than 3000 was approximately 75%. By 2050 this risk will have doubled to15% to 30% depending on the GCM. At MBR, where the risk is generally less that SGCP, the historical risk of an annual ∑FFDI of greater than 3000 is approximately 5%, but by 2050 the risk has increased to 35%.

The distribution of annual ∑FFDI can be seen from another perspective in the kernel estimate plots of Figure A3.9. At both locations, the shift of the distribution to one of greater fire danger by 2050 is very clear, yet different at the two sites. Remembering that these graphs are essentially histograms, at MBR the greatest occurrence is of an annual ∑FFDI of about 2200 which changes by 2050 to about 2500. At SGCP there is also an increase in this modal value, but the shape of the distribution of annual ∑FFDI changes in a different way to MBR. At SGCP the variability, that is the spread of the distribution increases.

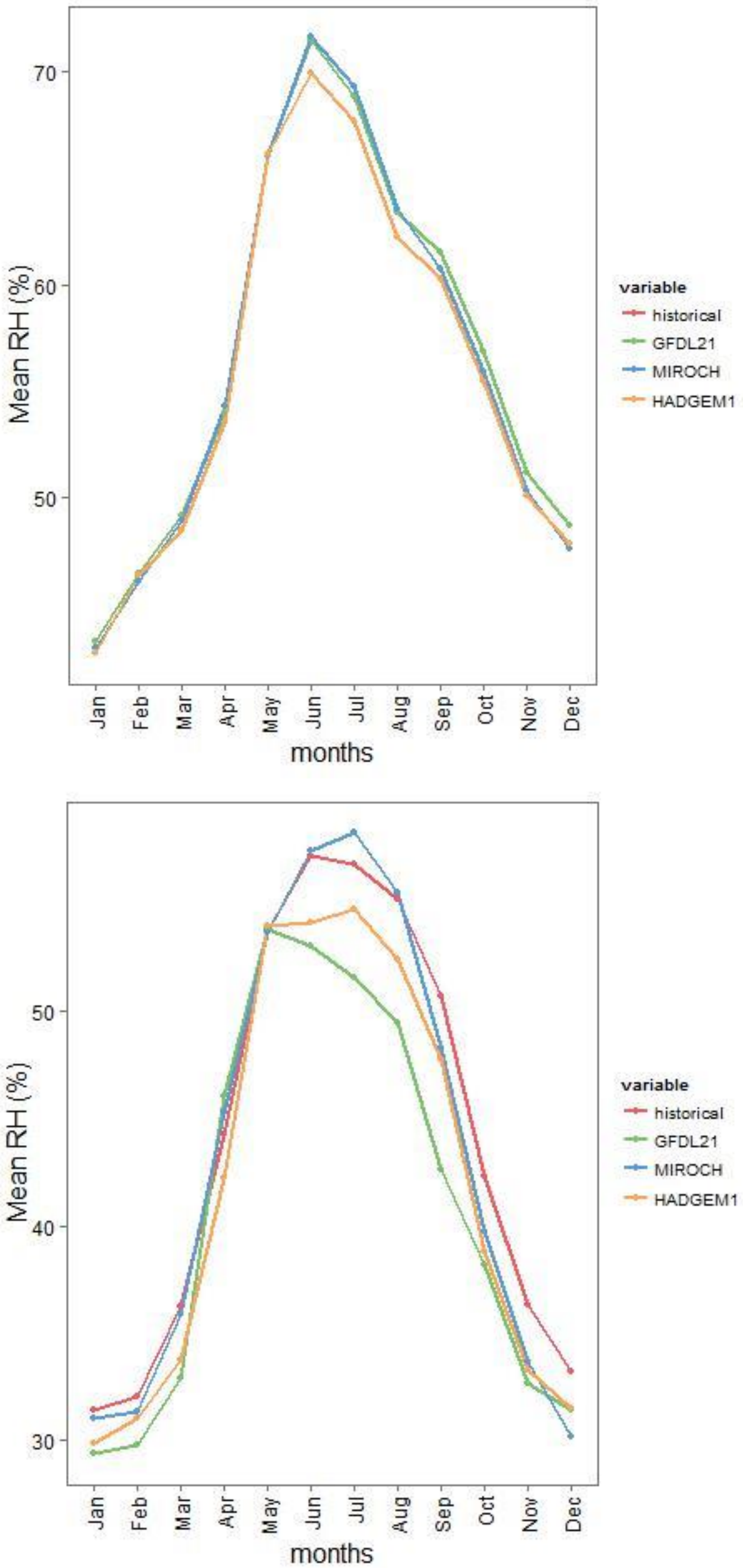

Figure A3.5: The cycle of mean monthly relative humidity or MBR (top) and SGCP (bottom) for the historical climate (red) and three possible future climates in 2050 as modelled by GFDL -21(green), MIROC-H (blue), and HADGEM1 (orange) using the A1FI high emissions SRES scenario. Note that for MBR the GFDL-21 RH data are the same as the historical data and are plotted on top of the historical plot. Hence only the GFDL-21 plot is seen.

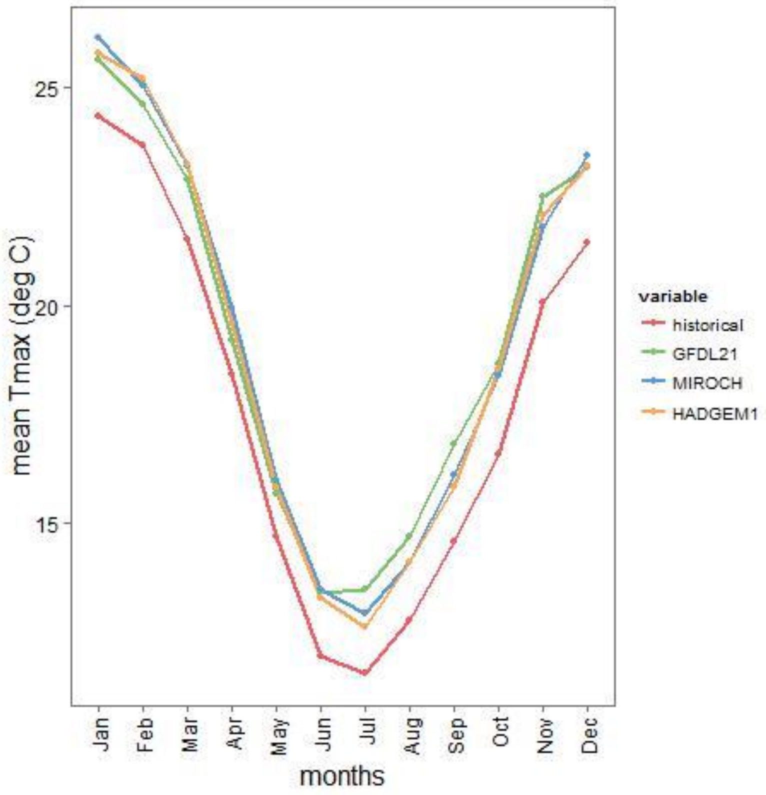

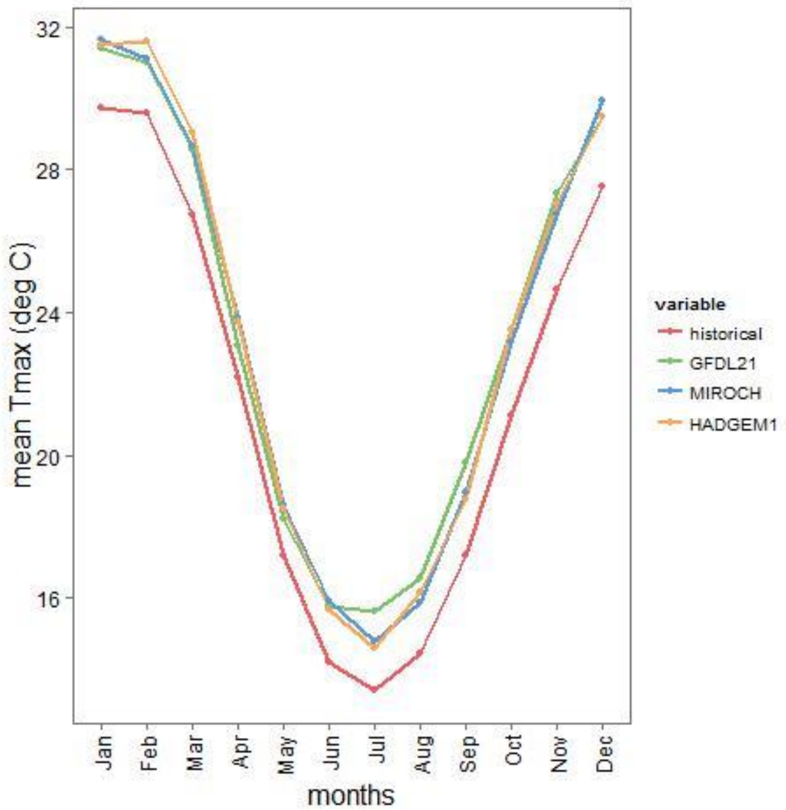

Figure A3.6: The cycle of mean monthly maximum temperature for MBR (top) and SGCP (bottom) for the historical climate (red) and three possible future climates in 2050 as modelled by GFDL -21(green), MIROC-H (blue), and HADGEM1 (orange) using the A1FI high emissions SRES scenario.

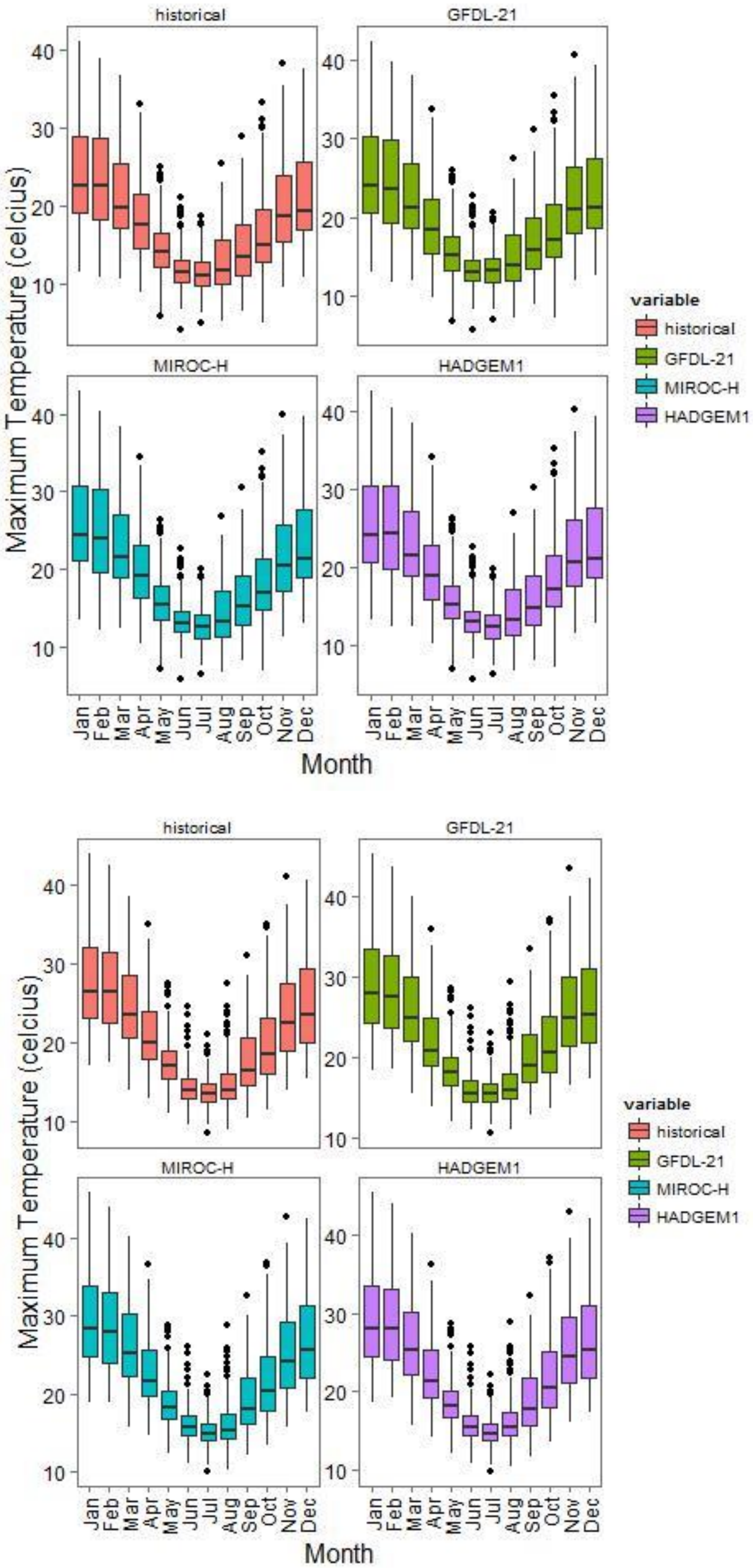

Figure A3.7: A box plot of the whole distribution of monthly maximum temperature for MBR (top) and SGCP (bottom) for the historical climate (red) and three possible future climates in 2050 as modelled by GFDL -21(green), MIROC-H (blue), and HADGEM1 (orange) using the A1FI high emissions SRES scenario.

CHANGES IN THE ANNUAL RISK OF MONTHLY ∑FFDI

Examining the mean monthly ∑FFDI enables an assessment of the severity of bushfire weather each month. The change in the mean of each month's ∑FFDI in 2050 (as shown in Figure A3.10) indicates the projected change in not only each month's fire severity but also a possible change in the seasonality of fire weather.

Historically SGCP has a greater monthly fire danger than MBR. Both locations have a maximum mean monthly ∑FFDI that occurs in January and February and a minimum in July.

The 2050 projections from all GCMs indicate an increase in monthly ∑FFDI at both sites. GFDL-21 has the largest increase. At MBR the changes are fairly uniform across all months, and the historical seasonality is maintained. However, in SGCP the seasonality changes in the GFDL-21 projection with the months of lowest ∑FFDI shifting from July-August to June-July. Perhaps the most significant change is the change in the start of the summer months: the MIROC-H projection shows the months of greatest severity shift forward from January-February in the historical data to December-January in 2050.

In the historical baseline data, May, June, and July have the greatest variability of ∑FFDI. Late spring has the least interannual variability. This seasonal pattern is maintained in 2050 in the MIROC-H and HADGEM1 projections, but in the GFDL2.1 projection the interannual variability increases in early spring (Figure A3.11).

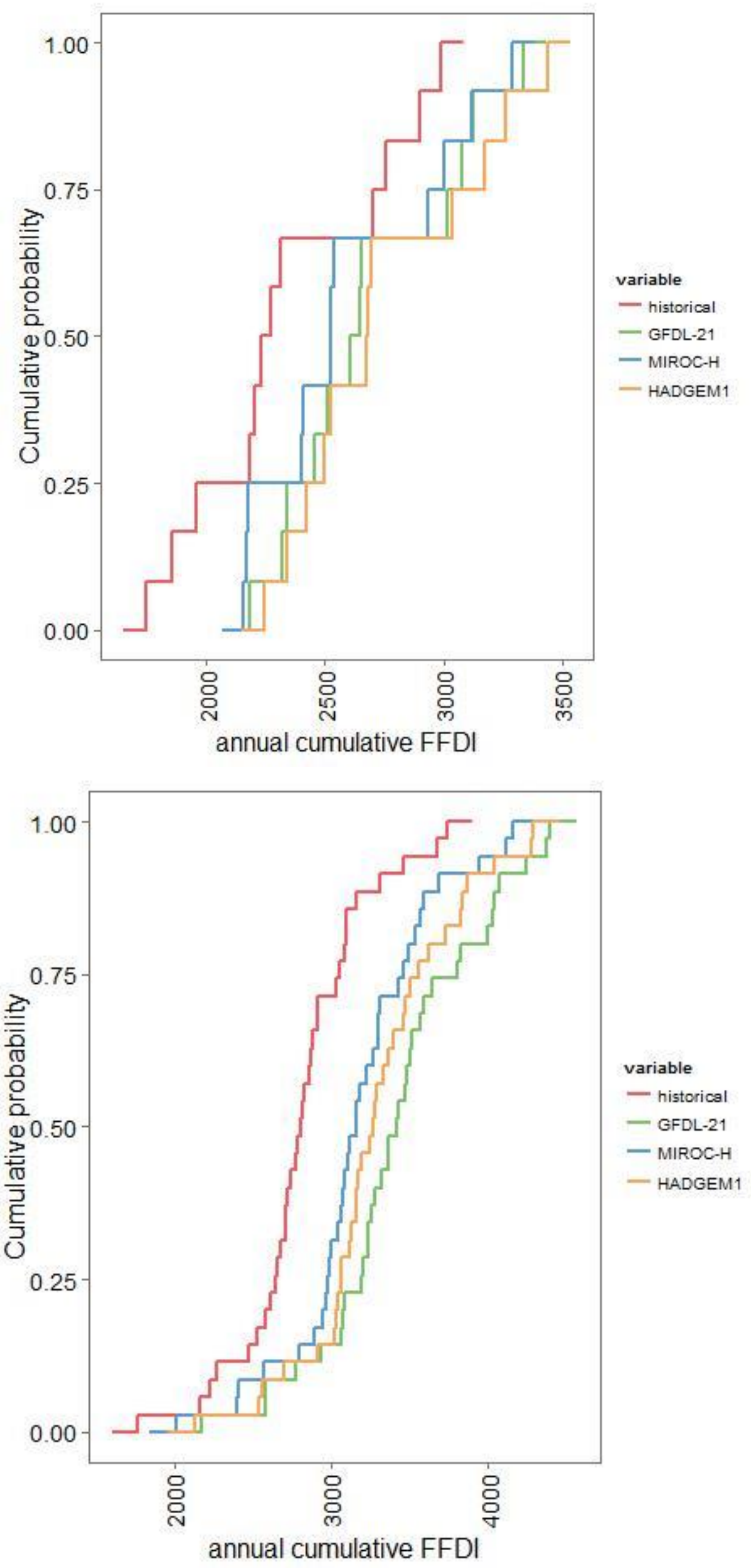

Figure A3.8: The cumulative probability of annual ∑FFDI for MBR (top) and SGCP (bottom) for the historical climate (red) and three possible future climates in 2050 as modelled by GFDL -21(green), MIROC-H (blue), and HADGEM1 (orange) using the A1FI high emissions SRES scenario.

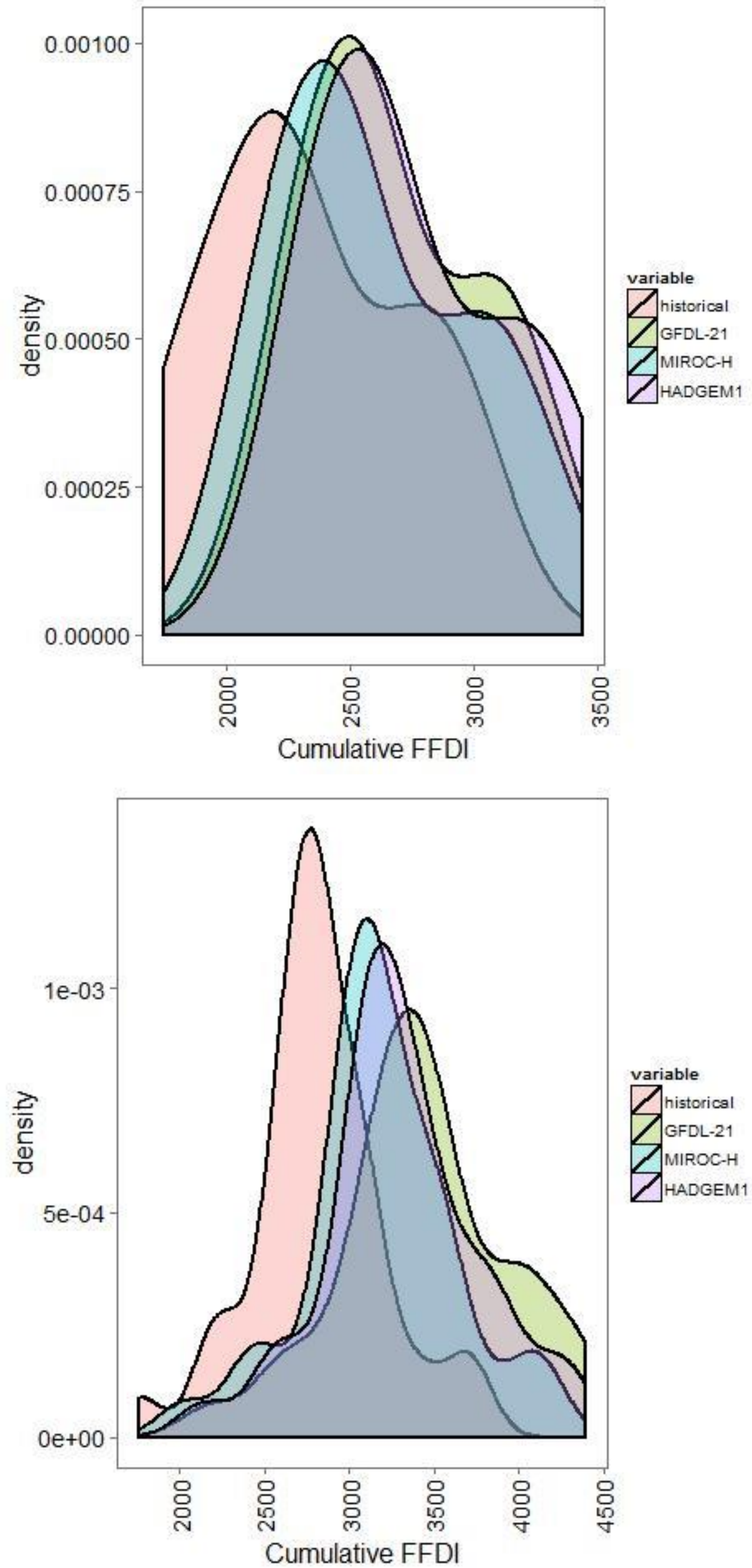

Figure A3.9: The kernel density estimate of annual ∑FFDI for MBR (top) and SGCP (bottom) for the historical climate (red) and three possible future climates in 2050 as modelled by GFDL -21(green), MIROC-H (blue), and HADGEM1 (orange) using the A1FI high emissions SRES scenario. A high density indicates a higher number of occurrences.

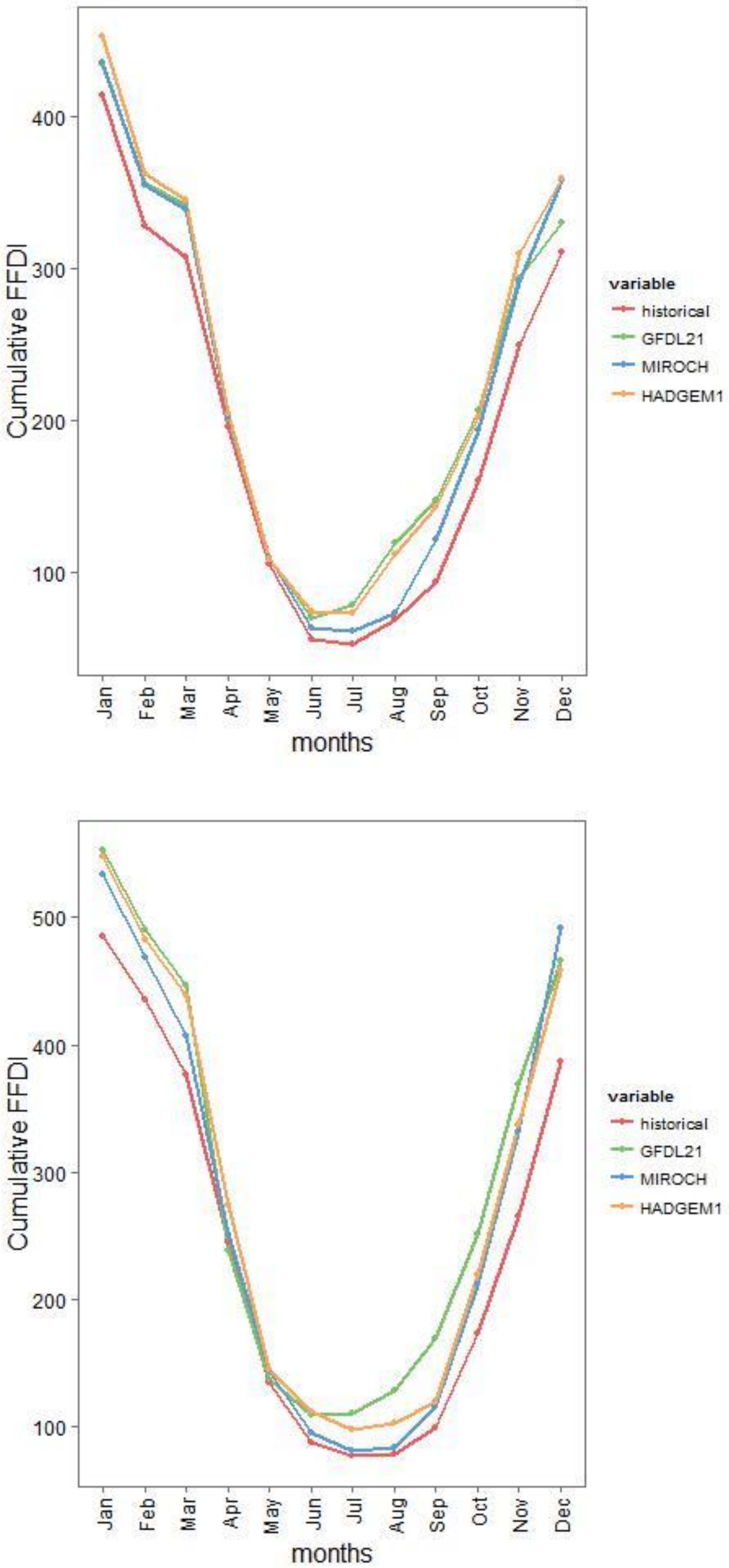

Figure A3.10: The cycle of mean monthly ∑FFDI for MBR (top) and SGCP (bottom) for the historical climate (red) and three possible future climates in 2050 as modelled by GFDL -21(green), MIROC-H (blue), and HADGEM1 (orange) using the A1FI high emissions SRES scenario. A high ∑FFDI indicates greater fire danger.

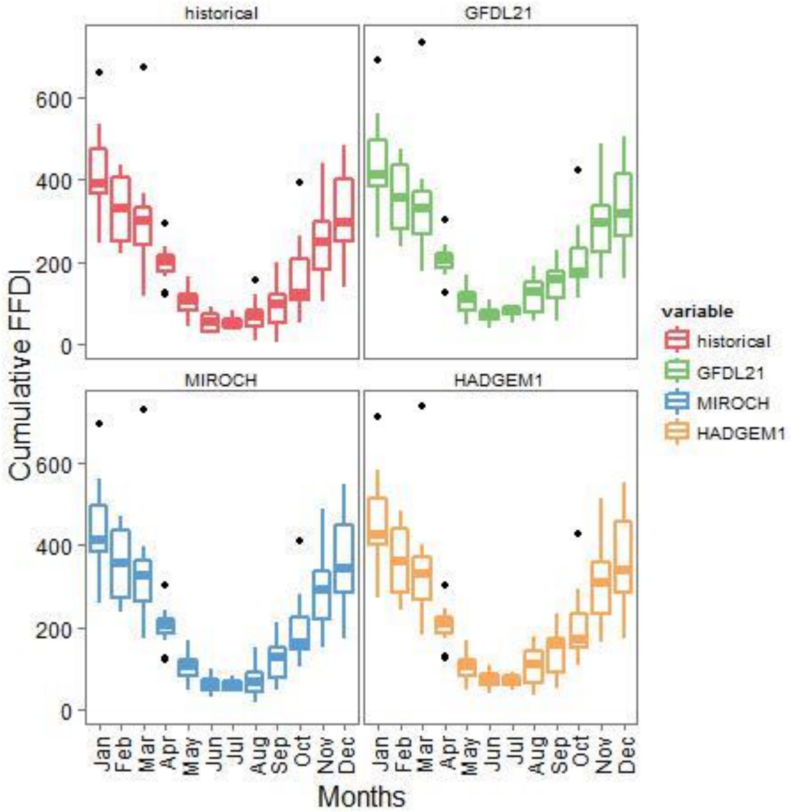

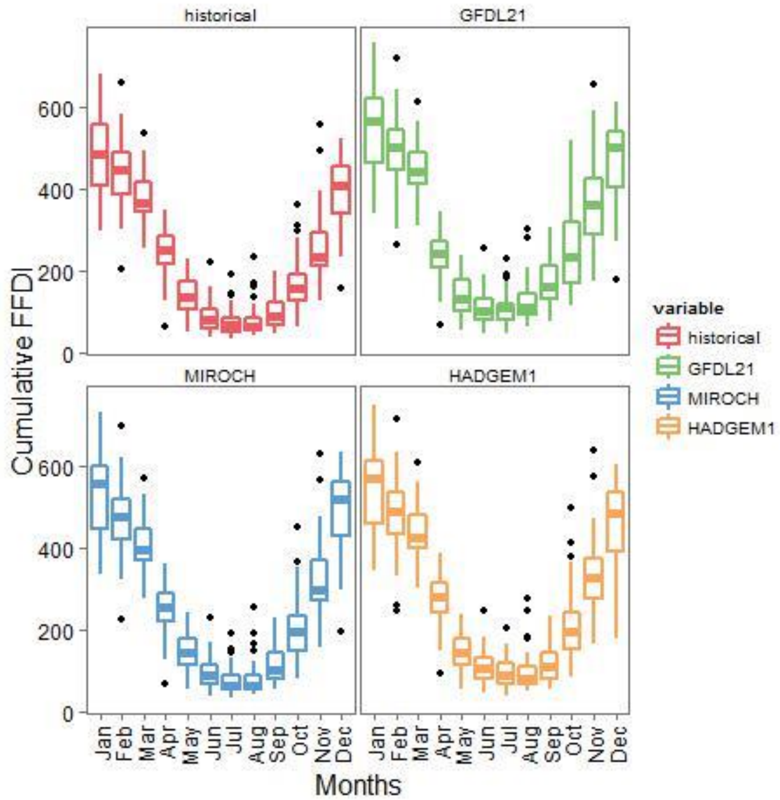

Figure A3.11: The annual cycle of monthly ∑FFDI for MBR (top) and SGCP (bottom) for the historical climate (red) and three possible future climates in 2050 as modelled by GFDL -21(green), MIROC-H (blue), and HADGEM1 (orange) using the A1FI high emissions SRES scenario.

DAILY THRESHOLD ANALYSIS

Changes in the number of very high to extreme FFDI days, that is days where the FFDI is greater than 25, provide additional insight into the possible changes of fire danger by 2050 (Tables A3.1 and A3.2 and Figure A3.12). Projected changes to daily fire-weather risk for each location are similar to those for the ∑FFDI.

At SGCP there is an increase in all of the FFDI threshold exceedance days from an historical mean of approximately 16 days each year for a FFDI>25 up to 23.4 days, 24.5 days, and 25.3 days in 2050 as projected by the MIROC-H, HADGEM1, and GFDL-21 GCMs respectively (Table A3.2). The entire distribution of the 2050 projections is shown in Figure A3.12 (bottom). The difference between the GCMs is not large although the GFDL-21 GCM does have a greater interannual variability in the FFDI>25 category compared with the other two GCMs.

Although the changes in the actual number of days of occurrence of the higher threshold exceedance events are small, if considered as a percentage change then they may be more significant in terms of fire management. For example in Table A3.1, the change at SGCP in the number of days that the FFDI>40 increases from an historical mean of 0.77 days/year to 2.66 days each year in the GFDL-21 2050 projection. This increase of approximately 200% is common when considering rarely occurring events.

Changes in the number of higher threshold exceedance events such as FFDI>75 need to be considered in the context of their return period (as per Lucas et al 2007). The return period is the typical number of years between occurrences. However, our datasets are not long enough to calculate such a measure.

The future projections of daily threshold occurrences in the MBR also increase (Table A3.1 and Figure A3.12 (top)). At MBR, although the historical number of days where FFDI >25 (16.7) is slightly greater than that at SGCP (16.0), there is a big difference in the future projections: the mean number of days FFDI >25 at MBR increases to about 20, whereas at SGCP it's about 24. The interannual variability of all threshold occurrences is much less at MBR than SGCP. Also, the interannual variability does not increase in all GCM projections of FFDI>25. In addition, the MIROC-H GCM has the great increase in the number of days in all categories, whereas at SGCP the GFDL-21 GCM has the greatest increases.

Table A3.1: The mean number of days where the FFDI is above a certain threshold at SGCP for the historical dataset and the three GCMS for the A1FI SRES scenario for the year 2050.

	FFDI>25	FFDI>40	FFDI>50
Historical	15.97	0.77	0.03
GFDL-21	25.34	2.26	0.09
MIROC-H	23.37	1.77	0.06
HADGEM1	24.46	2.11	0.06

Table A3.2: The mean number of days where the FFDI is above a certain threshold at MBR for the historical dataset and the three GCMS for the A1FI SRES scenario for the year 2050.

	FFDI>25	FFDI>40	FFDI>50
Historical	16.77	3.38	0.62
GFDL-21	19.15	4.69	1.08
MIROC-H	19.92	4.92	1.15
HADGEM1	21	5.62	1.77

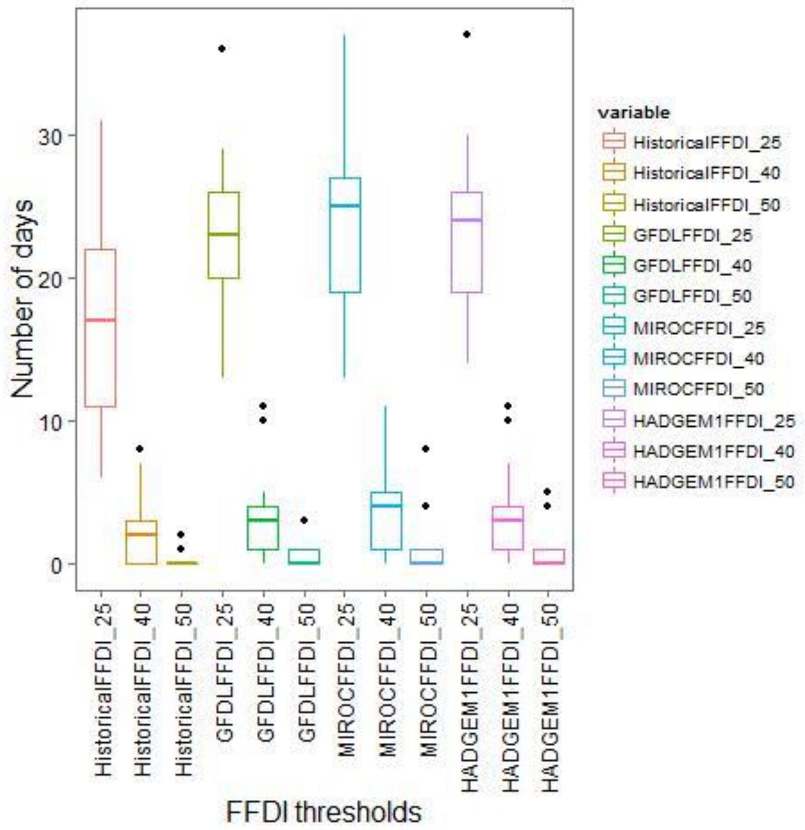

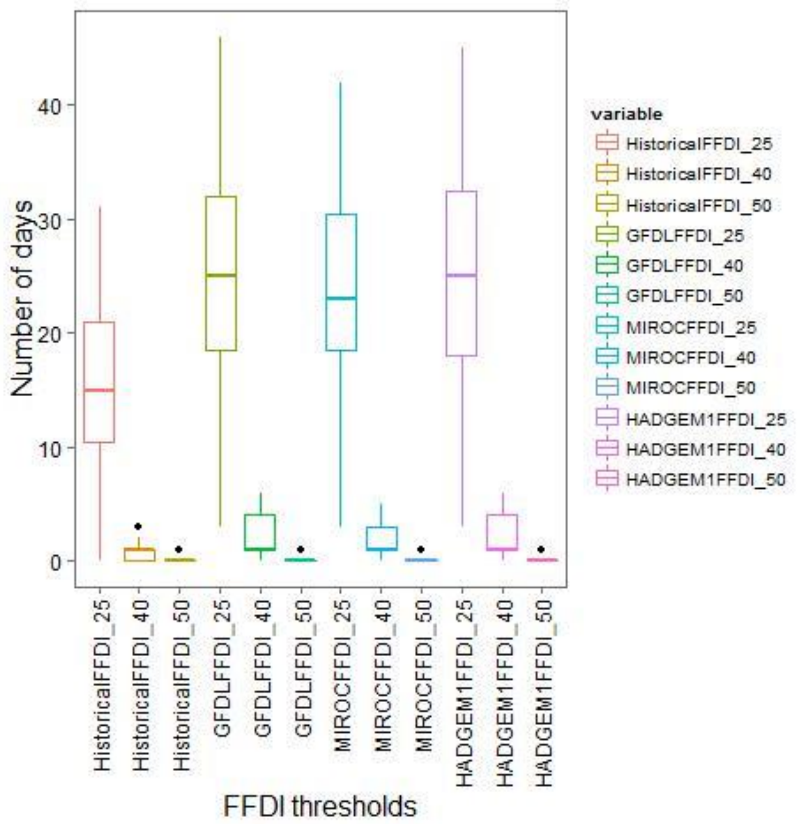

Figure A3.12: The distribution of the number of days when the FFDI was above three threshold levels: FFDI>25; FFDI> 40; and FFDI>50. The data for MBR (top) and SGCP (bottom) is for the historical climate (red) and three possible future climates in 2050 as modelled by GFDL -21(green), MIROC-H (blue), and HADGEM1 (orange) using the A1FI high emissions SRES scenario.

TEMPORAL ANALOGUES

The above assessment of future fire danger as produced by GCMs can be enhanced by considering climate analogues. In climate analogue analyses, future climates projected by GCMs for a location are compared with the climate throughout the historical record. Temporal analogues use historical climates and responses to climate variability, climate change and climate extremes to provide insights for vulnerability to climate change.

We present an analogue analysis only for SGCP, as the MBR record is too short for a meaningful analysis. For the SGCP, the annual rainfall anomalies are plotted against the annual temperature anomalies (Figure A3.13). The annual ΣFFDI is plotted as well. The climate projections for 2030 for mean annual rainfall and temperature are similar to the years 1961, 1965, 1980, 1988, 1990, 1991, and 1993. Interestingly, while the annual ΣFFDI in these years has been high, 1982 and 1967 had higher annual ΣFFDI.

The projections for temperature, rainfall and FFDI for the year 2050 were outside the range of the 1960-94 historical climate. However, more recent data that is not included here, may be an analogue for 2050.

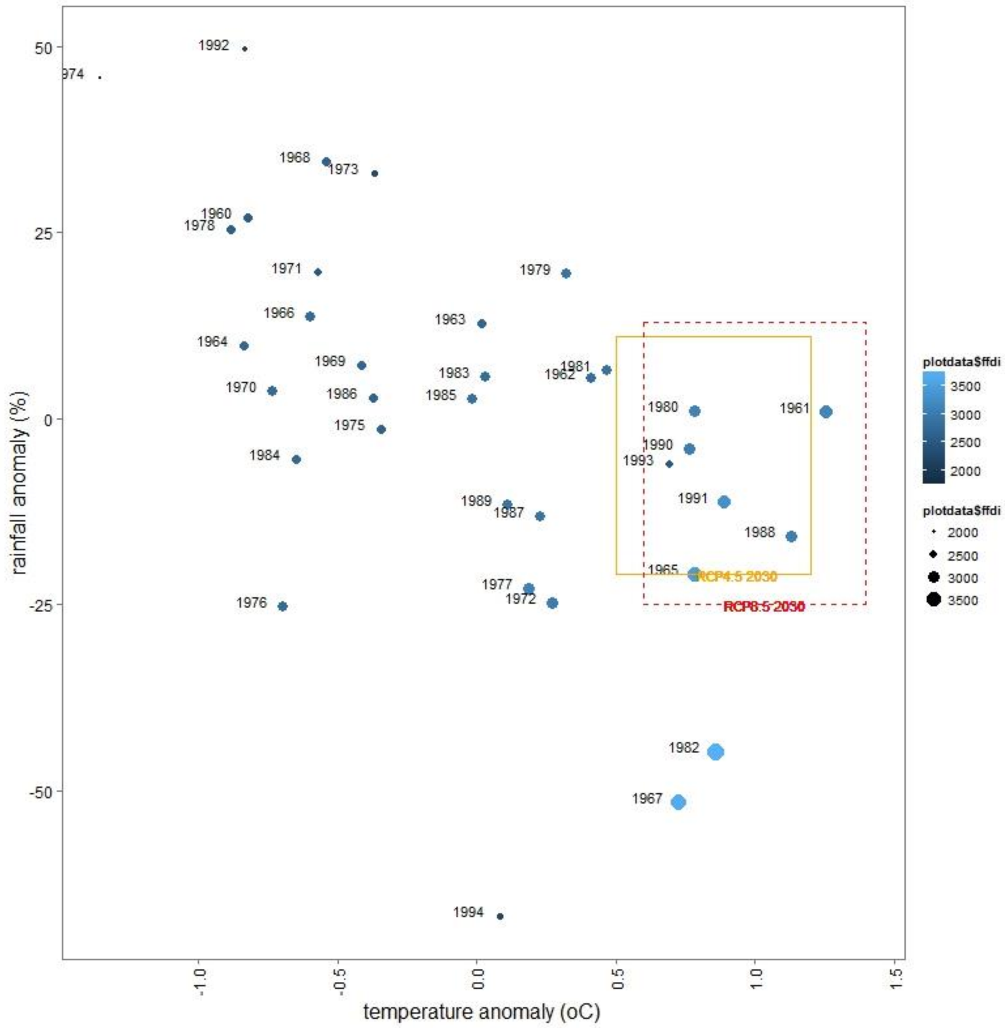

Figure A3.13: The historical annual rainfall anomalies and temperature anomalies from 1960-1994 for the SGCP, with the annual ΣFFDI superimposed on top. The boxes indicate the range of projections from the CMIP3 GCMs for rainfall and temperature in the year 2050 under A1FI emissions SRES scenario.

A3.6 CONCLUSIONS FROM THE PILOT STUDY ANALYSIS

The impact of climate change on bushfire risk at two pilot locations in South Australia has been examined. Future bushfire risk will be dependent on changes in a range of factors including climate, land use, population, and vegetation. This study has focussed solely on a range of projected changes of fire weather variables by 2050 that were then used to assess changes in fire danger as described by the Forest Fire Danger Index (FFDI).

Clare and Kuitpo have similar climatological features in terms of seasonaility and climate 'type'. However, there are differences that are reflected in the 2050 scenarios. Kuitpo is further south and in hillier terrain. It is wetter and more humid, windier, and cooler. The median ∑FFDI is less than at Clare. However Clare has greater interannual variability in climate. This difference means that it will have more extreme years of fire danger than Kuitpo. The seasonality of fire danger is the same at both sites.

Simulations from three CMIP3 GCMs run under the A1FI scenario were combined with historical weather observations to assess the changes to fire weather projected to occur by 2050. All three GCMs projected changes in the same direction across all months for temperature and relative humidity. That is, an increase in temperature and a decrease in relative humidity (except for the MIROC-H projection of changes in July).

The projections of monthly rainfall were also mostly consistent and showed a strong decrease in winter and spring. There was more variation between models for rainfall in summer.

The projections of wind speed, however, varied greatly between the GCMs, except for a consistent decrease in May wind speed. The greatest change in wind speed was in the winter months.

Therefore, with the exception of the uncertainty in the wind speed projections, the changes to fire weather conditions as a result of changes to rainfall, temperature and evaporation by 2050 would suggest an increase in fire danger.

Calculated changes to the FFDI include increases in the mean annual cumulative FFDI, and the interannual variability of annual ΣFFDI. Fire danger weather is therefore projected to increase at both locations compared to present day values. There are slight differences between the two regions.

Along with the projected increase in cumulative monthly and annual FFDI, an increase in the number of days with a FFDI of 'very high' or 'extreme' are also expected. The number of high fire danger days and above generally increases by 50-60%.

At both locations the fire seasons are likely to become longer, and start earlier in the year.

Generally the GFDL-21 GCM showed the greatest increase in FFDI.

These results are placed in the context of the current climate and its tendencies.

Overall, the future climate at SGCP is likely to be more variable than present, and the change in interannual variability greater at SGCP than at MBR. These conclusions may not apply across all of SA as although most regions are projected to warm in the future, if other regions have projected increases in precipitation and/or relative humidity then there may well be increased uncertainty in future fire danger projections.

The study of Lucas (2007) used longer historical time series and consequently was able to put these changes in an historical perspective. He concluded that during the last several years in southeast Australia, including the 2006-07 season, particularly severe fire weather conditions have been observed. In many cases, the conditions far exceed the projections in the high scenarios of 2050.

In terms of identifying long term trends in historical FFDI, there are not many more locations in addition to those studied by Lucas et al (2007) that are suitable for creating a long-term historic FFDI timeseries based on observed data. This limitation is mostly because of the lack of lengthy wind speed records.

However, there is an alternative methodology that will provide relatively long term data. This option involves using the SILO gridded dataset for temperature, rainfall, and vapour pressure, and a separate gridded wind speed dataset developed by CSIRO (McVicar et al.). This wind speed dataset was designed specifically to be integrated with SILO.

A3.7 CAVEATS

It is important to note the following caveats with respect to these analyses:

1. We have used proxies to represent the study areas of interest. We have used Clare as a proxy for SGCP and Kuitpo for MBR which we believe are relatively robust. However, local knowledge may need to be used to further interpret these results in terms of SGCP and MBR.

2. All climate change impact modelling studies have inherent uncertainties based on the future likely emissions, how the climate responds to those emissions and the accuracies of the GCMs to model the climate. This study has utilised the SRES A1FI emissions scenario, but has not addressed uncertainty that may arise from other scenarios or uncertainties.

3. We have aimed to capture a measure of the uncertainty resulting from the use of different GCMs by undertaking the analysis for three models. However, there may be GCMs that simulate other climate projections that may increase the range of risk from future climate change than that used in this analysis.

4. The primary assumption in the CCCS and Ozclim approach is that the spatial and temporal climate variability observed over the past 30 years will be maintained. With climate change, there may be changes in the frequency of certain types of events, for example the number of days of zero rainfall. Use of the Change Factor perturbation methodology does not capture changes in the frequency of dry days.

BIBILIOGRAPHY

Beer, T. and A. A. J. Williams (1995). "Estimating Australian forest fire danger as a result of doubled CO_2 concentrations." Climatic Change **29** (2).

Blanchi, R., C. Lucas, et al. (2010). "Meteorological conditions and wildfire-related house loss in Australia." International Journal of Wildland Fire **19**: 914–926.

Bradstock, R. A. (2010). "A biogeographic model of fire regimes in Australia: current and future implications." Global Ecology and Biogeography **19**(2): 145-158.

Bradstock, R. A. and A. M. Gill (2001). "Living with fire and biodiversity and the urban edge: in search of a sustainable solution to the human protection problem. ." Journal of Mediterranean Ecology **2**: 179–195.

Bureau of Meteorology. (2009). "Climate Change in Australia website." Retrieved 31 October, 2009, from http://www.climatechangeinaustralia.gov.au/.

Bureau of Meteorology. (2013). "Bureau of Meteorology Website." Retrieved April 2011, 2011, from http://www.bom.gov.au/.

Bureau of Meteorology. (2014a). "Fire Weather Warnings Web Page." Retrieved 18 September, 2014, from http://www.bom.gov.au/weather-services/bushfire/index.shtml.

Bureau of Meteorology. (2014b). "Climate and Past Weather page." Retrieved 18 September, 2014, from http://www.bom.gov.au/climate/.

Burgess, S., J. Ricketts, et al. (2012). Consistent Climate Scenarios Project User Guide: 'Change factor' and 'Quantile-matching' based climate projections data. . Queensland, Queensland Department of Science, Information Technology, Innovation and the Arts.

Byram, G. M. (1959). Combustion of forest fuels. Forest Fire: Control and Use. K. P. Davis. New York, McGraw-Hill**:** 61–89.

Caesar, J. and N. Golding (2011). Meteorological factors influencing forest fire risk under climate change mitigation. London, United Kingdom., AVOID: Avoiding dangerous climate change.**:** 30.

CFS. (2014). "More about Fire Danger Rating Webpage." Retrieved 18 September, 2014, from http://www.cfs.sa.gov.au/site/fire_bans_and_ratings/more_about_fire_danger_rating.jsp.

CFS (2014). South Australian Country Fire Service Standard Operating Procedures October 2013. S. A. C. F. Service. Adelaide, South Australian Government**:** 184.

Cheney, N. P., J. S. Gould, et al. (1998). "Prediction of fire spread in grasslands." International Journal of Wildland Fire **8**: 1-13.

Cheney, P. and A. Sullivan (1997). Grassfires: Fuel, Weather and Fire Behaviour. Melbourne, Australia, CSIRO Publishing.

Clarke, H., C. Lucas, et al. (2012). "Changes in Australian fire weather between 1973 and 2010." International Journal of Climatology **33**(4): 931-944.

Clarke, H., C. Lucas, et al. (2012). "Changes in Australian fire weather between 1973 and 2010." International Journal of Climatology: 14.

Clarke, H. G., P. L. Smith, et al. (2011). "Regional signatures of future fire weather over eastern Australia from global climate models." International Journal of Wildland Fire **20**: 550–562.

Clarke, H. G., P. L. Smith, et al. (2011). "Regional signatures of future fire weather over eastern Australia from global climate models." International Journal of Wildland Fire **20**: 550–562.

CO_2 Now.org. (2014). "Earth's CO_2 Home Page - Atmospheric CO_2 for August 2014." Retrieved 18 September, 2014, from http://co2now.org/.

CSIRO. (2011). "Q&A: Victorian bushfires." CSIRO Factsheets Retrieved 8 November 2011, from http://www.csiro.au/resources/Victorian-Bushfires-QA.html.

CSIRO and BoM (2007). Climate change in Australia Technical Report. Canberra, Commonwealth Scientific and Industrial Research Organisation.

CSIRO and BoM (2012). State of the Climate 2012., Commonwealth Scientific and Industrial Research Organisation and Bureau of Meteorology**:** 11.

Department of Environment and Natural Resources (2010). Spring Gully Conservation Park. D. o. E. a. N. Resources. Burra, South Australia, Department of Environment and Natural Resources.

Department of Environment and Natural Resources (2012). Overall fuel hazard guide for South Australia. Department of Environment and Natural Resources. Adelaide, Government of South Australia**:** 36.

Dowdy, A. J. and G. A. Mills (2009). Atmospheric states associated with the ignition of lightning-attributed fires, Centre for Australian Weather and Climate Research.

Dowdy, A. J., G. A. Mills, et al. (2009). Australian fire weather as represented by the McArthur forest fire danger index and the Canadian forest fire weather index, Citeseer.
Fuss, S., J. G. Canadell, et al. (2014). "Betting on negative emissions. ." Nature Climate Change **4**: 850-853.
Gifford, R., G. D. Farquhar, et al. (2004). Workshop summary on pan evaporation: An example of the detection and attribution of climate change variables. Pan Evaporation: An example of the detection and attribution of trends in climate variables, Canberra, Australian Academy of Science and the Australian Greenhouse Office.
Google Maps. (2014). "Maps of Mt Bold Reserve and Spring Hill Conservation Park." Retrieved 26 November 2014.
Griffiths, D. (1999). "Improved formula for the drought factor in McArthur's Forest Fire Danger Meter." Australian Forestry **62**(2): 202-206.
Hasson, A. E. A., G. A. Mills, et al. (2009). "Assessing the impact of climate change on extreme fire weather events over southeastern Australia." Climate research (Open Access for articles 4 years old and older) **39**(2): 159.
Hennessy, K. J., C. Lucas, et al. (2005). Climate change impacts on fire-weather in south-east Australia. CSIRO, Australian Government**:** 91.
Hwang, J., S. Lay, et al. (1994). "Nonparametric multivariate density estimation: a comparative study." Signal Processing, IEEE Transactions on **42**(10): 2795-2810.
IPCC (2007). Contribution of Working Group II to the Fourth Assessment Report of the Intergovernmental Panel on Climate Change - Summary for Policy Makers. Geneva, Switzerland, Intergovernmental Panel on Climate Change**:** 22.
IPCC (2013). IPCC Fifth Assessment Report - The Scientific Basis: Technical Summary., Intergovernmental Panel on Climate Change**:** 84.
Keetch, J. J. and G. M. Byram (1968). A Drought Index for Forest Fire Control. U.S. Department of Agriculture-Forest Service. Asheville, N.C. USA. **Research Paper E38,:** 32.
Kepert, J. D., A. Wain, et al. (2012). A comprehensive, nationally consistent climatology of fire weather parameters. Extended abstracts, Annual Conference of the Australasian Fire and Emergency Services Council and the Bushfire Cooperative Research Centre, Perth, August 28 to.
King, K. J., G. J. Cary, et al. (2012). "Implications of changing climate and atmospheric CO_2 for grassland fire in south-east Australia: insights using the GRAZPLAN grassland simulation model." International Journal of Wildland Fire **21**: 695–708.
Lucas, C. (2010). "On developing a historical fire weather data-set for Australia." Australian Meteorological and Oceanographic Journal **60**(1): 1.
Lucas, C., K. Hennessy, et al. (2007). Bushfire Weather in Southeast Australia: Recent Trends and Projected Climate Change Impacts. Melbourne, Bushfire Cooperative Research Centre and Bureau of Meteorology**:** 84.
McArthur, A. G. (1967). Fire Behaviour in Eucalypt Forest. Commonwealth of Australia Forestry and Timber Bureau. **Leaflet 107:** 25.
McArthur, A. G. (1973). Grassland Fire Danger Meter Mark 4. Commonwealth of Australia Forestry and Timber Bureau.
McVicar, T. R., T. G. Van Niel, et al. (2008). "Wind speed climatology and trends for Australia, 1975–2006: Capturing the stilling phenomenon and comparison with near-surface reanalysis output." Geophysical Research Letters **35**: L20403.
Moss, R. H., J. A. Edmonds, et al. (2010). "The next generation of scenarios for climate change research and assessment." Nature **463**: 747-756.
Nakicenovic, N. and R. Swat (2000). Special Report on Emissions Scenarios. Cambridge, UK., Cambridge University Press**:** pp 612.
Noble, I. R., G. A. V. Barry, et al. (1980). "McArthur's Fire-Danger Meters Expressed as Equations." Australian Journal of Ecology **5**: 201-203.
Pitman, A. J., G. T. Narisma, et al. (2007). "The impact of climate change on the risk of forest and grassland fires in Australia." Climatic Change **84**(3-4): 383-401.
Pittock, B. (2003). Climate Change: An Australian guide to the science and potential impacts. Canberra, Australian Greenhouse Office.
Price, C. (2009). Thunderstorms, Lightning and Climate Change. Lightning: Principles, Instruments and Applications. H. Betz, U. Schumann and P. Laroche, Springer Netherlands**:** 521-535.
Price, C. (2009). Thunderstorms, lightning and climate change. Lightning: Principles, Instruments and Applications - Review of modern lightening research. H. D. Betz, U. Schumann and P. Laroche. Netherlands, Springer Netherlands**:** 521-535.

Price, C. and D. Rind (1994). "Possible implications of global climate change on global lightning distributions and frequencies." Journal of Geophysical Research: Atmospheres **99**(D5): 10823-10831.
Ricketts, J. H. (2009). OzClim for the MTSRF region. . 18th World IMACS/MODSIM Congress. Cairns, Australia., MODSIM.
Sherwood, S. (2011). Climatic uncertainties: clouds, aerosol, water vapour and climate feedbacks. Greenhouse 2011: The science of climate change, Cairns, Queensland, Australia, CSIRO.
Solomon, S., D. Qin, et al. (2007). Climate change 2007: The physical science basis. Contribution of Working Group I to the fourth assessment report of the Intergovernmental Panel on Climate Change. . S. D. Solomon, IPCC.
Steffen, W. (2009). Climate Change 2009. Faster change and more serious risks. Canberra, Australian Department of Climate Change: 58.
Suppiah, R., B. Preston, et al. (2006). Climate change under enhanced greenhouse conditions in South Australia. Aspendale, Victoria, CSIRO: 82.
The Advertiser (2007). Fire ravages Kangarilla. The Advertiser,. Adelaide, South Australia.
Whetton, P., J. Katzfey, et al. (2001). "Developing scenarios of climate change for southeastern Australia: an example using regional climate model output. ." Climate research (Open Access for articles 4 years old and older) **16**(3): 181-201.
Whetton, P., K. McInnes, et al. (2005). Climate change projections for Australia for impact assessment and policy application: A review. . CSIRO Technical Paper. Australia, CSIRO.
Wild, M. (2004). Recent evidence on changes in surface solar radiation. Pan Evaporation: An example of the detection and attribution of trends in climate variables, Canberra, Australian Academy of Science and the Australian Greenhouse Office.
Williams, A. A., D. J. Karoly, et al. (2001). "The sensitivity of Australian fire danger to climate change." Climatic change **49**(1-2): 171-191.
Williams, R. J., R. A. Bradstock, et al. (2009). Interactions between climate change fire regimes and biodiversity in Australia - A preliminary assessment, Australian Government Department of Climate Change.